

UNCLASSIFIED

AD NUMBER
AD828633
NEW LIMITATION CHANGE
TO Approved for public release, distribution unlimited
FROM Distribution authorized to U.S. Gov't. agencies and their contractors; Critical Technology; FEB 1968. Other requests shall be referred to Air Force Weapons Lab., Attn: WLRT, Kirtland AFB, NM 87117.
AUTHORITY
Air Force Weapons Lab ltr dtd 30 Nov 1971

THIS PAGE IS UNCLASSIFIED

AD828633

AFWL-TR-67-127

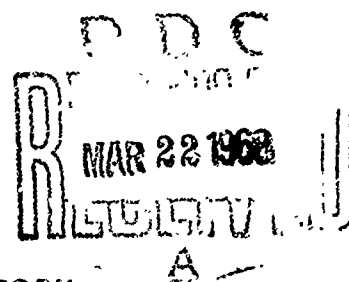
AFWL-TR-  
67-127

## HYDROCODE TEST PROBLEMS

Darrell Hicks

TECHNICAL REPORT NO. AFWL-TR-67-127

February 1968



AIR FORCE WEAPONS LABORATORY

Air Force Systems Command

Kirtland Air Force Base

New Mexico

This document is subject to special export controls and each transmittal to foreign governments or foreign nationals may be made only with prior approval of AFWL (WLRT), Kirtland AFB, NM, 87117.

AFWL-TR-67-127

ACCESSION NO.	
OFFICE	DATE
ROC	DATE
CLASSIFICATION/ASSOCIATION BY	
DISC.	AVAIL. DATE OF SPECIAL
2	

AIR FORCE WEAPONS LABORATORY  
Air Force Systems Command  
Kirtland Air Force Base  
New Mexico

When U. S. Government drawings, specifications, or other data are used for any purpose other than a definitely related Government procurement operation, the Government thereby incurs no responsibility nor any obligation whatsoever, and the fact that the Government may have formulated, furnished, or in any way supplied the said drawings, specifications, or other data, is not to be regarded by implication or otherwise, as in any manner licensing the holder or any other person or corporation, or conveying any rights or permission to manufacture, use, or sell any patented invention that may in any way be related thereto.

This report is made available for study with the understanding that proprietary interests in and relating thereto will not be impaired. In case of apparent conflict or any other questions between the Government's rights and those of others, notify the Judge Advocate, Air Force Systems Command, Andrews Air Force Base, Washington, D. C. 20331.

DO NOT RETURN THIS COPY. RETAIN OR DESTROY.

AFWL-TR-67-127

HYDROCODE TEST PROBLEMS

Darrell Hicks

TECHNICAL REPORT NO. AFWL-TR-67-127

This document is subject to special export controls and each transmittal to foreign governments or foreign nationals may be made only with prior approval of AFWL (WLPT), Kirtland AFB, NM, 87117. Distribution is limited because of the technology discussed in the report.

FOREWORD

This research was performed under Program Element 6.16.46.01.D, Project 5710, Subtask 15.G18, and was funded by the Defense Atomic Support Agency (DASA).

Inclusive dates of research were October 1966 to October 1967. The report was submitted 24 November 1967 by the Air Force Weapons Laboratory Project Officer, Mr. Darrell Hicks (WLRT).

The author wishes to express his appreciation to Robert M. Pelzl and Gail L. Houser for their help in preparing this report.

This technical report has been reviewed and is approved.

*Darrell Hicks*

DARRELL HICKS  
Project Officer

*Truman L. Franklin*

TRUMAN L. FRANKLIN  
Colonel, USAF  
Chief, Theoretical Branch

*Claude K. Stambaugh*

CLAUDE K. STAMBAUGH  
Colonel, USAF  
Chief, Research Division

ABSTRACT

(Distribution Limitation Statement No. 2)

The utility (accuracy, speed, etc.) of a hydrocode in solving the equations of hydrodynamics may be estimated by applying the hydrocode test problems described in this report. Given the estimations of the utilities of a pair of hydrocodes, we may decide which is the preferred hydrocode to use. The hydrocode test problems described in this report have solutions which are known exactly. Seven hydrocode test problems involving shocks, rarefactions, and interactions are investigated and applied to a typical hydrocode, AFWL's PUFF.

# CONTENTS

<u>Section</u>		<u>Page</u>
I	INTRODUCTION	1
	The Hydrocode Utility Problem	1
	An Example of a Typical Hydrocode	3
II	DESCRIPTIONS, DERIVATIONS, AND DETAILS	8
	Hydrocode Test Problem Sctp-I	10
	Hydrocode Test Problem Sctp-II	27
	Hydrocode Test Problem Sctp-III	47
	Hydrocode Test Problem Sctp-IV	62
	Hydrocode Test Problem Sctp-V	69
	Hydrocode Test Problem Sctp-VI	87
	Hydrocode Test Problem Sctp-VII	97
	APPENDIXES	
	I On the Equations Modeling Linear Flow Gas Hydrodynamics	105
	II Solution Methods	115
	III Error Formats and Error Functions	133
	IV Summary of PUFF Test Results	136
	INDEX	138
	DISTRIBUTION	143

PRECEDING  
PAGE BLANK

ILLUSTRATIONS

<u>Figure</u>		<u>Page</u>
1a	Pipe Plot for Sctp-I	10
1b	Eulerian Wave Plot for Sctp-I	11
2a	Pipe Plot for Sctp-II	27
2b	Eulerian Wave Plot for Sctp-II	31
2c	Velocity Plot for Sctp-II	34
2d	PUFF Sctp-II Error Graph	42
3a	Pipe Plot for Sctp-III	47
3b	Eulerian Wave Plot for Sctp-III	48
3c	Characteristic Lines Plot	52
3d	PUFF Sctp-III Error Graph	60
4a	Pipe Plot for Sctp-IV	62
4b	Wave Plot for Sctp-IV	62
4c	PUFF Sctp-III Error Graph	67
5a	Pipe Plot of Initial Conditions for Sctp-V	70
5b	Eulerian Wave Plot for Sctp-V	70
5c	Lagrangian Wave Plot	71
5d	Velocity Plot	71
5e	Pressure Plot	72
5f	Density Plot	72
5g	P, v Plot for Right Facing, Right Specified Shocks	75
5h	PUFF Error Graph on Sctp-V-A	83
5i	Error Graph for Sctp-V	83
6a	Pipe Plot for Sctp-VI Initial Values	88
6b	Lagrangian Wave Plot for Sctp-VI	88



## ILLUSTRATIONS (cont'd)

<u>Figure</u>		<u>Page</u>
6c	Pressure-Density Plot Prior to Collision	88
6d	Pressure Plot after Collision	89
6e	SCTP-VI Error Graph	94
6f	SCTP-VI-B Error Graph	95
7a	Pipe Plot for Initial Values in SCTP-VII	97
7b	Lagrangian Wave Plot for SCTP-VII	97
7c	Initial Pressure Plot for SCTP-VII	98
7d	After Overtake Pressure Plot for SCTP-VII	98
A-1	Domain of Dependence Graph for the Differential Solution	123
A-2	Domain of Dependence Graph for the Difference Solution	124
A-3	Relationship of the Domain of Dependence	124
A-4	PUFF Errors	136

## TABLES

<u>Table</u>		<u>Page</u>
I-A	PUFF Error Table for SCTP-I-A	26
I-B	PUFF Error Table for SCTP-I-B with $v_m = v_l$	26
II-A	PUFF Error Table for SCTP-II-A	44
II-B	PUFF Error Table for SCTP-II-B	44
II-C	PUFF Error Table for SCTP-II-C	45
II-D	PUFF Error Table for SCTP-II-D	45
II-E	PUFF Error Table for SCTP-II-E	46
III-A	PUFF Error Table for SCTP-III-A	61
III-B	PUFF Error Table for SCTP-III-B	61
IV-A	PUFF Error Table for SCTP-IV-A	68
IV-B	PUFF Error Table for SCTP-IV-B	68
V-A	Activity Table at Time $2 \times 10^{-3}$ Second on SCTP-V	85
V-B	PUFF Error Table for SCTP-V-A	85
V-C	PUFF Error Table for SCTP-V-B	86
V-D	PUFF Error Table for SCTP-V-C	86
VI-A	PUFF Error Table for SCTP-VI-A	96
VI-B	PUFF Error Table for SCTP-VI-B	96
VII-A	PUFF Error Table for SCTP-VII-A	103
VII-B	PUFF Error Table for SCTP-VII-B	103

## SECTION I

### INTRODUCTION

#### 1. THE HYDROCODE UTILITY PROBLEM

Hydrocodes are computer programs used to solve the equations of hydrodynamics. By "equations of hydrodynamics" we mean the equations arising from the conservation laws and thermodynamic laws. (See Appendix I for a detailed discussion of these equations.)

In particular, we shall restrict the hydrocodes in this report to be digital computer programs of finite difference schemes. We shall also restrict the discussion in this report to one-dimensional linear geometry hydrocodes. At the end of this section we shall give an example of a typical hydrocode. The purpose of this report is to present the development of a method of determining the utility (accuracy, speed, etc.) of a hydrocode.

Hydrocode solutions to the equations of hydrodynamics usually differ from the exact solutions. If the hydrocode solutions converge, this difference may be reduced by refining the mesh of the finite difference scheme used in the hydrocode. Thus, if the hydrocode solutions converge, the accuracy of the hydrocode solutions is directly related to the computational effort.

However, we have no proof of convergence of these schemes except when the solution is assumed smooth between a priori known shock positions.\* But the problems of interest involve shocks whose positions are not a priori known. Therefore, in the problems of interest, we have no proof of convergence.

The accuracy of the hydrocode solution is not necessarily directly related to the computational effort. That is, the mesh (space differences and time differences) might be refined and yet the accuracy might not be improved. Moreover, even if convergence were proved for a scheme, it still might not be of any practical use because the convergence might be too slow. That is, the computational effort required might be too much for practical purposes.

---

\*Lax and Keller, The Initial and Mixed Initial and Boundary Value Problem for Hyperbolic Systems, Los Alamos Report LAMS-1205, '951.

For the hydrocode to be useful, the error should be small and the computational effort must be within the capacity of the computer in relation to both memory and computation time. We will measure the computational effort by the running time required on the Air Force Weapons Laboratory's CDC 6600 computer. It is unfortunate that this running time also depends somewhat on the other programs which are being run in the 6600 because of its parallel processing. However, this was the only computing time number available.

When one uses a hydrocode to predict some phenomenon, he would like to know how accurate he can expect the hydrocode's prediction to be. That is, he would like to have a number or numbers which indicate to him what the deviations between the hydrocode numbers and the observed data will be. One place for deviations to enter is between the mathematical model of the phenomenon and the phenomenon itself. This report does not discuss that problem. (However, Appendix I does investigate the mathematical model.)

The problem we are trying to deal with is the deviation between the mathematical model (represented by the equations arising from the conservation laws and thermodynamic laws) and the hydrocode model (that is, the computed approximation to the solution of the equations arising from the conservation and thermodynamic laws). Therefore, we are going to call the solution to the mathematical model the "exact solution." We therefore want some number or numbers that indicate the "distance" between the hydrocode solution and the exact solution. The numbers will be like the maximum deviation between the exact pressure profile and the hydrocode's pressure profile, or the sum of the squares of the pressure deviations, etc. (See Appendix III for details on the error numbers.) These numbers will then give a measure of the utility of a hydrocode for a certain type of problem.

Hence, we developed a series of hydrocode test problems which are representative of the basic types of flow encountered in hydrodynamic problems and whose solutions are known exactly. By basic types of flow we mean flows including shocks, rarefactions, etc. (For details, see Section II.) Then we applied the hydrocode test problems to a typical hydrocode to give an example of the procedure that we have developed to measure the utility of a hydrocode.

2. AN EXAMPLE OF A TYPICAL HYDROCODE

As an example of the type of hydrocode that we are referring to, we shall present a sketch of AFWL's PUFF hydrocode which is described in detail in AFWL-TR-66-48.

PUFF is a modification of the hydrocode proposed by von Neumann and Richtmyer in their March 1950 Journal of Applied Physics paper. This paper introduced the notion of artificial viscosity. The equations they arrived at from the conservation laws, thermodynamic laws, and the introduction of an artificial viscosity were the following:

Consider a one-dimensional fluid motion. Let  $x$  be the Lagrangian coordinate, and  $X=X(x,t)$  be the Eulerian coordinate. That is,  $X(x,t)$  gives the position, at time  $t$ , of a fluid element that was initially at position  $x$ .

Let  $\rho_0(x)$  be the initial density, so that  $V$  and  $v$ , given by

$$V(x,t) = \left(1/\rho_0(x) (\partial X/\partial x)\right) \quad (1)$$

and

$$v(x,t) = \partial X/\partial t, \quad (2)$$

are the specific volume and fluid velocity, respectively.

The equations of motion, of energy, and of continuity are:

$$\rho_0 (\partial v/\partial t) = (\partial/\partial x)(p+q), \quad (3)$$

$$(\partial \epsilon/\partial t) + (p+q)(\partial V/\partial t) = 0, \quad (4)$$

and

$$\rho_0 (\partial V/\partial t) = (\partial v/\partial x). \quad (5)$$

In these equations,  $p = p(x,t)$  is the ordinary (or static) fluid pressure and  $\epsilon = \epsilon(x,t)$  is the internal energy per unit mass. A connection between  $\epsilon, p, V$  is established by an equation of state, which will be assumed, for the purpose of illustration, to have the form

$$\epsilon = (pV)/(\gamma-1) \quad (6)$$

which holds, for example, in the case of a perfect gas.

$\gamma$  is a constant  $>1$ .

It is supposed that the dissipative mechanism can be represented by the additional term  $q$  in the pressure, which is assumed to be negligibly small, except in the neighborhood of the shock.

The original  $q$  (artificial viscosity) was

$$q = - \frac{(\rho_0 c \Delta x)^2}{v} \left| \frac{\partial v}{\partial t} \right| \left| \frac{\partial v}{\partial t} \right| \quad (7)$$

Using (5), it can also be written

$$q = \frac{(c \Delta x)^2}{v} \left| \frac{\partial u}{\partial x} \right| \left| \frac{\partial u}{\partial x} \right| \quad (8)$$

where  $c$  is a dimensionless constant near 1 and  $\Delta x$  is the interval length used in the numerical integration of the hydrodynamic equations. PUFF's  $q$  is a modification of this.

Now we will describe PUFF's difference scheme to solve the foregoing equations.

Let the points of a rectangular network with spacings  $\Delta x$  and  $\Delta t$  be denoted by  $x_\ell$ ,  $t^n$  ( $\ell = 0, 1, 2, \dots, L$ ;  $n = 0, 1, 2, \dots$ ). We shall also have occasion to deal with intermediate points, having coordinates

$$x_{\ell+1/2} \equiv 1/2(x_{\ell+1} + x_\ell), \quad t^{n+1/2} \equiv 1/2(t^{n+1} + t^n).$$

To facilitate the writing, we introduce abbreviations such as

$$v_{\ell+1/2}^n \equiv v(x_{\ell+1/2}, t^n) \text{ etc.}$$

The difference equations with which PUFF approximates the differential equations (1) through (8) are the following:

$$\rho_0 \frac{u_{\ell}^{n+1/2} - u_{\ell}^{n-1/2}}{\Delta t} = - \frac{p_{\ell+1/2}^n + q_{\ell+1/2}^{n-1/2} - p_{\ell-1/2}^n - q_{\ell-1/2}^{n-1/2}}{\Delta x} \quad (9)$$

is PUFF's difference approximation to

$$\rho_o \frac{\partial U}{\partial t} = - \frac{\partial (P+q)}{\partial x} \quad (10)$$

$$\frac{X_{\ell}^{n+1} - X_{\ell}^n}{\Delta t} = U_{\ell}^{n+1/2}$$

is PUFF's difference approximation to

$$\frac{\partial X}{\partial t} = v$$

$$\rho_{\ell-1/2}^{n+1} = \frac{\rho_o \Delta x}{X_{\ell}^{n+1} - X_{\ell-1}^{n+1}} \quad (11)$$

is PUFF's difference approximation to

$$\frac{\rho_o}{\rho} = \frac{\partial X}{\partial x} \text{ or } \frac{v}{V_o} = \frac{\partial X}{\partial x}$$

because

$$\rho \equiv \frac{1}{v}$$

Now let

$$\Delta U \equiv U_{\ell}^{n+1/2} - U_{\ell-1}^{n+1/2}$$

Then PUFF's q is

$$q_{\ell-1/2}^{n+1/2} = (\Delta U \cdot C_o^2 - C_1 \cdot C_s) \cdot \Delta U \cdot \left( \frac{\rho_{\ell-1/2}^{n+1} + \rho_{\ell-1/2}^n}{2} \right) \quad (12)$$

where  $C_0 = 1.8$ ,  $C_1 = 0.25$ ,  $C_s =$  isothermal sound speed at time  $t^{n-1/2}$  and position  $\ell-1/2$ . That is,

$$C_s^2 \equiv \left. \frac{dP}{d\rho} \right|_{\epsilon \text{ const.}}$$

Then PUFF simultaneously solves

$$0 = \frac{\epsilon_{\ell-1/2}^{n+1} - \epsilon_{\ell-1/2}^n}{\Delta t} + \frac{P_{\ell-1/2}^{n+1} + q_{\ell-1/2}^{n+1/2} - P_{\ell-1/2}^n - q_{\ell-1/2}^{n-1/2}}{2} \cdot \frac{\Delta U}{\rho_0 \Delta x} \quad (13)$$

and

$$P_{\ell-1/2}^{n+1} = P(\epsilon_{\ell-1/2}^{n+1}, \rho_{\ell-1/2}^{n+1}) \quad (14)$$

(the equation of state).

The difference equation is the result of differencing

$$0 = \frac{\partial \epsilon}{\partial t} + (P+q) \frac{1}{\rho_0} \frac{\partial U}{\partial x}$$

which results from

$$0 = \frac{\partial \epsilon}{\partial t} + (P+q) \frac{\partial V}{\partial t} \text{ and } \frac{\partial V}{\partial t} = \frac{1}{\rho_0} \frac{\partial U}{\partial x}$$

PUFF's method of solution is this: Suppose that all quantities are known for superscript  $n$  or  $n-1/2$  (this is referred to as being at cycle  $n$ ); compute  $U_{\ell}^{n+1/2}$  for each  $\ell$  from (9), then compute  $X_{\ell}^{n+1}$  for each  $\ell$  from (1); next compute  $\rho_{\ell-1/2}^{n+1}$  for each  $\ell$  from (11), then compute  $q_{\ell-1/2}^{n+1/2}$  for each  $\ell$  from (12); next compute  $\epsilon_{\ell-1/2}^{n+1}$ ,  $P_{\ell-1/2}^{n+1}$  for each  $\ell$  by simultaneously solving (13) and (14). At this point, all variables have been advanced up to cycle  $n+1$ . Next, PUFF does its time-step computation to compute the next  $\Delta t$ . The time-step computation is based on a modification of the criterion developed by Courant, Friedrichs,



and Levy in their 1928 MATH. ANNALEN paper. The physical interpretation of this criterion is that the time step should be restricted so that a sound signal cannot travel across more than one zone in a time step. That is,  $C_{\ell}^n \Delta t^n \leq \Delta X_{\ell}^n$ , for all  $\ell$ , where  $C_{\ell}^n$  is the sound speed in the  $\ell$ th zone at cycle  $n$ ,  $\Delta t^n$  is the  $n$ th time step, and  $\Delta X_{\ell}^n$  is the width of the  $\ell$ th zone at cycle  $n$ .

Thus,  $\Delta t^n$  is usually defined as

$$\Delta t^n \equiv \theta \min_{\ell} \frac{\Delta X_{\ell}^n}{C_{\ell}^n}$$

where

$$0 < \theta \leq 1$$

$\theta$  is called the CFL number. PUFF uses a modification of this (see AFWL-TR-67-48). For more details about the CFL criterion, see Appendix II

## SECTION II

## DESCRIPTIONS, DERIVATIONS, AND DETAILS

To make this section easier to read, we include a discussion of the format used in presenting the hydrocode test problems. Seven hydrocode test problems are considered. The problems discussed in this report are labeled Sctp for Slab Code Test Problems. The "Slab" refers to the geometry, i.e., one-dimensional linear.

The labeling is further modified to indicate which problem, i.e., Sctp-I, Sctp-II, ..., Sctp-VII. The consideration of each problem is arranged in the following way:

n. HYDROCODE TEST PROBLEM Sctp-n

a. Description of Problem

Here we give a graphical and verbal description of the problem.

b. Derivation of Solution

Under this heading the exact mathematical solution is derived.

c. Application as a Test Problem

Now we get down to the numerous details and difficulties of applying the problem to a hydrocode, that is, how one inputs the initial and boundary values for various codes. The first division in variety of codes is whether the code is Eulerian or Lagrangian in its formulation of the hydrodynamics equations. Therefore, we introduce the following subdivisions.

(1) Eulerian Input

(a) Initial values

(b) Boundary values

(2) Lagrangian Input

(a) Initial values

(b) Boundary values

In the foregoing subdivisions we describe how the hydrocode test problems may be introduced into either an Eulerian or a Lagrangian hydrocode. That is, we give the specific processes for inputting the initial values and the boundary values.

Up to this point we have not specified any numbers for the initial pressures, densities, etc. These numbers are introduced in the following subdivision.

### (3) Numerical Values for SCTP-n

Here we give the initial and boundary value numbers which are used for both Eulerian and Lagrangian hydrocodes. Also, we give the resulting numbers which occur in the solution.

Next, we discuss what is to be expected from these problems when they are applied as hydrocode test problems. This is done under the heading

### (4) Comments on the Computer Solution

Under this heading we have two subdivisions:

#### (a) General comments

In this paragraph, we give a discussion of what can be said about the hydrocode test problems behavior in general. That is, how long the solution is as described without altering the boundary values, what mistakes a Lagrangian hydrocode will probably make, what errors an Eulerian hydrocode will probably commit, etc.

Lastly, as a final illustrative help to the reader who wishes to apply the hydrocode test problems, we present an application of the test problems. We apply the seven hydrocode test problems to the typical Lagrangian hydrocode PUFF (described in the introduction). This is done in the last heading:

#### (b) PUFF comments

Here we present the error graphs and error tables for PUFF to illustrate what we believe to be a reasonable way of describing the "distance" between the PUFF solutions and the exact solutions.

We did not illustrate the Eulerian input by applying the hydrocode test problems to an Eulerian code.

# 1. HYDROCODE TEST PROBLEM SCTP-I

## a. Description of Problem

This is the steady profile solution of a constant velocity piston compressing the fluid ahead of it. By steady profile solution it is meant that the fluid parameters from the piston face to the shock front are constant, and also to the right of the shock front the fluid parameters are constant. Therefore, the velocity of the piston and the velocity of the fluid between the piston and the shock front are the same.

Figure 1 attempts to explain the problem graphically.

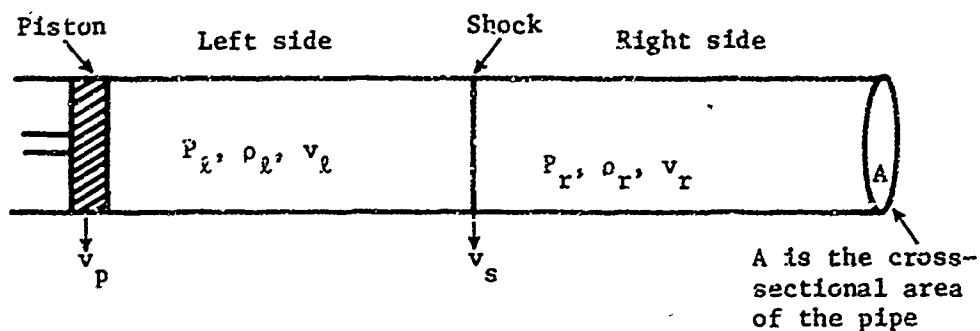


Figure 1a. Pipe Plot for Sctp-I

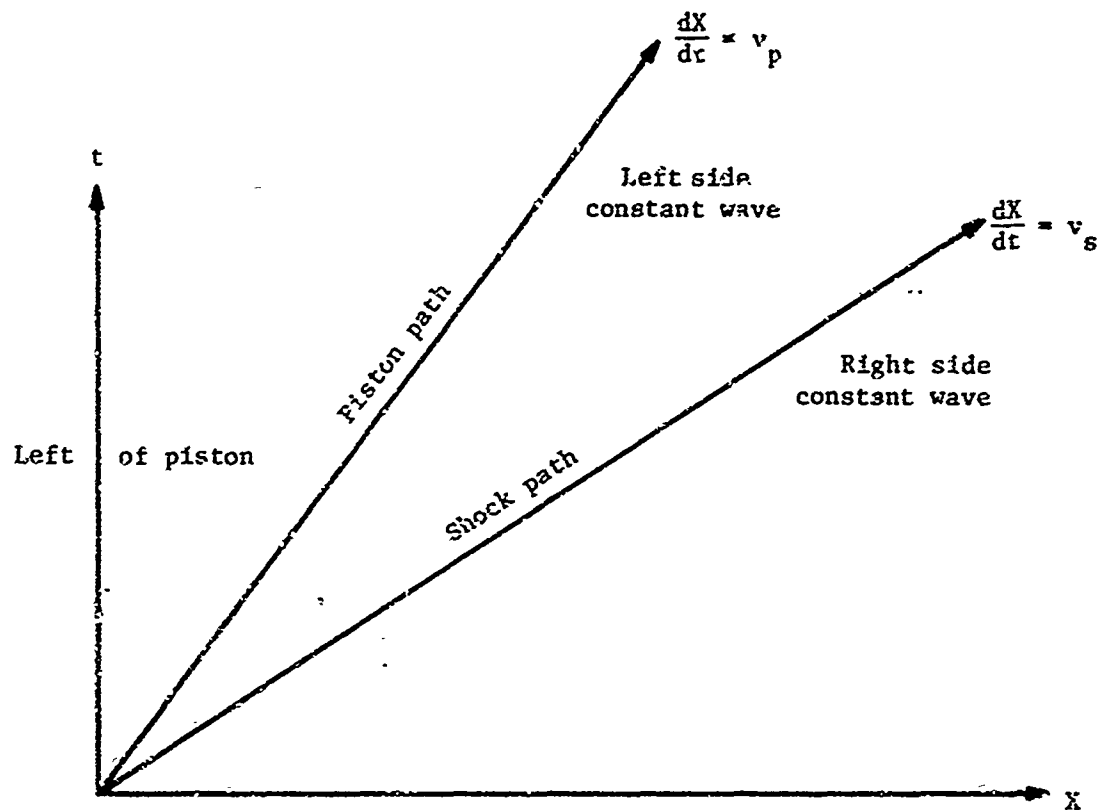


Figure 1b. Eulerian Wave Plot for SCTP-I

The variables used will be

- $A \equiv$  cross-sectional area of the pipe
- $C_L \equiv$  sound speed to the left of the shock
- $C_R \equiv$  sound speed to the right of the shock
- $P_L \equiv$  pressure to the left of the shock
- $P_R \equiv$  pressure to the right of the shock
- $\rho_L \equiv$  density to the left of the shock
- $\rho_R \equiv$  density to the right of the shock
- $V_L \equiv$  specific volume to the left of the shock
- $V_R \equiv$  specific volume to the right of the shock
- $v_L \equiv$  fluid velocity to the left of the shock
- $v_p \equiv$  piston velocity

$v_r \equiv$  fluid velocity to the right of the shock

$v_s \equiv$  shock velocity

b. Derivation of Solution

(1) Conservation of Mass or the Equation of Continuity

Looking from the right side of the shock wave, the mass engulfed in time  $\Delta t$  by the shock wave is

$$(v_s - v_r) \rho_r A \Delta t$$

Looking from the left side of the shock wave, the mass coming through the shock wave in time  $\Delta t$  is

$$(v_s - v_l) \rho_l A \Delta t$$

Let  $m$  be the mass per second per unit area passing through the shock. Then in time  $\Delta t$ , the mass  $m \Delta t$  will pass through the shock. Hence,

$$(v_s - v_l) \rho_l = m = (v_s - v_r) \rho_r \quad (1:CM)$$

So,

$$v_l = v_s - m/\rho_l \text{ and } v_r = v_s - m/\rho_r$$

Therefore,

$$v_l - v_r = m \left( \frac{1}{\rho_r} - \frac{1}{\rho_l} \right) = m (v_r - v_l)$$

(2) Newton's Second Law or the Equation of Motion or Conservation of Momentum Applied to Mass Passing through the Shock Wave

Suppose the mass  $m \Delta t$  passes through the shock wave in time  $\Delta t$ .

From  $F = d/dt (Mv)$  comes

$$F = \lim_{\Delta t \rightarrow 0} \frac{(m \Delta t) v_l - (m \Delta t) v_r}{\Delta t}$$

So,

$$F = mA(v_l - v_r)$$

Also,

$$F = (P_l - P_r)A$$

Therefore,

$$P_l - P_r = m(v_l - v_r) \quad (2: N2L)$$

### (3) Conservation of Energy or Energy Balance Equation

#### (a) Work done on a mass passing through shock wave

Recall that

$$W = \int \mathbf{F} \cdot d\mathbf{S}$$

The work done on the mass  $mA\Delta t$  entering the shock wave is  $(-P_r A)(v_r \Delta t)$ .

The work done on the mass  $mA\Delta t$  exiting the shock wave is  $(P_l A)(v_l \Delta t)$ .

Therefore, the work done on the mass  $mA\Delta t$  as it passes through the shock wave is

$$(P_l v_l - P_r v_r)A\Delta t$$

$\Delta W \equiv$  the work done on the mass  $mA\Delta t$  per area  $A$  per time  $\Delta t$ .

$$\Delta W = P_l v_l - P_r v_r$$

#### (b) Kinetic energy change in a mass passing through the shock wave

The change in kinetic energy of the mass  $mA\Delta t$  as it passes through the shock wave is  $1/2 mA\Delta t (v_l^2 - v_r^2)$ .

$\Delta K \equiv$  the change in kinetic energy of the mass  $mA\Delta t$  per area  $A$  per time  $\Delta t$ .

$$\Delta K = 1/2 m (v_l^2 - v_r^2)$$

(c) Internal energy change of a mass passing through the shock wave

The specific internal energy  $e$  is a function of the pressure and specific volume  $e = e(P, V)$ . So the internal energy of a gas with mass  $m\Delta t$  is  $(m\Delta t) e(P, V)$ .

$\Delta I \equiv$  the increase in the internal energy of the mass  $m\Delta t$  per area  $A$  per time  $\Delta t$  as it passes through the shock wave in time  $\Delta t$ .

$$\Delta I = m \left( e(P_l, V_l) - e(P_r, V_r) \right)$$

(d) Energy accounting

The increase in the mass  $m\Delta t$ 's internal energy plus the increase in its kinetic energy is equal to the work done on it. Symbolically,  $A\Delta t (\Delta I + \Delta K) = (\Delta W) A\Delta t$  or  $\Delta I + \Delta K = \Delta W$  or

$$m \left( e(P_l, V_l) - e(P_r, V_r) \right) + \frac{m}{2} (v_l^2 - v_r^2) = P_l v_l - P_r v_r \quad (3:CE)$$

(4) Equation of State

The equation of state used is that of the perfect or ideal gas model of standard air.

$$(\gamma-1) e = PV = RT \quad (4:EOS)$$

$\gamma \equiv$  the ratio of specific heats. It will be taken as 1.4 which is approximately the value for standard air

$e \equiv$  specific internal energy

$P \equiv$  pressure

$V \equiv$  specific volume

$R \equiv$  gas content

$T \equiv$  temperature



(5) The Rankine-Hugoniot Relation

By (2:N2L)

$$(P_\ell - P_r) (v_\ell + v_r) = m (v_\ell - v_r) (v_\ell + v_r)$$

so

$$\frac{m}{2} (v_\ell^2 - v_r^2) = (P_\ell - P_r) \left( \frac{v_\ell + v_r}{2} \right)$$

By (1:CM)

$$m = (v_\ell - v_r) / (v_r - v_\ell)$$

By (4:EOS)

$$e(P, V) = PV/(\gamma - 1)$$

Substituting these into (3:CE) yields

$$\frac{v_\ell - v_r}{v_\ell - v_r} (e_\ell - e_r) + (P_\ell - P_r) \left( \frac{v_\ell + v_r}{2} \right) = P_\ell v_\ell - P_r v_r$$

or

$$0 = e_\ell - e_r - \frac{P_\ell + P_r}{2} (v_\ell - v_r) \quad (5:RH)$$

(6) The Shock Speed Relations

Recall that by (1:CM)

$$(v_s - v_\ell) \rho_\ell = (v_s - v_r) \rho_r = m$$

By (2:N2L)

$$P_\ell - P_r = m (v_\ell - v_r)$$

By (3:CE)

$$\frac{m}{\gamma - 1} (P_\ell v_\ell - P_r v_r) + \frac{m}{2} (v_\ell^2 - v_r^2) = P_\ell v_\ell - P_r v_r$$

Eliminating  $m$ ,  $\rho_\ell$ ,  $V_\ell$ , and  $P_\ell$ , these equations yield

$$\frac{1}{\gamma-1} \left\{ P_r + (v_s - v_r) \rho_r (v_\ell - v_r) \right\} \frac{v_s - v_\ell}{v_s - v_r} v_r - P_r v_r + 1/2 (v_\ell^2 - v_r^2)$$

$$= \frac{\left\{ P_r + (v_s - v_r) \rho_r (v_\ell - v_r) \right\} v_\ell - P_r v_r}{(v_s - v_r) \rho_r}$$

This reduces to

$$v_s^2 - \left( \frac{1+\gamma}{2} v_\ell + \frac{3-\gamma}{2} v_r \right) v_s + \left( \frac{1+\gamma}{2} v_\ell + \frac{1-\gamma}{2} v_r \right) v_r - C_r^2 = 0$$

The solution to this is

$$v_s = \frac{1+\gamma}{4} v_\ell + \frac{3-\gamma}{4} v_r + \sqrt{\left( \frac{1+\gamma}{4} v_\ell + \frac{3-\gamma}{4} v_r \right)^2 + C_r^2} \quad (6:SS(v))$$

The plus sign is taken on the radical so that  $v_s > 0$ .

From (1:CM) and (2:N2L)

$$P_\ell - P_r = \rho_r (v_s - v_r) (v_\ell - v_r)$$

$$\frac{P_\ell - P_r}{\rho_r} = v_s v_\ell - v_s v_r - v_r v_\ell + v_r^2$$

Therefore,

$$\frac{-1+\gamma}{2} (v_s v_\ell - v_\ell v_r) = \frac{-1+\gamma}{2} \left( \frac{P_\ell - P_r}{\rho_r} + v_s v_r - v_r^2 \right)$$

Substituting this into the  $v_s$  quadratic yields

$$v_s^2 - \left(\frac{3-\gamma}{2} v_r\right) v_s - \frac{1+\gamma}{2} \left(\frac{P_\ell - P_r}{\rho_r} + v_s v_r - v_r^2\right) + \left(\frac{1-\gamma}{2}\right) v_r^2 - C_r^2 = 0$$

or

$$v_s^2 - 2v_r v_s + v_r^2 - \frac{1+\gamma}{2} \frac{P_\ell - P_r}{\rho_r} - C_r^2 = 0$$

So,

$$v_s = v_r + \sqrt{\frac{1+\gamma}{2} \frac{P_\ell - P_r}{\rho_r} + C_r^2}$$

So,

$$v_s = v_r + \sqrt{\frac{1}{\rho_r} \left( \frac{1+\gamma}{2} P_\ell + \frac{\gamma-1}{2} P_r \right)} \quad (7:SS(P))$$

By (5:RH)

$$P_\ell = \left( \frac{V_\ell}{\gamma-1} - \frac{V_r - V_\ell}{2} \right)^{-1} \left( \frac{P_r V_r}{\gamma-1} + \frac{P_r}{2} (V_r - V_\ell) \right)$$

Substituting this into (7:SS(P)) yields

$$v_s = v_r + \sqrt{\frac{2\gamma P_r V_r^2}{(\gamma+1) V_\ell - (\gamma-1) V_r}} \quad (8:SS(V))$$

Notice this requires that

$$(\gamma+1) v_\ell - (\gamma-1) v_r > 0$$

which requires that

$$\frac{\gamma+1}{\gamma-1} > \frac{\rho_\ell}{\rho_r}$$

Therefore, for  $\gamma = 1.4$ ,  $\rho_\ell/\rho_r < 6$  is required.

(7) Additional relations

Suppose the right side values are specified and

(a)  $v_\ell$  is specified

By (6:SS(v)),  $v_s$  is determined.

By (1:CM) and (2:N2L)

$$P_\ell = P_r + (v_s - v_r) \rho_r (v_\ell - v_r)$$

By (1:CM)

$$\rho_\ell = \frac{v_s - v_r}{v_s - v_\ell} \rho_r$$

(b)  $P_\ell$  is specified.

By (7:SS(P)),  $v_s$  is determined.

By (1:CM) and (2:N2L)

$$v_\ell = v_r \frac{P_\ell - P_r}{v_s - v_r} + v_r$$

By (1:CM)

$$\rho_\ell = \frac{v_s - v_r}{v_s - v_\ell} \rho_r$$

(c)  $v_\ell$  is specified.

Recall (8:SS(V)) is

$$v_s = v_r + \sqrt{\frac{2\gamma P_r V_r^2}{(\gamma+1) v_\ell - (\gamma-1) v_r}}$$

In order for the radical to be defined, it is required that

$$v_\ell < v_r \frac{\gamma-1}{\gamma+1}$$

If this restriction is satisfied, then  $v_s$  is determined.

By (1:CM)

$$v_\ell = v_s - v_\ell (v_s - v_r) \rho_r$$

By (2:N2L)

$$P_\ell = P_r + (v_s - v_r) \rho_r (v_\ell - v_r)$$

### c. Application as a Test Problem

#### (1) Eulerian Input

##### (a) Initial values

To the right of  $X_s$ , the initial shock position, define the velocity to be  $v_r = 0$ , the pressure to be  $P_r > 0$ , the density to be  $\rho_r > 0$ . From this,  $C_r^2 = \gamma P_r V_r$  is determined.

Let  $v_p = MC_r$  for some  $M > 0$ . Now the shock velocity is determined by (6:SS(v)),

$$v_s = C_r M \left( \frac{\gamma+1}{4} \right) \left( 1 + \sqrt{1 + \frac{4}{(\gamma+1) M}} \right)$$

For  $0 \leq X \leq X_s$ , the velocity is defined by  $v_\ell = v_p$ , the pressure is defined by  $P_\ell = P_r + v_s v_p \rho_r$ . (2:N2L) and (1:CM) defines the density  $\rho_\ell = v_s \rho_r / (v_s - v_p)$ .

(b) Boundary values

At  $X = 0$ , hold the velocity at  $v_\ell$ , the pressure at  $P_\ell$ , and the density at  $\rho_\ell$ . Notice that for an Eulerian code, this is as if the piston were always to the left of 0 and the computer solution were exact from the piston to 0.

(2) Lagrangian Input

(a) Initial values

The Lagrangian input is the same as the Eulerian input.

(b) Boundary values

The Lagrangian input is the same as the Eulerian input.

(Notice that the interpretation of the boundary value is much more satisfactory now because the piston is always at  $x = 0$ .)

(3) Numerical values for SCTP-I

(a) SCTP-I-A

$M = 1$ ,  $\Delta X = 1$  meter,  $X_s = 50$  meters

$P_r = 10^4$  dynes/cm<sup>2</sup>

$\rho_r = 10^{-5}$  gm/cm<sup>3</sup>

$v_r = 0$

Right boundary at 300 meters. These values yield

$v_\ell \approx 1.18 \times 10^5$  cm/sec

$v_s \approx 2.08 \times 10^5$  cm/sec

$P_\ell \approx 3.47 \times 10^4$  dynes/cm<sup>2</sup>

$\rho_\ell \approx 4.34 \times 10^5$  cm<sup>3</sup>/gm

A reasonable output recipe is to run the problem to 0.1 second with prints at 0.01 second intervals. The 300th zone should remain inactive so total energy sums will be taken out to there. With the CFL number set to 1, the first  $\Delta t$  will be about  $6.9 \times 10^{-4}$  sec. After the first time step, the time steps should all be about  $3 \times 10^{-4}$  sec. Therefore, it should take about 335 cycles for a CFL number of 1.

## (b) SCTP-I-B

Same as A except  $M = 100$ . This yields

$$v_l \approx 1.18 \times 10^7 \text{ cm/sec}$$

$$P_l \approx 1.68 \times 10^8 \text{ dynes/cm}^2$$

$$V_l \approx 1.67 \times 10^5 \text{ cm}^3/\text{gm}$$

$$C_l \approx 6.26 \times 10^6 \text{ cm/sec}$$

$$v_s \approx 1.42 \times 10^7 \text{ cm/sec}$$

A reasonable output recipe is to run the problem to  $10^{-3}$  sec with prints at  $10^{-4}$  sec. With a CFL number of 1, the first time step will be  $\approx 1.6 \times 10^{-5}$  sec. After the first time step, the time steps should run about  $2.7 \times 10^{-6}$  sec. Thus, it should take about 375 cycles to run to  $10^{-3}$  sec if the CFL number is 1. As in SCTP-I-A, the 300th zone should remain inactive so total energy sums will be taken from zone 1 to zone 300.

## (4) Comments on the Computer Solution

## (a) General comments

If the hydrocode is solving this problem correctly, the velocity of the shock will be about  $v_s$ . The quantities to the left of the shock should remain at  $v_l$ ,  $P_l$ ,  $\rho_l$ , and the quantities to the right should be  $v_r$ ,  $P_r$ ,  $\rho_r$ .

The shock front should remain sharp and not smeared over too many zones. The specific internal energy on the left should be  $P_l V_l / (\gamma - 1)$ ; on the right, it should be  $P_r V_r / (\gamma - 1)$ . The specific kinetic energy on the left should be  $1/2 v_l^2$ ; on the right, it should be  $1/2 v_r^2$ .

The specific total energy should be  $1/2 v_l^2 + P_l V_l / (\gamma - 1)$  on the left and  $P_r V_r / (\gamma - 1)$  on the right. To check conservation of total energy, sum  $\left( 1/2 v_I^2 + P_I V_I / (\gamma - 1) \right) M_I$ , where  $M_I$  is the mass of the  $I$ th zone, from the piston face to some fixed point on the right which remains undisturbed throughout the problem (zone 300 for SCTP-I-A or SCTP-I-B). This value should increase by  $P_l v_l t$ , where  $t$  is time, for a Lagrangian code. For a Eulerian code, take the above sum over  $I$  and subtract  $t v_l \left( 1/2 v_l^2 + P_l V_l / (\gamma - 1) \right) P_l$  because of the interpretation mentioned in (1)(b). After this is subtracted from the total energy sum, the remainder should increase by  $P_l v_l t$ . The reason for the time step sequence as mentioned in (3)(a) is that if the CFL number is

1, then for the first time step  $\Delta t_1 = \Delta X/C_2 \approx 6.9 \times 10^{-4}$ ; but after one of the zones on the right has been compressed, it should be about 43.4 cm long; then

$$\Delta t_2 \approx \frac{43.4 \text{ cm}}{C_2} \approx 3 \times 10^{-4} \text{ sec}$$

The shock speed is moving at about  $2 \times 10^5$  cm/sec, so in the first time step it moves about 140 cm, which will engulf the first zone to the right. After the first time step, the first zone on the right should be compressed to about 43.4 cm.

Care should be taken in determining the correct time and position of all quantities produced by the code being tested. For example, in PUFF, the velocities are one half time step behind in time and the Jth values of the pressures, densities, and internal energies are halfway between X(J-1) and X(J). Errors on the order of 5 or 10 percent can arise if these variables are not plotted at the right time and place. The energy partition is of interest because it indicates whether or not the energy dissipation rate associated with entropy increase across a shock is correct. In particular, if the code uses an artificial viscosity as a dissipation mechanism, the energy partition can indicate whether it introduces too much or too little dissipation.

#### (b) PUFF Comments

##### 1. SCTP-I-A

ACCURACY: Overall accuracy was on the order of 1 percent except for the region of the initial discontinuity zone and the zones where the shock transition occurs. That is, P, V, v, e, and the shock speed were all within about 1 percent except at zone 52 (zone directly in front of the initial discontinuity) where e and V were about 13 percent high and in the shock transition zones where the P, V, v, e take about six zones to change from within 1 percent of the left state to within 1 percent of the right state. To change from 10 percent of the left state to 10 percent of the right state takes about three zones. I believe that the e, V peak in zone 52 was caused by the conversion of kinetic to internal energy by the artificial viscosity which was intensified here by the sharp jump at the initial shock wave position. After the shock had been rounded off a bit, the artificial viscosity term reduced and remained uniform for the balance of the problem. This increase in internal energy combined with constant pressure produced a higher specific volume because the specific volume is proportional to the internal energy/pressure quotient.



Behind the shock, there is a little rarefaction dip in density and pressure which is traveling to the left. At early times this dip exceeds 1 percent but does not reach 2 percent, and at later times it fades away.

The above statements indicate that the Rankine-Hugoniot relations are being satisfied asymptotically. PUFF's total energy, total internal energy, and total kinetic energy errors (deviations from the exact solutions) are small as indicated in Table I, thus indicating approximate conservation of energy and correct energy partition. In particular, the Q (artificial viscosity) conversion of kinetic energy to internal energy was operating at about the correct rate.

TIME: PUFF took 1033 cycles, giving it an "effective CFL number" of  $335/1033 \approx 0.32$ . PUFF's rezon. capability was not utilized. PUFF took 72 seconds CDC 6600 central processor time to run 1033 cycles on this problem.

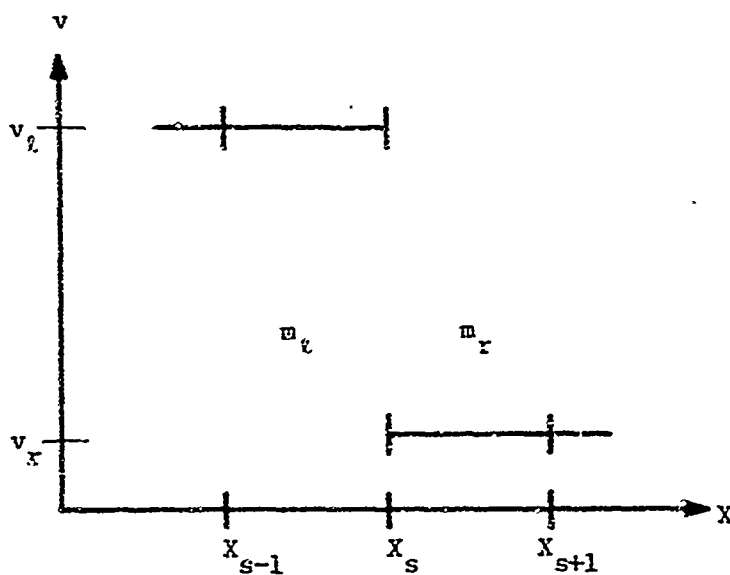
## 2. SCTP-I-B

ACCURACY: Again, the only distortions were associated with the initial discontinuity and the later shock positions. The internal energy peak in zone 52 was at about  $12.7 \times 10^{13}$  ergs/gm while it should have been about  $7.00 \times 10^{13}$  ergs/gm. The pressure was correct in zone 52 so there was a corresponding peak in the specific volume at zone 52. The rarefaction dip in the pressure and density which is seen at early times is less than 3 percent. By cycle 1495, this rarefaction dip is down to 1 percent or less. The shock transition is again about six zones for 1 percent of the left to 1 percent of the right and about three zones for 10 percent to 10 percent. Except for the above mentioned distortions, the PUFF solution to SCTP-I-B has at most about 1 percent error for all other zones. Again, the sum total energy, sum internal energy, and sum kinetic energies are close as indicated by Table I.

TIME: PUFF took 1463 cycles, giving an effective CFL number of  $375/1463 \approx 0.26$ . PUFF took 75 seconds CDC 6600 central processor time to run 1463 cycles on this problem.

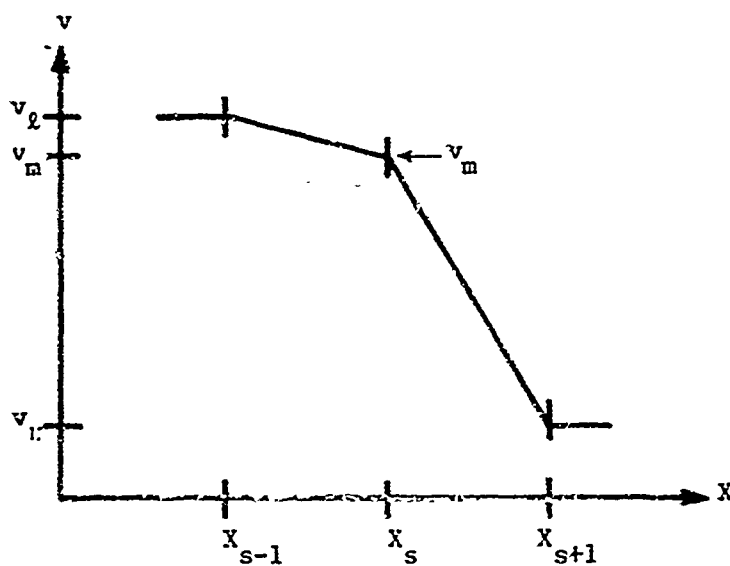
## 3. Discussion of the initial discontinuity

In inputting a discontinuous velocity profile into PUFF, there are several alternatives in selecting  $v_m$  (the value of the velocity at the discontinuity). Graphically, the exact picture is this:



where  $m_l$  is the mass in the zone to the left of the discontinuity and  $m_r$  is the mass of the zone to the right of the discontinuity.  $x_s$  is the position of the discontinuity,  $x_{s-1}$  is the adjacent zone boundary to the left, and  $x_{s+1}$  is the zone boundary to the right.

Since PUFF uses a linear interpolation on its velocities, the PUFF profile will look like this when a value  $v_m$  is given:



Some alternatives for  $v_m$ :

- (1) Set  $v_m$  to either  $v_l$  or  $v_r$ .
- (2) Minimize the maximum deviation of PUFF's velocity profile from the exact velocity profile. This leads to

$$v_m = \frac{v_l + v_r}{2}$$

- (3) Conserve the momentum of the exact profile. This yields

$$v_m = \frac{m_l v_l + m_r v_r}{m_l + m_r}$$

- (4) Conserve the energy of the exact profile. This yields

$$v_m = - \left( \frac{m_l v_l + m_r v_r}{m_l + m_r} \right) + \sqrt{ \left( \frac{m_l v_l + m_r v_r}{m_l + m_r} \right)^2 + 3 \left( \frac{m_l v_l^2 + m_r v_r^2}{m_l + m_r} \right)}$$

which, when  $v_r = 0$ , becomes

$$\left( -1 + \sqrt{1 + \frac{3m_r}{m_l}} \right) \frac{m_l v_l}{m_l + m_r}$$

Notice that if  $v_r = 0$ , the  $v_m$  of (4) is bigger than the  $v_m$  of (3) which in turn is bigger than the  $v_m$  of (2) when  $m_l < m_r$ . So we have, when  $v_r = 0$  and  $m_l < m_r$ ,

$$v_r < v_m^{(2)} < v_m^{(3)} < v_m^{(4)} < v_l$$

Now the internal energy spike increases as one increases the upper index of  $v_m^{(i)}$  (let  $v_m^{(1)} = v_r$  and  $v_m^{(5)} = v_l$ ), but the rarefaction dip and the associated hump leading it decrease. In all subsequent shock inputs in this report, we set  $v_m = v_l$ .

Table I-A\*

PUFF ERROR TABLE FOR SCTP-I-A WITH  $v_m = v_\ell$ 

Problem time = 0.1 sec

PUFF cycle = 1033

Computer time = 72 sec

Number of active zones = 267

	<u>Sum Sqr. Err.</u>	<u>Max. Err.</u>	<u>Position of Max. Err.</u>
Pressure	0.0251	+0.339	$X_s$
Velocity	0.0423	+0.583	$X_s$
Density	0.0229	+0.292	$X_s$

	<u>Sum Int. Energy</u>	<u>Sum Kin. Energy</u>	<u>Sum Tot. Energy</u>
EXACT	$1.324 \times 10^9$	$2.270 \times 10^8$	$1.551 \times 10^9$
PUFF	$1.324 \times 10^9$	$2.264 \times 10^8$	$1.550 \times 10^9$

Table I-B

PUFF ERROR TABLE FOR SCTP-I-B WITH  $v_m = v_\ell$ Problem time =  $1.0 \times 10^{-3}$  sec

PUFF cycle = 1463

Computer time = 75 sec

Number of active zones = 198

	<u>Sum Sqr. Err.</u>	<u>Max. Err.</u>	<u>Position of Max. Err.</u>
Pressure	0.0486	+0.644	$X_s$
Velocity	0.0764	+0.850	$X_s$
Density	0.0568	+0.577	$X_s$

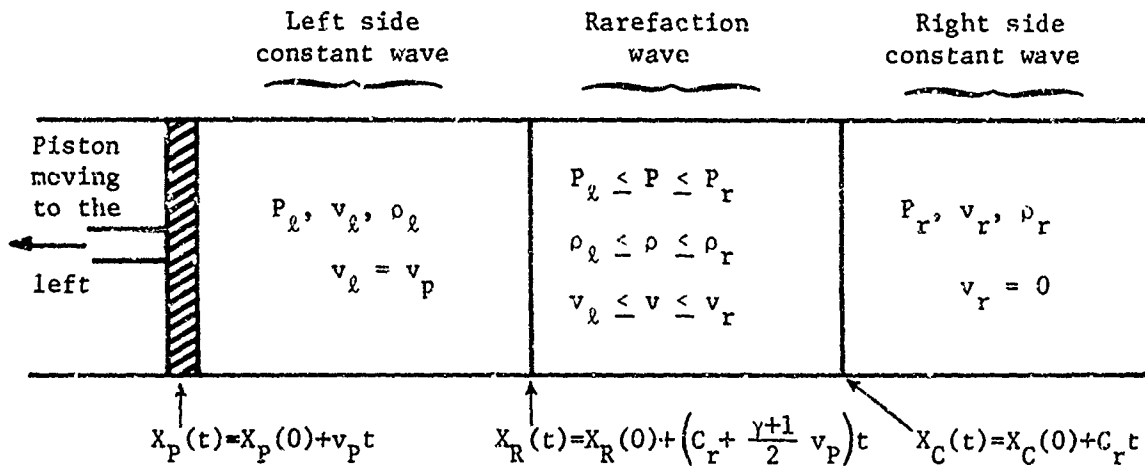
  

	<u>Sum Int. Energy</u>	<u>Sum Kin. Energy</u>	<u>Sum Tot. Energy</u>
EXACT	$3.095 \times 10^{12}$	$3.093 \times 10^{12}$	$6.188 \times 10^{12}$
PUFF	$3.098 \times 10^{12}$	$3.087 \times 10^{12}$	$6.185 \times 10^{12}$

\*See Appendix III for a discussion of the Error Tables.

2. HYDROCODE TEST PROBLEM SCTP-IIa. Description of Problem

In this problem, a piston moving with constant velocity  $v_p \ll 0$  to the left evacuates a pipe in which the gas was initially at rest. In so doing, a rarefaction wave moving to the right is formed. See figures 2a through 2d for a graphical description.



$X_p(t)$  moves to the left with velocity  $v_p < 0$ .

$X_R(t)$  may move right or left or be stationary depending upon whether its velocity  $C_r + \gamma+1/2 v_p$  is positive, negative, or zero.

$X_C(t)$  moves to the right with velocity  $C_r > 0$ .

Figure 2a. Pipe Plot for SCTP-II

b. Derivation of Equation

## (1) The Eulerian Equations

Consider the Eulerian formulation of a homentropic (see index for definition) hydrodynamic process for an ideal gas (see Appendix I for a derivation of the following equations):

Equation of continuity:

$$\rho_t + v\rho_x + \rho v_x = 0$$

Equation of motion:

$$v_t + v v_x + \frac{1}{\rho} P_x = 0$$

Equation of state:

$$(\gamma-1) e = PV$$

Since the process is homentropic,

$$P = P_o \left( \frac{\rho}{\rho_o} \right)^\gamma$$

and

$$C^2 \equiv \left. \frac{dP}{d\rho} \right|_S = \frac{dP}{d\rho}$$

So,

$$P_X = \frac{dP}{d\rho} \rho_X = C^2 \rho_X$$

Therefore, the equations form the homogeneous hyperbolic system:

$$\begin{pmatrix} \rho_t \\ v_t \end{pmatrix} + \begin{pmatrix} v & \rho \\ \frac{C^2}{\rho} & v \end{pmatrix} \begin{pmatrix} \rho_X \\ v_X \end{pmatrix} = \begin{pmatrix} 0 \\ 0 \end{pmatrix}$$

The method of characteristics will be used to derive the solution.

## (2) The Method of Characteristics

### (a) Canonical form

For convenience, introduce  $\sigma$  such that  $d\sigma = C d\rho/\rho$ . For

$$P = P_o \left( \frac{\rho}{\rho_o} \right)^\gamma$$

$\sigma = 2C/(\gamma-1) + \text{const.}$  So, define  $\sigma$  as  $2C/(\gamma-1)$ . Then

$$\begin{pmatrix} \sigma_t \\ v_t \end{pmatrix} + \begin{pmatrix} v & C \\ C & v \end{pmatrix} \begin{pmatrix} \sigma_X \\ v_X \end{pmatrix} = \begin{pmatrix} 0 \\ 0 \end{pmatrix}$$

Let  $v \equiv v + \sigma$ ,  $\omega \equiv v - \sigma$ . Then

$$\begin{pmatrix} v_t \\ \omega_t \end{pmatrix} + \begin{pmatrix} v + c & 0 \\ 0 & v - c \end{pmatrix} \begin{pmatrix} v_x \\ \omega_x \end{pmatrix} = \begin{pmatrix} 0 \\ 0 \end{pmatrix}$$

Notice that the matrix is now in characteristic form. That is, its characteristic values are on the diagonal and zeros are elsewhere.

(b) Characteristic curves

Consider the curves in the  $X, t$  plane which are solutions of the ordinary differential problems:

$$X^+(t_0^+) = X_0^+ \text{ and } \frac{dX^+}{dt} = v + c$$

or

$$X^-(t_0^-) = X_0^- \text{ and } \frac{dX^-}{dt} = v - c$$

Notice that

$$\frac{d}{dt} v(X^+(t), t) = v_x \frac{dX^+}{dt} + v_t = 0$$

and likewise,

$$\frac{d}{dt} \omega(X^-(t), t) = 0$$

$v$  and  $\omega$  are called Riemann invariants because  $v$  is constant on the curve  $(X^+(t), t)$  which is called a characteristic curve and likewise,  $\omega$  is constant on the characteristic curve  $(X^-(t), t)$ . Therefore,

$$v(X^+(t), t) = v(X_0^+, t_0^+)$$

and

$$\omega(X^-(t), t) = \omega(X_0^-, t_0^-)$$

Hence, if  $v(X_0, t_0)$ ,  $\sigma(X_0, t_0)$  are known for some  $(X_0, t_0)$  the values of  $v \pm \sigma$  are known at all points along the curve  $(X^\pm(t), t)$ . The initial and/or boundary data for the original partial differential problem can be used to determine values of  $v$  and  $\sigma$  at some  $(X_0, t_0)$ . That is, the initial data specifies

$v(X_0, t_0)$  and  $\sigma(X_0, t_0)$  for  $t_0 = 0$ . We repeat that the curves  $(X^+(t), t)$  and  $(X^-(t), t)$  are called characteristic curves. The family of curves in the  $(X, t)$  plane with slope  $v + C$  is designated  $C_+$  characteristics. Likewise, the family of curves in the  $(X, t)$  plane with slope  $v - C$  is designated  $C_-$  characteristics. Notice that on a  $C_+$  characteristic  $dv/d\rho = dv/d\rho + d\sigma/d\rho = 0$  and  $d\sigma/d\rho = C/\rho$  so  $dv/d\rho = -C/\rho$ . With this relation, we may define a mapping from  $C_+$  characteristics into curves in the  $(v, \rho)$  plane. Let the curve  $(X^+(t), t)$  with initial values  $(X_0, t_0)$  be mapped into the curve  $(v(\rho), \rho)$  with initial values  $(v_0, \rho_0)$  where  $v_0 = v(X_0, t_0)$ ,  $\rho_0 = \rho(X_0, t_0)$  and  $dv/d\rho = -C/\rho$ . This family of curves in the  $(v, \rho)$  plane is designated  $\Gamma_+$  characteristics (because they are the images of the  $C_+$  characteristics). Likewise, the family of curves in the  $(v, \rho)$  plane with slope  $C/\rho$  is designated  $\Gamma_-$  characteristics (because they are the images of the  $C_-$  characteristics).

The method of characteristics will now be applied to SCTP-II. Remember that SCTP-II can be interpreted as a piston withdrawing from a pipe containing a gas initially at rest. Let  $X_p(t)$  be the position of the piston at time  $t$ ,  $X_p(0) = 0$ . Let  $v_p$  be the velocity of the piston,  $v_p < 0$ . Now the information that the piston is being removed travels back into the undisturbed gas with the speed of sound of the resting gas,  $C_r$ . So, in the  $X, t$  plane a wave plot looks like figure 2b. First  $C(X_p(t), t)$ , the sound speed at the face of the piston, will be determined by the method of characteristics. Notice (in figure 2b) that the  $C_-$  characteristics have  $(X_0, t_0)$  in the undisturbed region (therefore,  $v(X_0, t_0)$  and  $\sigma(X_0, t_0)$  are known) and the  $C_-$  characteristics intersect the piston path line. The  $C_-$  characteristics will intersect the piston path line because a  $C_-$  characteristic will start out in the undisturbed region with slope  $-C_r$ ; then where the  $C_-$  characteristic enters the rarefaction wave, its slope  $v - C$  becomes more negative than the fluid velocity as long as  $C > 0$ .  $C$  will be positive if the piston is not withdrawn too fast for the gas to follow (that is, if no vacuum is formed between the gas and the piston). When no vacuum is formed, the gas will be in contact with the piston face and there it will have the velocity  $v_p$  of the piston. Therefore, the  $C_-$  characteristics intersect the piston path. Hence, if  $(X_0, t_0)$  is in the undisturbed region (e.g., if  $t_0 = 0$  and  $X_0 > 0$ ),  $v(X_0, t_0) = 0$ ,  $\sigma(X_0, t_0) = 2C_r/(\gamma-1)$ , and  $v(X_0, t_0) - \sigma(X_0, t_0) = v(X_p(t), t) - \sigma(X_p(t), t)$ . So,  $-2C_r/(\gamma-1) = v_p - 2C(X_p(t), t)/(\gamma-1)$ . Therefore,  $C(X_p(t), t) = \gamma-1/2 v_p + C_r$ .



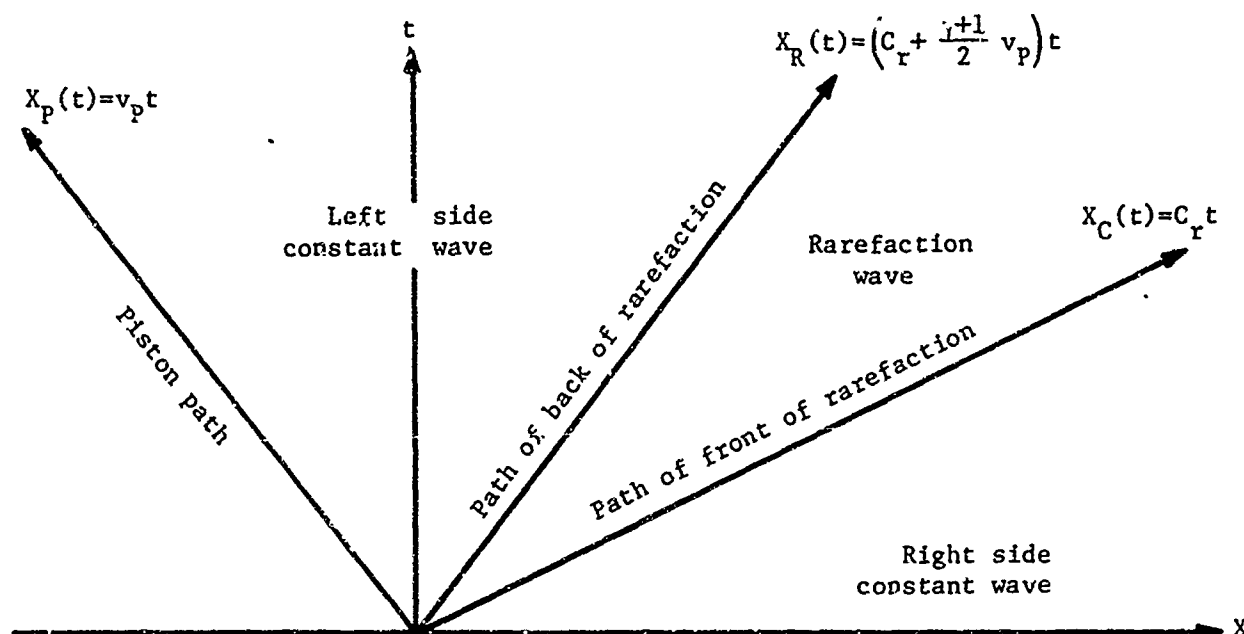


Figure 2b. Eulerian Wave Plot for SCTP-II

## (c) Simple waves

Note that  $v - \sigma$  is the same constant,  $-\sigma_r$ , for the entire rarefaction region. Such a region is called a  $C_-$  simple wave. Also, if  $v + \sigma$  is the same constant in a region, then the region is called a  $C_+$  simple wave. Since  $v - \sigma = -\sigma_r$  in this region,  $v = \sigma - \sigma_r$  so  $v$  depends only on  $\sigma$ . But  $\sigma$  depends only on  $C$  which depends only on  $\rho$ . Therefore,  $P$ ,  $v$ ,  $\sigma$ ,  $C$  depend only on  $\rho$ . Notice that if  $\sigma - \sigma_r$  is substituted for  $v$  in

$$\begin{pmatrix} \sigma_t \\ v_t \end{pmatrix} + \begin{pmatrix} v & C \\ C & v \end{pmatrix} \begin{pmatrix} \sigma_X \\ v_X \end{pmatrix} = \begin{pmatrix} 0 \\ 0 \end{pmatrix}$$

then the one equation  $\sigma_t + (\sigma - \sigma_r + C) \sigma_X = 0$  results. Since  $C = \gamma - 1/2 \sigma$ , this equation is of the form  $\sigma_t + (a\sigma + b) \sigma_X = 0$  where  $a$  and  $b$  are constants. The general solution to equations of this type may be expressed implicitly as  $\sigma(X, t) = F(X - (a\sigma(X, t) + b)t)$ .

So,

$$\sigma(X, t) = F\left(X - \left(\sigma - \sigma_r + C\right)t\right) = F\left(X - (v + C)t\right) = F\left(X - \left(\frac{\gamma+1}{2} \sigma - \sigma_r\right)t\right)$$

F can be determined by the condition at the piston face. For  $t < 0$ ,

$$\sigma(X_p(t), t) = \sigma_r = F(-C_r t)$$

Therefore, for  $\xi > 0$ ,

$$F(\xi) = \sigma_r$$

For  $t > 0$ ,

$$\sigma(X_p(t), t) = \sigma_p = \sigma_r + v_p = F(X_p(t) - (v_p + C_p)t)$$

If  $v_p$  is constant, then  $X_p(t) = v_p t$ , so  $\sigma_p = F(-C_p t)$ . Therefore, for  $\xi < 0$ ,  $F(\xi) = \sigma_r + v_p$ . Summarizing,

$$F(\xi) = \begin{cases} \sigma_r & \text{if } \xi > 0 \\ \sigma_r + v_p & \text{if } \xi < 0 \end{cases}$$

From  $t > 0$  and from the formula for  $F(\xi)$  where  $\xi = X - \left(\frac{\gamma+1}{2} \sigma - \sigma_r\right)t$ , it follows that

$$X > \left(\frac{\gamma+1}{2} \sigma - \sigma_r\right)t \iff X/t > C_r$$

and

$$X < \left(\frac{\gamma+1}{2} \sigma - \sigma_r\right)t \iff X/t < C_r + \frac{\gamma+1}{2} \cdot v_p$$

Therefore,

$$X = \left(\frac{\gamma+1}{2} \sigma - \sigma_r\right)t \iff$$

$$\left[X \neq \left(\frac{\gamma+1}{2} \sigma - \sigma_r\right)t\right] \wedge \left[X \neq \left(\frac{\gamma+1}{2} \sigma - \sigma_r\right)t\right] \iff C_r \leq X/t \leq C_r + \frac{\gamma+1}{2} v_p$$

Hence,

$$X/t < C_r + \frac{\gamma+1}{2} v_p \Rightarrow \sigma = \sigma_r + v_p$$

and

$$C_r + \frac{\gamma+1}{2} v_p \leq X/t \leq C_r \Rightarrow X/t + \sigma_r \frac{2}{\gamma+1} = \sigma$$

and

$$X/t > C_r \Rightarrow \sigma = \sigma_r$$

Thus  $\sigma(X,t)$  is completely defined. Now the relation between  $\sigma$  and  $\rho$  is one to one so  $\rho$  is completely defined. As mentioned previously,  $P$ ,  $v$ ,  $c$  are all functions of  $\rho$ , so  $P$ ,  $v$ ,  $c$  are completely defined. Notice that  $\sigma_p = \sigma_r + v_p$ ; therefore,  $\sigma_p$  will be positive if  $|v_p| < \sigma_r$ . Since  $\sigma_p = 2/(\gamma-1) C_p$ , for the piston not to leave the gas (i.e., no vacuum) it is required that  $|v_p| < C_r \frac{2}{\gamma-1}$ . In the left side constant wave, the fluid velocity is  $v_p$ . In the rarefaction wave, the fluid velocity goes linearly from  $v_p$  to 0. In the right side constant wave, the fluid velocity is zero. See figure 2c. Since there is a one-to-one relation between velocity and density, all variables may be written in terms of the velocity because by the equation of state  $P$  is a function of  $\rho$ .

$$X_p(t) = X_p(0) + v_p t$$

$$X_R(t) = X_F(0) + \left( C_r + \frac{\gamma+1}{2} v_p \right) t$$

$$X_C(t) = X_p(0) + C_r t$$

For

$$X_p(t) \leq X \leq X_R(t)$$

$$v(X,t) = v_p$$

For

$$X_R(t) \leq X \leq X_C(t)$$

$$v(X,t) = v_P \frac{X - X_C(t)}{X_R(t) - X_C(t)}$$

For

$$X > X_C(t)$$

$$v(x,t) = 0$$

Then

$$C(X,t) = C_r + \frac{\gamma-1}{2} v(X,t)$$

$$\rho(X,t) = \rho_r \left( 1 + \frac{\gamma-1}{2} \frac{v(X,t)}{C_r} \right)^{\frac{2}{\gamma-1}}$$

and

$$P(X,t) = P_r \left( 1 + \frac{\gamma-1}{2} \frac{v(X,t)}{C_r} \right)^{\frac{2\gamma}{\gamma-1}}$$

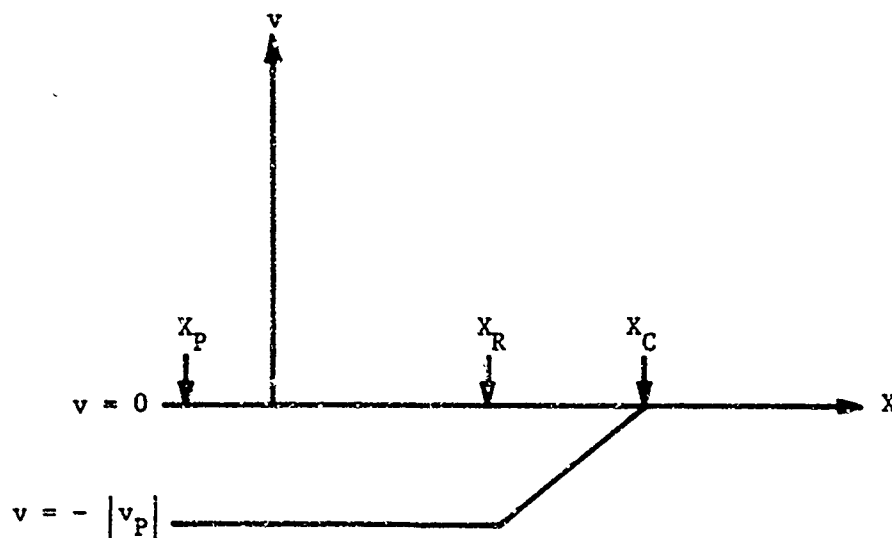


Figure 2c. Velocity Plot for SCTP-II

Or they could be written as

$$\rho(X,t) = \rho_r \left( \frac{C(X,t)}{C_r} \right)^{\frac{2}{\gamma-1}}$$

and

$$P(X,t) = P_r \left( \frac{C(X,t)}{C_r} \right)^{\frac{2\gamma}{\gamma-1}}$$

The total energy TE at time zero from the piston face at  $X_p(0)$  to a position  $X_Q$  far enough to the right so that it is quiet (at rest, stationary) throughout the problem time is

$$\left( X_Q - X_p(0) \right) \frac{P_r}{\gamma-1} \equiv TE(0)$$

The total energy from the piston face  $X_p(t)$  to  $X_Q$  at some later time  $t > 0$  is  $TE(t) = TE(0) + P_p v_p t$  where  $P_p$  is the pressure at the piston and  $v_p = -|v_p|$  is the velocity at the piston. The total kinetic energy TKE is initially zero ( $t = 0$ ). At later times,

$$(t > 0) \text{ TKE}(t) = \left( X_R(t) - X_p(t) \right) \frac{1}{2} \rho_p v_p^2 + \int_{X_R(t)}^{X_C(t)} \frac{1}{2} \rho(X) v^2(X) dX$$

$$\int_{X_R}^{X_C} dX \frac{1}{2} \rho(X) v^2 = \int_{v_p}^0 \rho(v) v^2 X'(v) dv$$

$$\rho(v) = \rho_r \left( 1 + \frac{\gamma-1}{2} \frac{v}{C_r} \right)^{\frac{2}{\gamma-1}}$$

and

$$\frac{2}{\gamma-1} = 5 \text{ if } \gamma = 1.4$$

$$X'(v) = \frac{X_C - X_R}{0 - v_P} = \frac{X_R - X_C}{v_P}$$

So the kinetic energy from  $X_R$  to  $X_C$  is

$$\begin{aligned} \frac{1}{2} \int_{v_P}^0 \rho_r \left( 1 + \frac{\gamma-1}{2} \frac{v}{C_r} \right)^5 v^2 \left( \frac{X_R - X_C}{v_P} \right) dv &= \frac{\rho_r (X_C - X_R)}{2} v_P^2 \left[ \frac{1}{3} + \frac{5B}{4} + \frac{10B^2}{5} \right. \\ &\quad \left. + \frac{10}{6} B^3 + \frac{5}{7} B^4 + \frac{B^5}{8} \right] \end{aligned}$$

where

$$B = \frac{\gamma-1}{2} \frac{v_P}{C_r}$$

Then the total internal energy is the total energy minus the total kinetic energy.

### c. Application as a Test Problem

#### (1) Eulerian Input

##### (a) Initial values

For  $0 < X \leq X_P(0)$

$$v = -|v_P|$$

$$P = P_r \left( 1 - \frac{\gamma-1}{2} \frac{|v_P|}{C_r} \right)^{\frac{2\gamma}{\gamma-1}}$$

$$\rho = \rho_r \left( 1 - \frac{\gamma-1}{2} \frac{|v_P|}{C_r} \right)^{\frac{2}{\gamma-1}}$$

For  $X > X_P(0)$

$$v = 0$$

$$P = P_r$$

$$\rho = \rho_r$$

(b) Boundary values

For  $X = 0$

$$v = -|v_p|$$

$$P = P_r \left( 1 - \frac{\gamma-1}{2} \frac{|v_p|}{C_r} \right)^{\frac{2\gamma}{\gamma-1}}$$

$$\rho = \rho_r \left( 1 - \frac{\gamma-1}{2} \frac{|v_p|}{C_r} \right)^{\frac{2}{\gamma-1}}$$

(2) Lagrangian input

(a) Initial values

For  $x > 0$

$$v = 0$$

$$P = P_r$$

$$\rho = \rho_r$$

(b) Boundary values

For  $x = 0$

$$v(0,t) = -|v_p|$$

$$X(0,t) = X(0,0) - |v_p|t$$

or, since  $X_p(t) \equiv X(0,t)$ , then

$$X_p(t) = X_p(0) - |v_p|t$$

(3) Numerical Values for SCTP-II

(a) SCTP-II-A

$$P_r = 10^4 \text{ dynes/cm}^2$$

$$\rho_r = 10^{-6} \text{ gm/cm}^3$$

$$C_r^2 = \gamma P_r V_r = 1.4 \times 10^{10} \text{ cm}^2/\text{sec}^2$$

$$|v_p| = C_r / (\gamma + 1)$$

$$\Delta X = 100 \text{ cm}$$

$$X_F(0) = 100 \text{ meters}$$

$$X_Q = 300 \text{ meters}$$

A reasonable output recipe is to run for 0.1 second and print every 0.01 second. This takes about 120 cycles for a CFL number of 1.

(b) SCTP-II-B

Same as A except  $|v_p| = 2C_r / (\gamma + 1)$

(c) SCTP-II-C

Same as A except  $|v_p| = 2C_r / (\gamma - 1)$

(d) SCTP-II-D

Same as A except  $|v_p| = 4C_r / (\gamma - 1)$

(e) SCTP-II-E

Same as A except free boundary condition on the left in place of withdrawing piston on the left.

(4) Comments on the Computer Solution

(a) General

If specific volume is used in a code instead of density, then it cannot solve those problems where vacuums occur (C, D, and E) because the specific volume becomes infinite. Whereas, if density is used, the vacuum condition is expressed by the density going to zero. Also, the Eulerian



formulation cannot give the correct answers because in the equation of motion the density (as a function of time) is used as a divisor. (In Lagrangian formulation it is the initial density which is used as a divisor.) The mathematical solution to C, D, and E is the same. However, it cannot be expected that the computer solutions will be the same. Notice that in C, the left boundary of the gas is forced to move at the correct escape velocity. In D, the left boundary of the gas is constrained to move too fast to the left. In E, the code is allowed to calculate what the escape velocity should be. Because the masses of the zones of the fluid do not go to zero at the left boundary, the escape velocity that the code computes will be too low. That is, in the mathematical solution, the fluid starts moving with the escape velocity instantly upon its release. For a nonzero mass of fluid to jump from zero velocity to a constant nonzero velocity requires an infinite force. The mathematical continuum model is not, however, predicting such a thing. The continuum model is requiring that an "infinitesimal mass" start moving with a constant velocity and is thus not requiring an infinite force. To state this precisely, let  $x_\ell$  be the label of the gas point, to the left of which is a vacuum, i.e.,  $X(x_\ell, t) = X_R(t)$ . Let  $x_r$  be the label of the gas point, which at time  $t$  is at the boundary of the undisturbed gas and the gas which has started moving toward the vacuum, i.e.,  $X(x_r, t) = X_C(t)$ . Let  $x_q$  be the label of some fixed gas point such that in the time interval of interest  $[0, T]$ ,  $T > 0$ , the gas point labeled  $x_q$  is quiet or undisturbed, i.e.,  $x_q > x_r$  for  $0 \leq t \leq T$  ( $x_r$  is a function of time), e.g., let  $X(x_q, t) = X_Q$ . Now the force on the left boundary of the gas at time zero is the negative (the force is directed to the left) of the initial pressure  $P$  of the gas times the cross-sectional area of the pipe (which is a unit area) and this is equal to the time rate of change of the momentum of the gas at time zero. Expressed symbolically, this is

$$-P = \lim_{\substack{t \rightarrow 0 \\ t > 0}} \frac{d}{dt} \int_{X(x_\ell, t)}^{X(x_q, t)} \hat{\rho}(X, t) \hat{v}(X, t) dx$$

where  $\hat{f}(X(x, t), t) \equiv f(x, t)$ , or by a change of variables in the integral, we have

$$-P = \lim_{\substack{t \rightarrow 0 \\ t > 0}} \frac{d}{dt} \int_{x_l}^{x_q} \rho(x, 0) v(x, t) dx$$

(This can be further reduced to

$$-P = \rho \lim_{\substack{t \rightarrow 0 \\ t > 0}} \frac{\int_0^{C_x t} v(x, t) dx}{t}$$

by defining  $x_l = 0$ .) So that, although the time derivative of  $v$  at  $x_l$  and time zero is not defined, the time derivative of the momentum is defined and finite. So in the mathematical continuum model, the jumping of the left hand boundary to a nonzero constant velocity at time zero does not require an infinite force. However, in the discrete model, the finite zoning produces a positive mass for the left boundary so that it cannot jump from a zero to a nonzero constant velocity by the application of a finite force. The finite force used in a code should be just the negative of the initial pressure at the left hand boundary. Then the acceleration of the left boundary is  $-P$  divided by the mass associated by the code with the left zone boundary (which, for example, in PUFF, is  $1/2$  the left zone mass). In C and D, there will be a couple of compensating errors influencing the total energy computation. An error that will tend to reduce the total energy is caused by the fact that the pressure at the left zone boundary  $P_p$  will not be zero; therefore, the work done on the gas at the left boundary,  $P_p v_p t$ , will be negative. This causes an internal energy decrease by the first law of thermodynamics. An error that will tend to increase the total kinetic energy and, therefore, the total energy is the numerical integration of the kinetic energy. The typical code's numerical integration of

$$1/2 \int_{x_I}^{x_{I+1}} \rho(x) v^2(x) dx$$

will yield too large a value for the kinetic energy because this will be approximated by something like

$$1/2 v^2(X_{I+1/2}) \int_{X_I}^{X_{I+1}} \rho(X) dX$$

where

$$X_{I+1/2} \text{ is } \frac{X_{I+1} + X_I}{2}$$

This approximation is too large because of the characteristics of the particular  $\rho$  and  $v$  encountered in this problem. This error affects both C and D. A further erroneous increase that arises in D is caused by the left boundary's overly high velocity. Thus, the kinetic energy of the left zone is erroneously increased; therefore, the errors affect the energy partition by erroneously increasing the kinetic and decreasing the internal energy. The total energy may either increase or decrease, depending on which error dominates. Also, the discrete models will not allow the density to go to zero at the piston face because the left zone started with a finite mass and is just being stretched out as the problem progresses. Other points of interest in the continuum solutions which should be approximated by the discrete solutions are these: In A,  $X_R(t)$  moves to the right with velocity  $C_r/2$ . In B,  $X_R(t)$  is stationary. In C, D, E,  $X_r(t)$  moves to the left with velocity  $-2C_r/(\gamma-1)$  and  $X_R(t)$  marks the boundary between vacuum and gas. The gas can just keep up with the piston in C, i.e.,  $X_p = X_R$ , and at the piston face, the values of the pressure and density are zero. In D, the piston leaves the gas behind with a vacuum between the piston at  $X_p$  and the gas front at  $X_R$ . The gas front can move into a vacuum with, at most, the velocity  $-2C_r/(\gamma-1)$ , which is known as the escape velocity. So, in C, D, E,  $X_R(t) = X_p(0) - 2C_r t/(\gamma-1)$ . The total energy from the piston to an undisturbed point  $X_Q$  on the right increases (or decreases) by  $P_p v_p t$  where  $P_p$  and  $v_p$  are the pressure and velocity at the piston face. In A, B,  $P_p > 0$ , but in C, D, E,  $P_p = 0$ , so in A, B, the total energy should decrease, but in C, D, E, it should remain constant from start to finish.

(b) PUFF comments

1. SCTP-II-A

The typical PUFF profiles in velocity, pressure, and density deviated from the exact solution in the manner described in figure 2d.

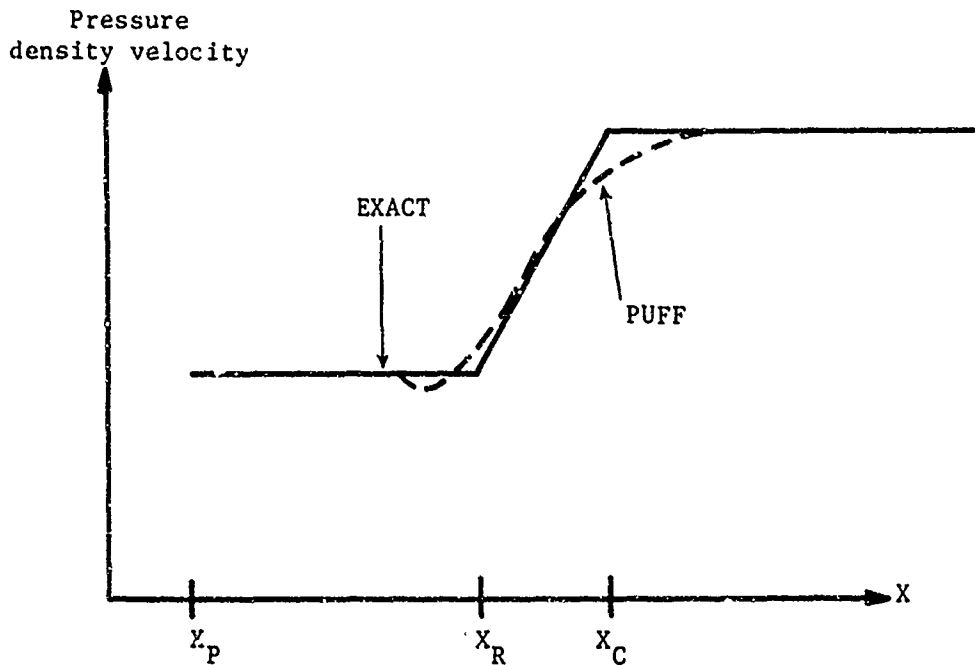


Figure 2d. PUFF SCT-II Error Graph

Reading figure 2d from right to left, we first see an underround at  $X_C$ , then an overround followed by an undershoot at  $X_R$ . At time 0.1 (170 PUFF cycles) second, the velocity deviations at the undershoot and the underround are both about 3 percent (the base for percentages was the piston velocity). If we take the initial pressure and density as bases for the percentage deviation in the pressure and density, respectively, then we get about 2 percent as the maximum error for the pressure and density. The total energy computations yielded the following:

$X_Q$  was chosen 200 meters to the right of  $X_P(0)$ . This yielded a total internal energy at time zero of  $5 \times 10^8$  ergs. Since the velocity and, therefore, the total energy is zero at time zero, the initial total energy is the same as the initial internal energy. After 170 cycles, PUFF reached the problem time 0.1 sec and the energy deviations are presented in table II-A. Refer to the energy numbers in table II-A. These numbers are  $\times 10^8$  ergs.

PUFF took 31 seconds central processor time on the CDC 6600 and 170 cycles to run this problem to the problem time of 0.1 second. With a CFL number of 1, it would have taken 120 cycles, so that PUFF's effective CFL is  $120/170 \sim 0.7$  on this problem.

2. SCTP-II-B

See figure 2d again for the typical PUFF profiles. The results on percentage underground and undershoot are about the same as in SCTP-II-A. The total energy computations yield the following:

$X_Q$  was again chosen 200 meters to the right of  $X_p(0)$ ; the initial total internal and total energy, therefore, are  $5 \times 10^8$  ergs. After 170 cycles, PUFF reaches the problem time 0.1 second and table II-B displays the energy deviations.

PUFF took 19 seconds CDC 6600 central processor time on this problem. Again, PUFF's effective CFL is  $120/170 \sim 0.7$  on this problem.

3. SCTP-II-C

See table II-C for the error numbers.

This took PUFF 170 cycles and 21 seconds CDC 6600 computer time to run to the problem time of 0.1 second. Thus, the effective CFL number is  $120/170 \sim 0.7$ .

4. SCTP-II-D

See table II-D for the error numbers.

This problem took PUFF 170 cycles and 30 seconds CDC 6600 computer time to run to the problem time of 0.1 second. The effective CFL number is  $120/170 \sim 0.7$ .

5. SCTP-II-E

As discussed earlier, the gas front at the free boundary of the gas in a finite difference solution will not move instantly with the escape velocity because the left zone has a nonzero mass. This causes a "truncation of the profile." That is, the graphs appear about the same, but they are not extended as far to the left as the exact solution. See table II-E for the error numbers.

PUFF took 170 cycles and 29 seconds CDC computer time to run to 0.1 second. Thus, effective CFL number is  $120/170 \sim 0.7$ .

Table II-A

## PUFF ERROR TABLE FOR SCTP-II-A

Problem time = 0.1 sec

PUFF cycle = 170

Computer time = 31 sec

Number of active zones = 134

	<u>Sum Sqr. Err.</u>	<u>Max. Err.</u>	<u>Position of Max. Err.</u>
Pressure	0.0032	-0.0136	$X_C$
Velocity	0.0076	+0.0248	$X_R$
Density	0.0025	-0.0097	$X_C$
	<u>Sum Int. Energy</u>	<u>Sum Kin. Energy</u>	<u>Sum Tot. Energy</u>
EXACT	$4.629 \times 10^8$	$1.027 \times 10^7$	$4.732 \times 10^8$
PUFF	$4.629 \times 10^8$	$1.025 \times 10^7$	$4.731 \times 10^8$

Table II-B

## PUFF ERROR TABLE FOR SCTP-II-B

Problem time = 0.1 sec

PUFF cycle = 170

Computer time = 19 sec

Number of active zones = 134

	<u>Sum Sqr. Err.</u>	<u>Max. Err.</u>	<u>Position of Max. Err.</u>
Pressure	0.0032	-0.0146	$X_C$
Velocity	0.0048	-0.0178	$X_R$
Density	0.0027	-0.0104	$X_C$
	<u>Sum Int. Energy</u>	<u>Sum Kin. Energy</u>	<u>Sum Tot. Energy</u>
EXACT	$4.432 \times 10^8$	$2.923 \times 10^7$	$4.725 \times 10^8$
PUFF	$4.431 \times 10^8$	$2.920 \times 10^7$	$4.723 \times 10^8$

Table II-C

## PUFF ERROR TABLE FOR SCTP-II-C

Problem time = 0.1 sec

PUFF cycle = 170

Computer time = 21 sec

Number of active zones = 135

	<u>Sum Sqr. Err.</u>	<u>Max. Err.</u>	<u>Position of Max. Err.</u>
Pressure	0.0036	-0.0157	$x_C$
Velocity	0.0006	-0.0022	$x_C$
Density	0.0027	-0.0112	$x_C$
	<u>Sum Int. Energy</u>	<u>Sum Kin. Energy</u>	<u>Sum Tot. Energy</u>
EXACT	$4.260 \times 10^8$	$7.395 \times 10^7$	$5.000 \times 10^8$
PUFF	$4.249 \times 10^8$	$8.045 \times 10^7$	$5.053 \times 10^8$

Table II-D

## PUFF ERROR TABLE FOR SCTP-II-D

Problem time 0.1 sec

PUFF cycle = 170

Computer time = 30 sec

Number of active zones = 135

	<u>Sum Sqr. Err.</u>	<u>Max. Err.</u>	<u>Position of Max. Err.</u>
Pressure	0.0038	-0.0158	$x_C$
Velocity	0.0007	-0.0023	$x_C$
Density	0.0028	-0.0113	$x_C$
	<u>Sum Int. Energy</u>	<u>Sum Kin. Energy</u>	<u>Sum Tot. Energy</u>
EXACT	$4.260 \times 10^8$	$7.395 \times 10^7$	$5.000 \times 10^8$
PUFF	$4.245 \times 10^8$	$9.919 \times 10^7$	$5.237 \times 10^8$

Table II-E

## PUFF ERROR TABLE FOR SCTP-II-E

Problem time = 0.1 sec

PUFF cycle = 170

Computer time = 29 sec

Number of active zones = 134

	<u>Sum Sqr. Err.</u>	<u>Max. Err.</u>	<u>Position of Max. Err.</u>
Pressure	0.0025	-0.0140	$x_C$
Velocity	0.0006	-0.0048	free boundary
Density	0.0019	-0.0100	$x_C$
	<u>Sum Int. Energy</u>	<u>Sum Kin. Energy</u>	<u>Sum Tot. Energy</u>
EXACT	$4.260 \times 10^8$	$7.395 \times 10^7$	$5.000 \times 10^8$
PUFF	$4.261 \times 10^8$	$7.374 \times 10^7$	$4.998 \times 10^8$



3. HYDROCODE TEST PROBLEM SCTP-IIIa. Description of Problem

In this problem, a piston proceeds with a constant acceleration into a gas initially at rest (by "gas initially at rest" is meant that the initial conditions are: velocity is zero; density, pressure and all other fluid parameters are constant). This forms what is called a compression wave. At time  $t_s = 2C_r/a(\gamma+1)$ , a shock wave is formed ( $t_s \equiv$  time of shock formation,  $C_r \equiv$  sound speed of the gas at rest,  $a \equiv$  acceleration of the piston). Until time  $t_s$ , the variables are continuous and the solution is easily found.\* Moreover, except for one point (the front of the compression wave), the variables are smooth prior to  $t_s$ . Figure 3 attempts a graphical representation and description of the problem. As shown in figure 3b, the compression wave front up to time  $t_s$  is  $X_c(t) = c_r t$ . After that time, the compression wave front is a shock, i.e., there is a discontinuity in pressure, density, velocity, etc.

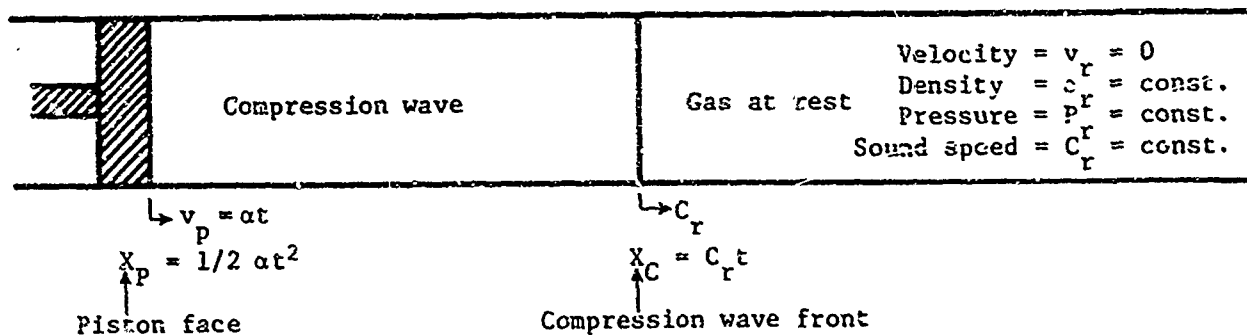


Figure 3a. Pipe Plot for SCTP-III

\*See K. O. Friedrichs' paper in 1948 C.P.A.M., page 211, for an investigation of the solution after shock formation.

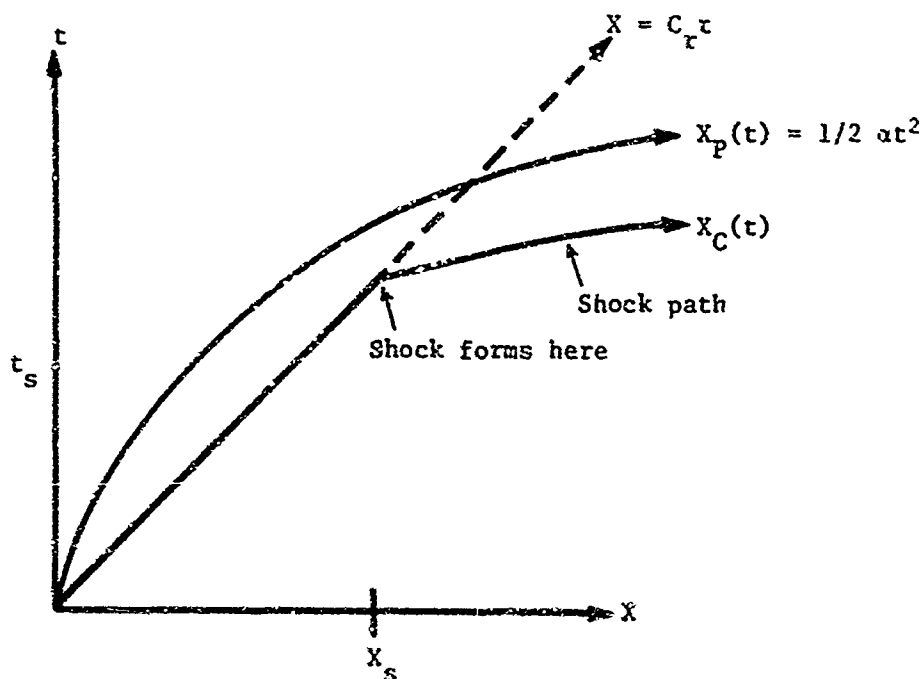


Figure 3b. Eulerian Wave Plot for SCTP-III

#### b. Derivation of Solution

We present here the solution for the preshock region. The preshock region is the set of all points  $(X, t)$  such that  $0 \leq t \leq t_s$ , i.e., the set of points in the  $X, t$  plane below the line  $t = t_s$  and above the line  $t = 0$ . This derivation depends on three key points. First key: there is a one-to-one relation between the density and the velocity and the pressure of the fluid. Second key: the values of the density, pressure, and velocity are known at the piston face. Third key: the density surface may be described in terms of its level lines in the  $X, t$  plane.

Now we will establish the first key. In the preshock region,  $v - \sigma = v_r - \sigma_r = -\sigma_r$ . This is because the  $\lambda_-$  characteristics ( $dx/dt = v - c$ ) extend from the  $t = 0$  line, where  $v = v_r = 0$  and  $\sigma = \sigma_r$ , into the preshock region, and, of course,  $v - \sigma$  is constant on  $\lambda_-$  characteristics. Therefore, the preshock region is a  $\lambda_-$  simple wave, i.e.,  $v - \sigma$  is the same constant in the entire region. And the part of the simple wave between  $X_p(t)$  and  $X_c(t)$  is a compression wave ( $X_p(t)$  is piston face position,  $X_c(t)$  is sound signal front). Now, for  $0 \leq t \leq t_s$ ,  $v(\rho) = \sigma(\rho) - \sigma_r$ ,  $\sigma(\rho) = 2c(\rho)/(\gamma - 1)$ ,  $c^2(\rho) = dP/d\rho(\rho)$ ,  $c(\rho) \geq 0$ ,  $P(\rho) = k\rho^\gamma$ ,  $k = P_r/\rho_r^\gamma$ . This establishes the one-to-one relations

mentioned in the first key point. Now we will establish the second key. The velocity at the piston is  $v_p = at$ . So,  $\sigma(\rho) = \sigma_r + at$  at the piston face. Then utilizing the relations between  $\sigma$  and  $c$  and  $P$  and  $\rho$ , the second key is established. So, at the point  $(X_p(t), t)$ , i.e., the piston face, we know the density, pressure, and velocity. By the first key, if we knew  $\rho(X, t)$  for all values of  $X$  and  $t$ , we would know the complete solution. By the second key, we know  $\rho(1/2 at^2, t)$ . The third key suggests that we represent the density surface in terms of its level lines. Therefore, we investigate the level lines of the density surface. That is, we will investigate the paths in the  $x, t$  plane on which the density is constant. To be precise, we should denote points on this path by  $(X(\rho_0; t), t)$  such that for  $0 \leq t \leq t_s$   $\rho(X(\rho_0; t), t) = \rho_0$ . That is,  $X$  is defined to be a function of two variables, density and time. Or, as some phrase it,  $X$  is a one-parameter (density) family of functions of one variable (time). Let us denote by  $(X_0, t_0)$  one point such that  $\rho(X_0, t_0) = \rho_0$ . So,  $\rho(X(\rho_0; t), t) = \rho(X_0, t_0) = \rho_0$  for  $0 \leq t \leq t_s$ . Now the level line representation procedure is composed of two parts. First part: for all numbers,  $\rho_0$ , in the range of the function  $\rho$ , find numbers  $X(\rho_0), t(\rho_0)$  such that  $\rho(X(\rho_0), t(\rho_0)) = \rho_0$ . Second part: on a level line,

$$0 = \frac{d\rho}{dt} = \rho_X \frac{dX}{dt} + \rho_t$$

so

$$\frac{dX}{dt} = - \left. \frac{\rho_t}{\rho_X} \right|_{\rho=\rho_0}$$

Therefore,

$$X = X_0 - \int_{t_0}^t \left( \left. \frac{\rho_t}{\rho_X} \right|_{\rho=\rho_0} \right) dt$$

Then let  $X_0 = X(\rho_0)$ ,  $t_0 = t(\rho_0)$ . Then we solve for  $\rho_0$  and this gives us  $\rho_0(X, t)$  which is the representation of the density surface we desire, i.e.,  $\rho_0(X, t) = \rho(X, t)$ . At this point, we know of two previous points which might bother the reader (we hope there are only two). First point: we have been saying "level line representation" and to be precise, perhaps we should have

said "level curve representation." We will prove that the level curves are lines. Second point:

$$\int_{t_0}^t \left( \frac{\rho_t}{\rho_X} \right)_{\rho=\rho_0} dt$$

is a bit vague perhaps, but it turns out that

$$\left( \frac{\rho_t}{\rho_X} \right)_{\rho=\rho_0} = \left( \frac{d(v\rho)}{d\rho} \right)_{\rho=\rho_0}$$

so that

$$- \int_{t_0}^t \left( \frac{\rho_t}{\rho_X} \right)_{\rho=\rho_0} dt = \left( \frac{d(v\rho)}{d\rho} \right)_{\rho=\rho_0} (t-t_0)$$

This last relation, by the way, proves the first point about the level curves being lines. Now we will establish that

$$- \frac{\rho_t}{\rho_X} \Big|_{\rho=\rho_0} = \frac{d(v\rho)}{d\rho} \Big|_{\rho=\rho_0}$$

In a smooth flow, conservation of mass is expressed by  $\rho_t + (\rho v)_X = 0$ . By the first key,  $v = v(\rho)$ , so

$$\rho_t + \frac{d(\rho v)}{d\rho} \rho_X = 0$$

Therefore,

$$- \frac{\rho_t}{\rho_X} = \frac{d(\rho v)}{d\rho}$$

AFWL-TR-67-127

Therefore,

$$-\left. \frac{\rho}{\rho_X} \right|_{\rho=\rho_0} = \left. \frac{d(\rho v)}{d\rho} \right|_{\rho=\rho_0}$$

and

$$\frac{dX}{dt} = \left. \frac{d(\rho v)}{d\rho} \right|_{\rho=\rho_0}$$

is the differential equation for the level line with density  $\rho_0$ . Hence,

$$X(\rho_0; t) = X_0 + \left[ \left. \frac{d(\rho v)}{d\rho} \right|_{\rho=\rho_0} \right] (t - t_0)$$

$$\frac{dv}{d\rho} = v + \rho \frac{dv}{d\rho}$$

and

$$\rho \frac{dv}{d\rho} = C \text{ by } v = \sigma - \sigma_r$$

$$\sigma = \frac{2C}{\gamma-1}$$

$$C^2 = \frac{dP}{d\rho}$$

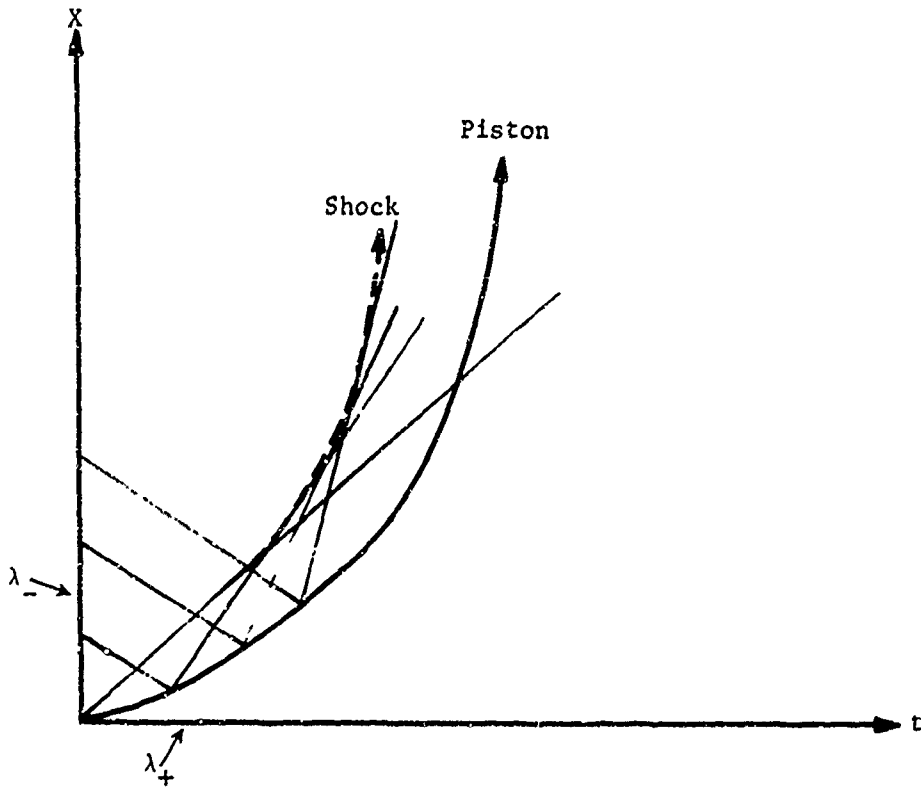
and

$$P = k\rho^\gamma$$

So,

$$\frac{dX}{dt} = \left. \frac{d(\rho v)}{d\rho} \right|_{\rho=\rho_0} = (v+C) \Big|_{\rho=\rho_0}$$

Therefore, the level lines are  $\lambda_+$  characteristics. Thus, in short summary, the density level curves are lines and also they are  $\lambda_+$  characteristics (figure 3c).



$\lambda_-$  characteristics have slope  $-C_r$ .

$\lambda_+$  characteristics have slope  $(\gamma+1)/2$  at  $+C_r$  at the point  $(1/2 at^2, t)$ .

Figure 3c. Characteristic Lines Plot

If the minimum intersection time of the  $\lambda_+$  characteristics is computed, it is found to be  $2C_r/a(\gamma+1)$ . A point where  $\lambda_+$  characteristics cross may indicate a discontinuity. This is because  $v + \sigma$  is a different constant on different  $\lambda_+$  characteristics. So, when two characteristics cross, the contradiction can sometimes be resolved by a discontinuity at the point. And, of course, the discontinuity is known as a shock. Now we have  $X(\rho; t)$  and the problem is to find  $\rho(X, t)$ ; so we must "invert" the relation

$$X = X_0 + \left( v(\rho_0) + C(\rho_0) \right) (t - t_0)$$

where

$$\rho_o = \rho(X_o, t_o)$$

By the second key,  $v$ ,  $\sigma$ ,  $C$ ,  $P$ ,  $\rho$  are known at the piston face. All values of the velocity that are taken on will be taken on at some time at the piston face. Therefore, by the first key, all values of  $\sigma$ ,  $C$ ,  $P$ ,  $\rho$  will be taken on at some time at the piston face. By the first key, if we know the velocity surface, we know the complete solution. It is computationally convenient to switch to the velocity as the function to determine first. By the first key, the density level lines are also velocity level lines. Thus, for any value of the velocity that is taken on in the preshock region, we can find an  $X_o, t_o$  on the piston path such that  $v(X_o, t_o) = v_o$ . Thus, we can produce the  $X(v_o), t(v_o)$  such that  $v(X(v_o), t(v_o)) = v_o$  which is required by the first part of the level curve representation procedure.

$$X = 1/2 a t_o^2 + \left( a t_o + C \left( 1/2 a t_o^2, t_o \right) \right) (t - t_o)$$

and

$$t_o = t(v_o) = \frac{v_o}{a}$$

Therefore,

$$X = 1/2 a \left( \frac{v_o}{a} \right)^2 + \left( v_o + C(v_o) \right) \left( t - \frac{v_o}{a} \right)$$

Solving for  $v_o$ , we get

$$v_o = v(X, t) = \frac{-\left(C_r - 1/2 (\gamma+1) a t\right) + \sqrt{\left(C_r - \frac{\gamma+1}{2} a t\right)^2 + 2a\gamma \left(C_r t - X\right)}}{\gamma}$$

for

$$X_p \leq X \leq C_r t$$

and

$$0 \leq t \leq t_s$$

Also,  $v(X,t) = 0$  for  $X > C_r t$  and  $0 \leq t \leq t_s$ . Then using the simple wave formulas:

$$C = C_r \left( 1 + \frac{\gamma-1}{2} \frac{v}{C_r} \right)$$

$$\rho = \rho_r \left( \frac{C}{C_r} \right)^{\frac{2}{\gamma-1}}$$

$$P = P_r \left( \frac{C}{C_r} \right)^{\frac{2\gamma}{\gamma-1}}$$

Notice that at time  $t_s = 2C_r/a(\gamma+1)$  and position  $X_s = C_r t_s$ , the

$$\lim_{X \rightarrow X_s} v_X(X, t_s) = -\infty$$

This indicates that a shock forms at  $(X_s, t_s)$ . Now we compute the total energy and energy partition. The total energy should increase according to the amount of work done on the gas by the piston, which is

$$\int_0^t P_p(\tau) v_p(\tau) d\tau = \int_0^t P_r \left( 1 + \frac{\gamma-1}{2} \frac{at}{C_r} \right)^{\frac{2\gamma}{\gamma-1}} a d\tau$$

Integrating by parts, this becomes

$$\begin{aligned} &= \frac{2C_r P_r}{3\gamma-1} \left( 1 + \frac{\gamma-1}{2} \frac{at}{C_r} \right)^{\frac{3\gamma-1}{\gamma-1}} t \\ &+ \frac{2C_r P_r}{a(3\gamma-1)(2\gamma-1)} \left[ 1 - \left( 1 + \frac{\gamma-1}{2} \frac{at}{C_r} \right)^{\frac{4\gamma-2}{\gamma-1}} \right] \end{aligned}$$



To get the energy partition, we have the choice of computing either the kinetic or the internal and subtracting from the total energy to get the other. We will compute the internal energy in the compression wave.

$$\text{Internal energy} = \int_{X_p}^{X_c} \rho e dX = \int_{X_p}^{X_c} \frac{P}{\gamma-1} dX$$

by the equation of state. Using the velocity level line equation which is a quadratic in the velocity, we get

$$dX = -\frac{1}{a} \left( c_r - \frac{\gamma+1}{2} at + \gamma v \right) dv$$

At  $X_p$ ,  $v = v_p = at$ . At  $X_c$ ,  $v = v_r = 0$ . Using these substitutions, we get

$$\text{Internal energy} = \frac{1}{a(\gamma-1)} \int_0^{at} P(v) (A + \gamma v) dv$$

where

$$A = c_r - \frac{\gamma+1}{2} at$$

Then, using the simple wave formula for  $P(v)$ , the integral is

$$\frac{1}{a(\gamma-1)} \int_0^{at} P_r \left( 1 + \frac{\gamma-1}{2} \frac{v}{c_r} \right)^{\frac{2\gamma}{\gamma-1}} (A + \gamma v) dv$$

and this can be integrated by parts.

$$\text{Internal energy} = \frac{P_r}{a(\gamma-1)} \left[ \frac{\left(1 + \frac{\gamma-1}{2} \frac{v}{c_r}\right)^{\frac{2\gamma}{\gamma-1} + 1}}{\left(\frac{2\gamma}{\gamma-1} + 1\right)} \left(\frac{2c_r}{\gamma-1}\right) (A+\gamma v) \right]_0^{\text{at}}$$

$$- \left[ \frac{\left(1 + \frac{\gamma-1}{2} \frac{v}{c_r}\right)^{\frac{2\gamma}{\gamma-1} + 2}}{\left(\frac{2\gamma}{\gamma-1} + 1\right) \left(\frac{2\gamma}{\gamma-1} + 2\right)} \left(\frac{2c_r}{\gamma-1}\right)^2 \gamma \right]_0^{\text{at}}$$

Finally, kinetic energy = total energy - internal energy. For computation purposes, it seems best to choose a point,  $X_Q$ , far enough to the right of the piston so that the fluid is quiet (at rest) at  $X_Q$  throughout the course of the problem. Then take the initial total energy, which will be

$$(X_Q - X_P(0)) \rho_r e_r = \frac{P_r}{\gamma-1} (X_Q - X_P(0))$$

and add the total energy increase,

$$\int_0^t P_P v_p d\tau$$

This gives the total energy from  $X_P$  to  $X_Q$ . Then the internal energy will be the internal energy in the compression wave, computed above, plus the internal energy from  $X_C$  to  $X_Q$ , which is

$$(X_Q - X_C) \cdot \rho_r \cdot e_r = (X_Q - X_C) \frac{P_r}{\gamma-1}$$

Finally, the kinetic energy from  $X_p$  to  $X_Q$  will be the total energy from  $X_p$  to  $X_Q$  minus the internal energy from  $X_p$  to  $X_Q$ . Note that the kinetic energy from  $X_C$  to  $X_Q$  is zero because the velocity is zero.

c. Application as a Test Problem

(1) Eulerian Input

(a) Initial values

$$P = P_r, \rho = \rho_r, v = v_r = 0$$

(b) Boundary values

$$\text{Let } X(I) = I\Delta X$$

Let GI be the greatest integer function:

$$I(t) = GI(1/2 at^2/\Delta X)$$

Then the left-hand boundary (piston face) will be zone I(t) and the boundary values there will be

$$\begin{aligned} \text{velocity} &= at \\ \text{pressure} &= P_r \left( 1 + \frac{\gamma-1}{2} \frac{at}{c_r} \right)^{\frac{2\gamma}{\gamma-1}} \end{aligned}$$

$$\text{density} = \rho_r \left( 1 + \frac{\gamma-1}{2} \frac{at}{c_r} \right)^{\frac{2}{\gamma-1}}$$

(2) Lagrangian Input

(a) Initial values

$$\text{pressure} = P$$

$$\text{density} = \rho_r$$

$$\text{velocity} = v_r = 0$$

(b) Boundary values

at  $x = 0$  (piston position)

$$X_p = 1/2 at^2 \text{ and } v_p = at$$

## (3) Numerical Values for SCTP-III

## (a) SCTP-III-A

$$P_r = 10^4 \text{ dynes/cm}^2$$

$$\rho_r = 10^{-6} \text{ gm/cm}^3$$

$$c_r^2 = \gamma P_r / \rho_r = 1.4 \times 10^{10} \text{ cm}^2/\text{sec}^2$$

$$a = c_r / 1 \text{ sec}$$

$$\Delta x = 10 \text{ meters}$$

Right boundary at 1500 meters

A reasonable recipe for output is as follows: Run for 1 sec (problem time not computer time) and print at 0.1 sec intervals and at time  $2/(\gamma+1)$  (when the shock forms). If the CFL number equals 1, this takes 218 cycles. This follows from

$$\Delta t^n = \min_I \frac{\Delta x_I^n}{c_I^n} = \frac{\Delta x_{\text{piston}}^n}{c_{\text{piston}}^n}$$

Then by conservation of mass,

$$\frac{\Delta X}{\Delta x} = \frac{\rho_r}{\rho}$$

So,

$$\Delta t^n = \frac{\Delta x}{c_r} \frac{1}{\left(\frac{\rho}{\rho_r}\right) \left(\frac{c}{c_r}\right)}$$

By the simple wave formulas

$$\frac{\rho}{\rho_r} = \left(\frac{c}{c_r}\right)^{\frac{2}{\gamma-1}}$$

and

$$\frac{c}{c_r} = 1 + \frac{\gamma-1}{2} \frac{at}{c_r}$$

Thus,

$$t^0 = 0$$

$$t^n = \sum_{i=1}^n \Delta t^i$$

and

$$\Delta t^n = \frac{\Delta x}{c_r} \frac{1}{\left(1 + \frac{\gamma-1}{2} \frac{at^{n-1}}{c_r}\right)^{\frac{\gamma+1}{\gamma-1}}}$$

Then solve the recursion relation for the smallest N such that  $t^N \geq 1$ .

#### (4) Comments on the Computer Solution

##### (a) General

The characteristics solution is valid until the  $\lambda_+$  characteristics cross at time  $t_s = 2c_r/a(\gamma+1)$  (shock formation time) at distance  $X_s = 2c_r/a(\gamma+1)$  (shock formation position) from the original position of the piston  $X_p(0)$ . At this time,  $t_s$ , the piston is traveling with velocity  $2c_r/(\gamma+1)$ . After time  $t_s$ , the characteristics solution method is not valid.\* For all time the total energy formula is correct. But the energy partition derivation depended on the characteristics solution method, so it is valid only up to shock formation time.

##### (b) PUFF comments

The boundary condition should be  $v_p = a(t-\Delta t/2)$ , not  $v_p = at$  because PUFF in the velocity, pressure, density profiles is the "compression overround" at  $X_c$  displayed in figure 3d.

---

\*See Friedrichs' 1948 C.P.A.M. paper mentioned in an earlier footnote for discussion of solution after shock.

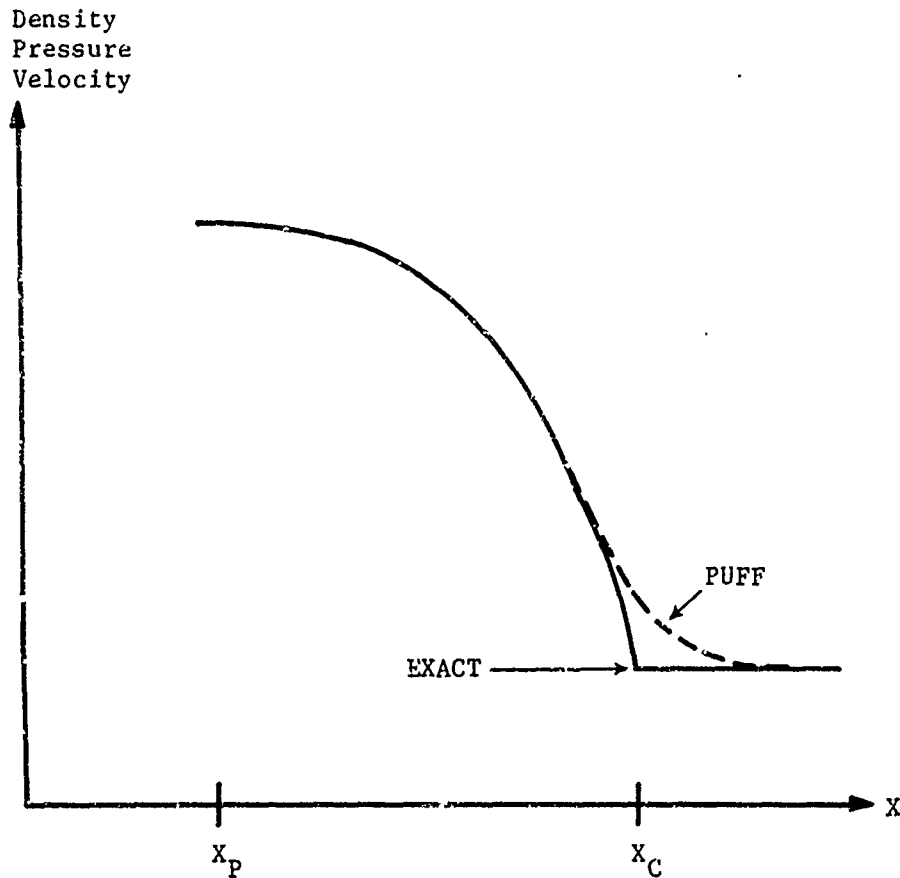


Figure 3d. PUFF SCTP-III Error Graph

1. SCTP-III-A

ACCURACY: See table III-A.

TIMING: PUFF took 245 cycles and 19 seconds CP time (CDC 6600) to run to 0.8333 second. Effective CFL number =  $218/324 \approx 0.68$  on run to 1.0 second.

2. SCTP-III-B

ACCURACY: See table III-B.

TIMING: PUFF took 245 cycles and 21 seconds CP time (CDC 6600) to run to 0.08333 second. Effective CFL number =  $218/324 \approx 0.68$  on run to 0.1 second.

Table III-A

## PUFF ERROR TABLE FOR SCTP-III-A

Problem time = 0.8333 sec

PUFF cycle = 245

Computer time = 19 sec

Number of active zones = 19

	<u>Sum Sqr. Err.</u>	<u>Max. Err.</u>	<u>Position of Max. Err.</u>
Pressure	0.0057	0.0426	$X_C$
Velocity	0.0125	0.0909	$X_C$
Density	0.0053	0.0407	$X_C$
	<u>Sum Int. Energy</u>	<u>Sum Kin. Energy</u>	<u>Sum Tot. Energy</u>
EXACT	$4.36800 \times 10^9$	$2.62864 \times 10^8$	$4.63087 \times 10^9$
PUFF	$4.37190 \times 10^9$	$2.64055 \times 10^8$	$4.63595 \times 10^9$

Table III-B

## PUFF ERROR TABLE FOR SCTP-III-B

Problem time = 0.08333 sec

PUFF cycle = 245

Computer time = 21 sec

Number of active zones = 119

	<u>Sum Sqr. Err.</u>	<u>Max. Err.</u>	<u>Position of Max. Err.</u>
Pressure	0.0057	0.0426	$X_C$
Velocity	0.0125	0.0909	$X_C$
Density	0.0053	0.0407	$X_C$
	<u>Sum Int. Energy</u>	<u>Sum Kin. Energy</u>	<u>Sum Tot. Energy</u>
EXACT	$4.36800 \times 10^8$	$2.62864 \times 10^7$	$4.63087 \times 10^8$
PUFF	$4.37190 \times 10^8$	$2.64055 \times 10^7$	$4.63595 \times 10^8$

#### 4. HYDROCODE TEST PROBLEM SCTP-IV

##### a. Description of Problem

In this problem, a piston has a constant acceleration out of a gas at rest. Eventually, the piston velocity exceeds the speed with which the gas can move into a vacuum. This speed is  $2c_r/(\gamma-1)$  and when the piston exceeds it, a vacuum occurs. Figure 4 presents a graphical explanation.

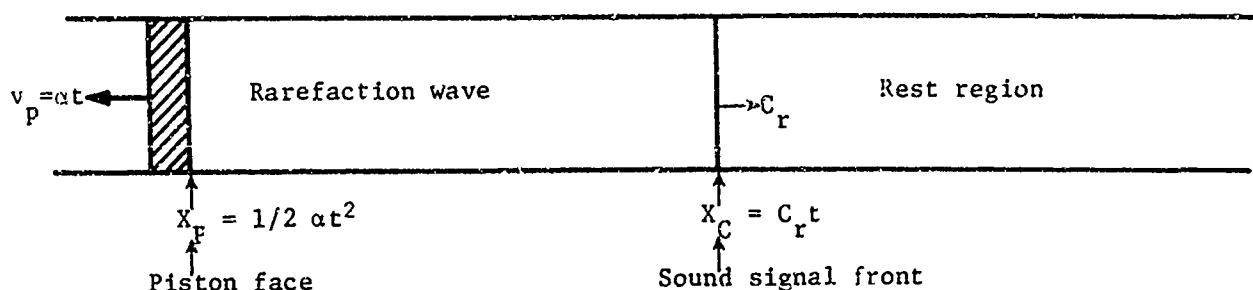


Figure 4a. Pipe Plot for SCTP-IV

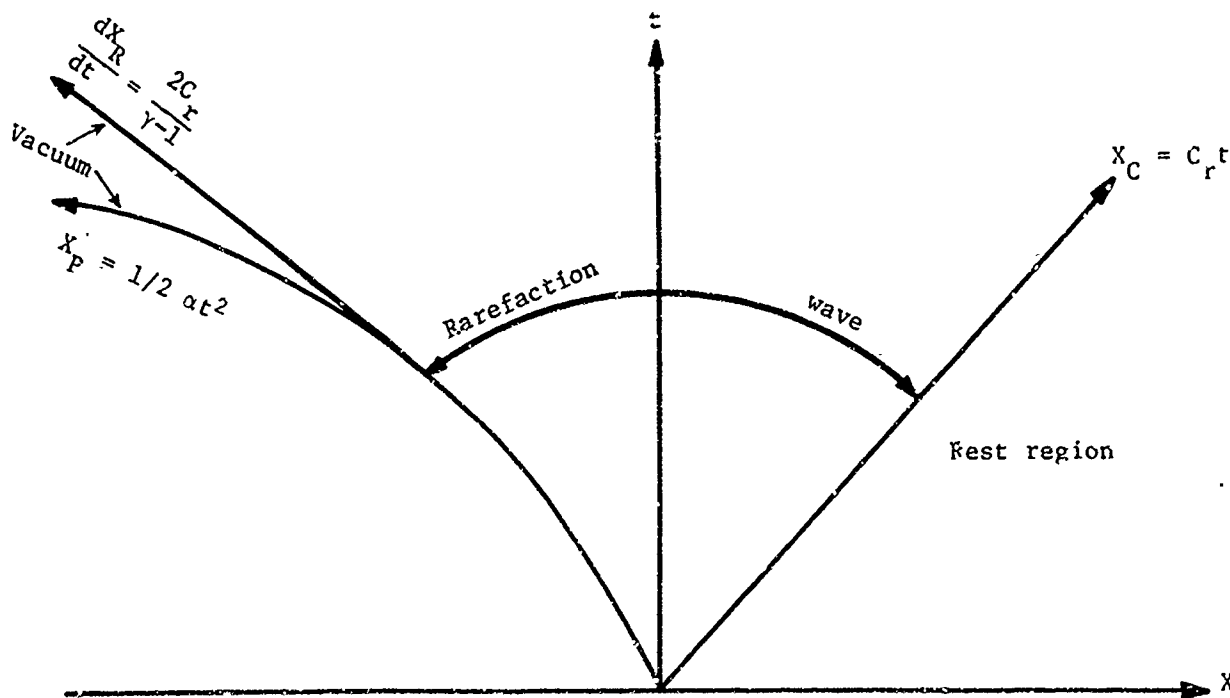


Figure 4b. Wave Plot for SCTP-IV



b. Derivation of Solution

The analysis is the same as for SCTP-III.

$$v(X,t) = \frac{-\left(c_r - \frac{\gamma+1}{2} at\right) + \sqrt{\left(c_r - \frac{\gamma+1}{2} at\right)^2 + 2a\gamma(c_r t - X)}}{\gamma}$$

for  $at^2/2 \leq X \leq c_r t$ .  $v(X,t) = 0$  for  $X \geq c_r t$ . For

$$|v| \leq \frac{2c_r}{\gamma-1}$$

$$c = c_r + \frac{\gamma-1}{2} v$$

$$P = P_r \left(\frac{c}{c_r}\right)^{\frac{2\gamma}{\gamma-1}}$$

$$\rho = \rho_r \left(\frac{c}{c_r}\right)^{\frac{2}{\gamma-1}}$$

For

$$|v| > \frac{2c_r}{\gamma-1}$$

there is a vacuum; therefore,  $0 = P = \rho = c$  from  $X_p(t)$  to

$$X_p(t_v) - \frac{2c_r}{\gamma-1} (t-t_v)$$

$t_v$  is the time the vacuum is formed,

$$|a| t_v = \frac{2c_r}{\gamma-1}$$

The energy decrease is the amount of work done on the piston by the gas which is

$$\int_0^t P_p(t) v_p(t) dt = \frac{2c_r P_r}{3\gamma-1} \left( 1 + \frac{\gamma-1}{2} \frac{at}{c_r} \right)^{\frac{3\gamma-1}{\gamma-1}} t$$

$$+ \frac{2c_r^2 P_r}{a(3\gamma-1)(2\gamma-1)} \left( 1 - \left( 1 + \frac{\gamma-1}{2} \frac{at}{c_r} \right)^{\frac{4\gamma-2}{\gamma-1}} \right)$$

until time

$$t_v = \frac{2c_r}{|a|(\gamma-1)}$$

at which time

$$\int_0^{t_v} P_p(t) v_p(t) dt = \frac{2c_r^2 P_r}{a(3\gamma-1)(2\gamma-1)}$$

The energy partition is also computed exactly like SCTP-III.

c. Application as a Test Problem

(1) Eulerian Input

(a) Initial values

$$P = P_r, \rho = \rho_r, v = v_r = 0$$

(b) Boundary values

$$\text{Let } X(I) = \Delta X \cdot I$$

$$I(t) = GI - 1/2 |a| t^2 / \Delta X$$

$I(t)$  will be the piston face zone and at the piston face

$$v = -|a|t$$

$$P = P \left( \frac{-|a|t^2}{2}, t \right)$$

$$\rho = \rho \left( \frac{-|a|t^2}{2}, t \right)$$

(2) Lagrangian Input

(a) Initial values

$$P = P_r, \rho = \rho_r, v = v_r = 0$$

(b) Boundary values

At  $x = 0$ ,

$$x = -1/2|a|t^2, v = -|a|t$$

(3) Numerical Values for SCTP-IV

(a) SCTP-IV-A

$$P_r = 10^4 \text{ dynes/cm}^2$$

$$\rho_r = 10^{-6} \text{ gm/cm}^3$$

$$c_r^2 = \gamma P_r v_r = 1.4 \times 10^{10} \text{ cm}^2/\text{sec}^2$$

$$a = -c_r/1 \text{ sec}$$

$$\Delta x = 1 \text{ meter}$$

Right boundary at 150 meters.

A reasonable output recipe is to run for 10 seconds with prints at 1, 4, 5, 6, and 10 seconds.

(b) SCTP-IV-B

Same as A but  $a = -10 c_r/1 \text{ second}$  and print at 0.1, 0.4, 0.5, 0.6, and 1.0 second.

(4) Comments on the Computer Solution

(a) General comments

After time

$$t_v = \frac{2c_r}{|a|(\gamma-1)}$$

there is a vacuum between the piston and the gas at

$$1/2 at_v^2 + \frac{2c_r}{\gamma-1} (t-t_v)$$

the pressure and density are zero for  $t \geq t_v$ . From the left edge of the gas at

$$1/2 at_v^2 + \frac{2c_r}{\gamma-1} (t-t_v)$$

the same formulas hold as before  $t_v$ . If the hydrocode uses specific volume as a variable instead of density, there will be an overflow when the density goes to zero. The total energy should decrease until the vacuum is formed, but after  $t_v$ , the total energy should not change. The energy decrease is the work done at the piston

$$\int_0^t P_p(t) v_p(t) dt$$

This was computed in the derivation of solution. A Lagrangian code with zone center pressures will not compute the energy decrease correctly because the piston face zone will never have zero pressure. The energy partition should also be checked against the EXACT solution as computed in the derivation of solution. For further comments, look back to the comments in SCTP-II.

(b) PUFF comments

As previously observed, it is impossible for PUFF to conserve energy on this problem. The worst behaving variable is the nonprimary\* variable, momentum; the reason this is off so much is because its computation involves

---

\*Primary and nonprimary variables are defined in Appendix III, Error Functions and Error Formats.

the mixing of a zone center quantity (density) and a zone boundary quantity (velocity), thus introducing interpolation errors which cannot be ascribed to PUFF. PUFF's primary\* variables are quite near the EXACT solution. See figure 4c and tables IV-A and IV-B for accuracy.

TIMING: PUFF took 25 seconds CDC 6600 CP time and 169 cycles to run to 10.0 seconds on SCTP-IV-A. On SCTP-IV-B, PUFF took 16 seconds CDC 6600 CP time and 19 cycles to run to 1.0 second.

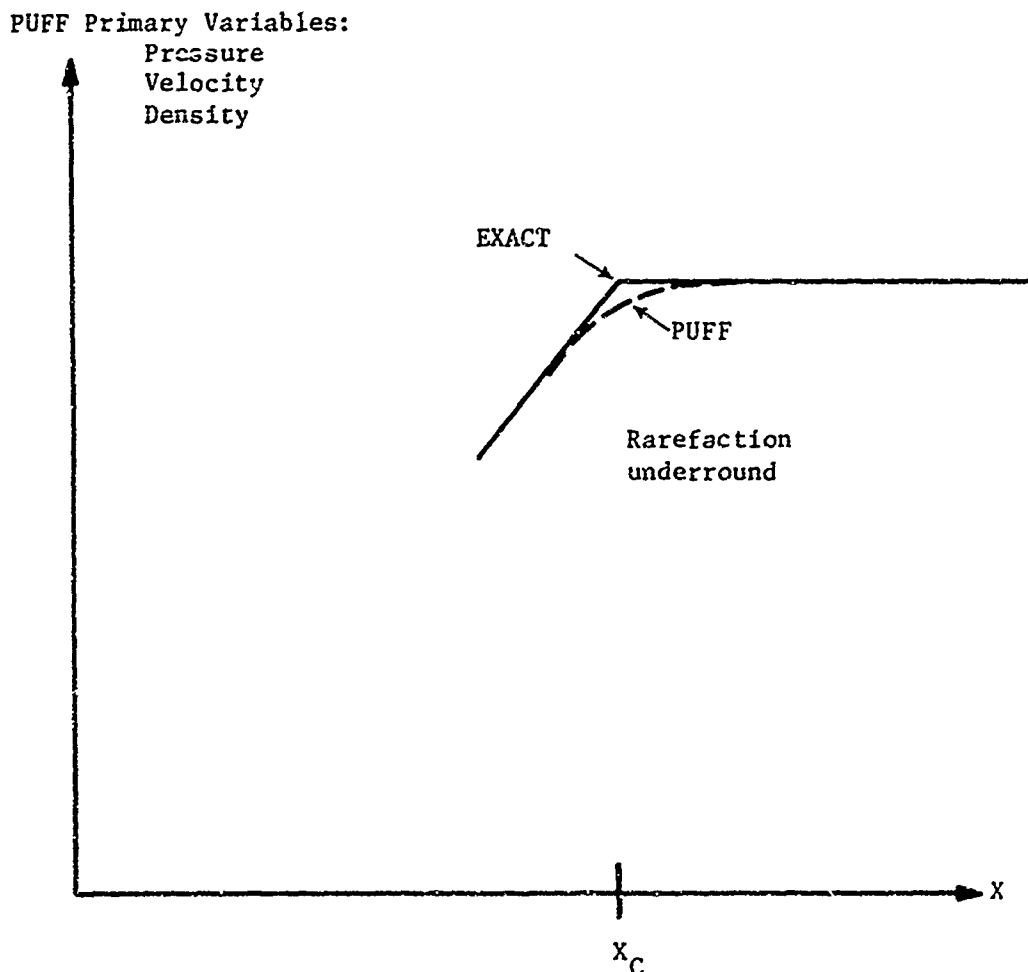


Figure 4c. PUFF SCTP-IV Error Graph

\*See Appendix III for definition of primary variables.

Table IV-A

## PUFF ERROR TABLE FOR SCTP-IV-A

Problem time = 10 sec

PUFF cycle = 169

Computer time = 25 sec

Number of active zones = 134

	<u>Sum Sqr. Err.</u>	<u>Max. Err.</u>	<u>Position of Max. Err.</u>
Pressure	0.0017	-0.0099	$x_C$
Velocity	0.0004	-0.0038	$x_P$
Density	0.0013	-0.0071	$x_C$

	<u>Sum Int. Energy</u>	<u>Sum Kin. Energy</u>	<u>Sum Tot. Energy</u>
EXACT	$3.09266 \times 10^{10}$	$6.98426 \times 10^9$	$3.79108 \times 10^{10}$
PUFF	$3.04551 \times 10^{10}$	$8.92017 \times 10^9$	$3.93752 \times 10^{10}$

Table IV-B

## PUFF ERROR TABLE FOR SCTP-IV-B

Problem time = 1 sec

PUFF cycle = 19

Computer time = 16 sec

Number of active zones = 21

	<u>Sum Sqr. Err</u>	<u>Max. Err.</u>	<u>Position of Max. Err.</u>
Pressure	0.0166	-0.0492	$x_C$
Velocity	0.0018	-0.0042	$x_C$
Density	0.0132	-0.0358	$x_C$

	<u>Sum Int. Energy</u>	<u>Sum Kin. Energy</u>	<u>Sum Tot. Energy</u>
EXACT	$3.684 \times 10^{10}$	$6.984 \times 10^8$	$3.754 \times 10^{10}$
PUFF	$3.671 \times 10^{10}$	$2.844 \times 10^8$	$3.956 \times 10^{10}$

5. HYDROCODE TEST PROBLEM SCTP-Va. Description of Problem

This is called the shock tube problem. It is an example of the more general Riemann problem. The Riemann problem is that of determining the flow after the conjunction of two states, left state and right state, with  $P_l, \rho_l, v_l$  the constant values of the left state and  $P_r, \rho_r, v_r$  the constant values of the right state. In the shock tube problem,  $v_r$  and  $v_l$  are no longer arbitrary but are set to zero. So the problem may be interpreted as the determination of the flow after removal of a membrane separating two constant states at rest. We choose to make as a convention  $P_l \geq P_r \geq 0$ . Then in the code test problem we will run through the three possibilities

$$\rho_l > \rho_r$$

$$\rho_l = \rho_r$$

$$\rho_l < \rho_r$$

At time zero, the membrane is removed. The resultant action is a rarefaction wave traveling into the left state and a shock traveling into the right state. The velocity is  $v_l = 0$  to the left of the rarefaction wave. From the left of the rarefaction wave to the right, the velocity rises linearly from 0 to  $v_m > 0$ . The velocity is constant at  $v_m$  from the right of the rarefaction wave rightward toward the shock. At the shock, the velocity jumps from  $v_m > 0$  down to  $v_r = 0$ . See figure 5d for a velocity plot. The pressure drops continuously across the rarefaction wave from  $P_l$  to  $P_m$ . The pressure has the value  $P_m$  constantly from the right of the rarefaction wave to the shock. The pressure drops from  $P_m$  to  $P_r$  across the shock. See figure 5e for a pressure plot. The density drops continuously across the rarefaction wave from  $\rho_l$  to a  $\rho_{ml}$  which value it maintains from the right of the rarefaction wave to the point in the fluid where the initial discontinuity\* was and there the density jumps up to  $\rho_{mr}$ . From the initial discontinuity point to the shock, the density is  $\rho_{mr}$ . At the shock,

---

\*This density discontinuity is called a contact discontinuity.

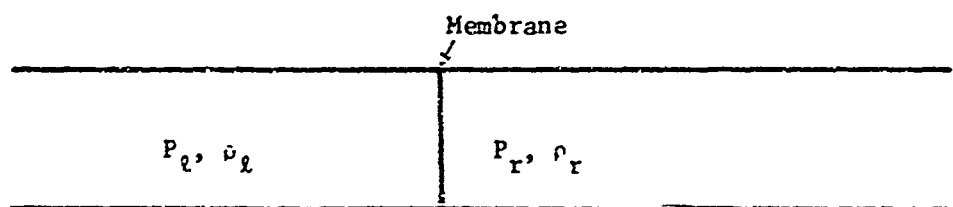


Figure 5a. Pipe Plot of Initial Conditions for Sctp-V

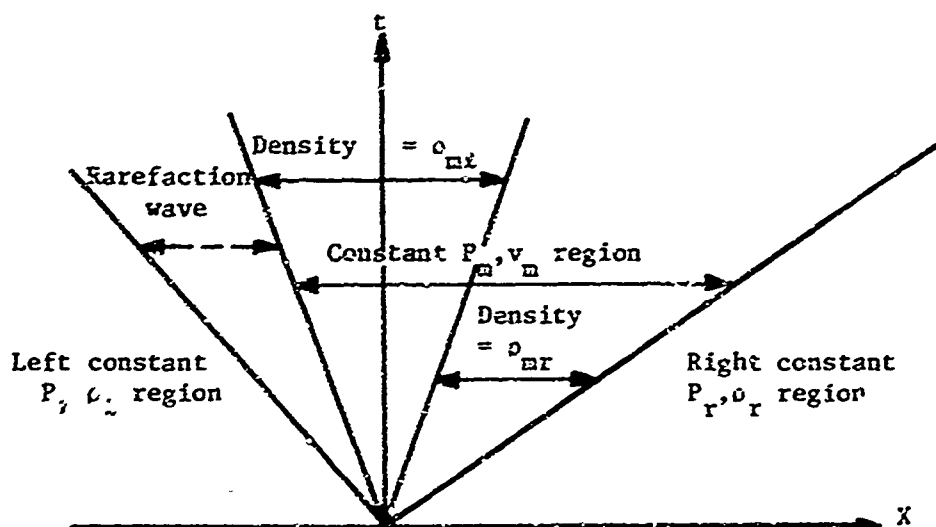


Figure 5b. Eulerian Wave Plot for Sctp-V



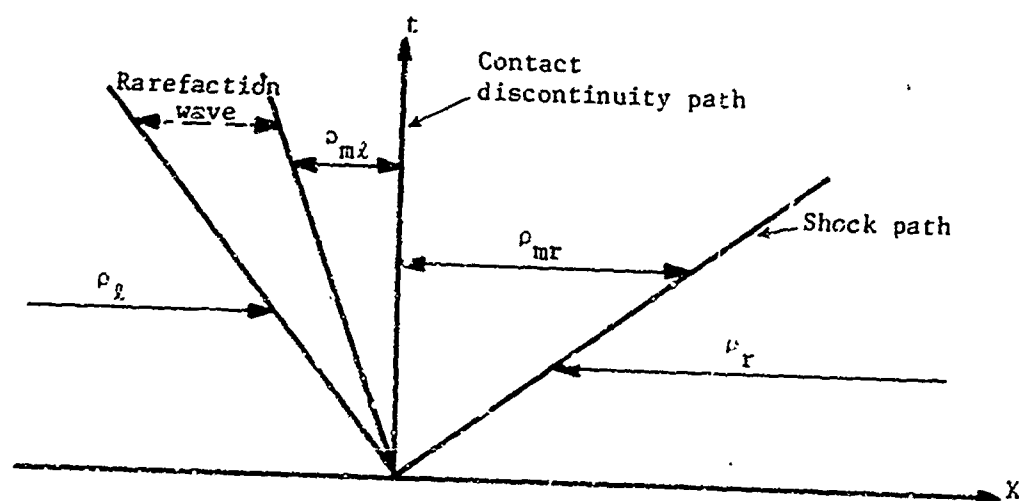


Figure 5c. Lagrangian Wave Plot

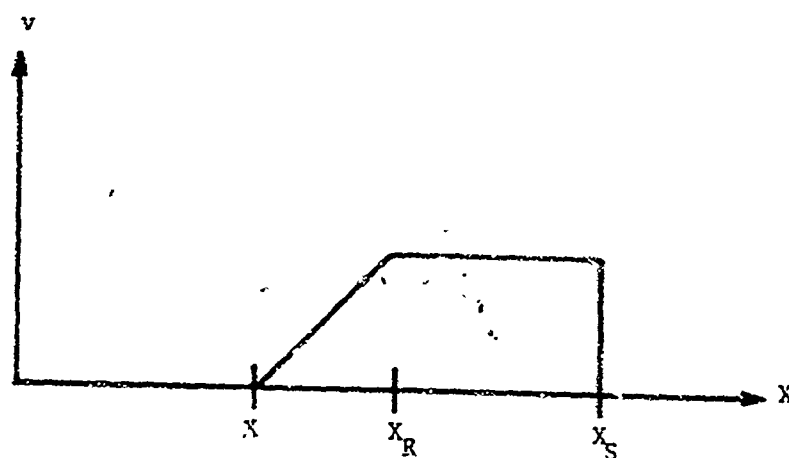


Figure 5d. Velocity Plot

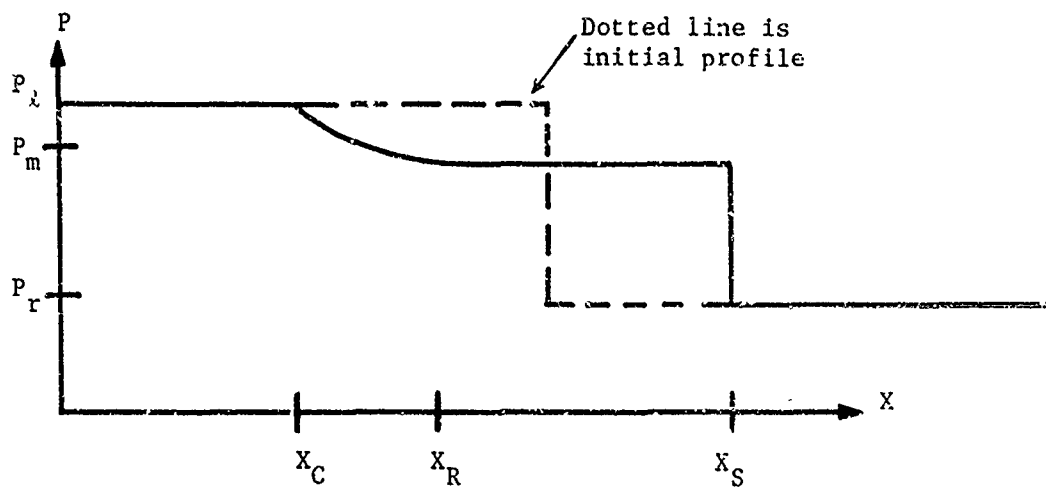


Figure 5e. Pressure Plot

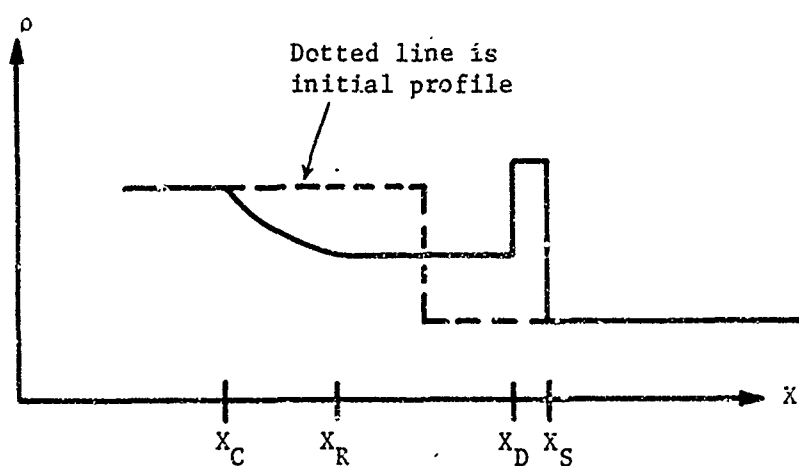


Figure 5f. Density Plot

the density jumps down from  $\rho_{mr}$  to  $\rho_r$  which value is maintained all the way to the right. See figure 5f for a density plot. We will mention again that this is a special case of the Riemann problem because in the Riemann problem, the velocities are also arbitrary along with  $P_\ell$ ,  $\rho_\ell$ ,  $P_r$ ,  $\rho_r$ . Figures 5a through 5i give graphic explanations.

b. Derivation of Solution

Assume states m and r are connected by a shock facing to the right, i.e.,  $P_m > P_r$ . By the conservation of momentum relation, (2:N2L), derived for SCTP-I,

$$m(v_m - v_r) = P_m - P_r$$

By the conservation of mass relation, (1:CM), derived for SCTP-I,

$$v_r = v_s - \frac{m}{\rho_r}$$

$$v_m = v_s - \frac{m}{\rho_m}$$

So

$$m\left(\frac{m}{\rho_r} - \frac{m}{\rho_m}\right) = P_m - P_r$$

or

$$m^2(v_r - v_m) = P_m - P_r$$

and

$$m^2 = \frac{P_m - P_r}{\frac{v_r - v_m}{\gamma + 1}}$$

By the Rankine-Hugoniot relation, (5:RH), derived for SCTP-I, the  $v_m$  may be eliminated to yield

$$m^2 = \frac{P_m + P_r \frac{\gamma-1}{\gamma+1}}{\frac{\gamma}{\gamma+1} v_r} = \frac{(\gamma+1) P_m + (\gamma-1) P_r}{2v_r}$$

or  $V_r$  may be eliminated to yield

$$m^2 = \frac{(\gamma+1) P_r + (\gamma-1) P_m}{2V_m}$$

By (2:N2L),

$$v_m = v_r + \frac{P_m - P_r}{m}$$

So,

$$v_m = v_r + (P_m - P_r) \sqrt{\frac{2V_r}{(\gamma+1) P_m + (\gamma-1) P_r}}$$

Then

$$v_m = v_r + \phi_r(P_m)$$

and

$$v_r = v_l + \phi_m(P_r)$$

Figure 5g is a plot of the possible  $P_m$ ,  $v_m$  values for a shock facing to the right when the right state  $(P_r, v_r)$  is prescribed. That is, it is a plot of the right facing, right specified shock relation for  $P$ ,  $v$  which is

$$v = v_r + \phi_r(P)$$

So if  $P_m$  is determined, then  $v_m$  is determined by

$$v_m = v_r + \phi_r(P_m)$$

In the analysis for SCTP-II, it was demonstrated that across a rarefaction wave traveling to the left, the Riemann invariant  $v + \sigma$  is constant (recall  $\sigma \equiv 2C/(\gamma-1)$ ). That is, a rarefaction moving to the left is a  $\lambda_+$  simple wave. Therefore,

$$v_l - v_m + \frac{2}{\gamma-1} (C_l - C_m) = 0$$

If the initial state was homentropic, then

$$\frac{P_\ell}{P_m} = \left( \frac{\rho_\ell}{\rho_m} \right)^\gamma$$

since the changes in state in a rarefaction wave are isentropic. Combining  $C^2 = \gamma PV$  and

$$\frac{P_\ell}{P_m} = \left( \frac{\rho_\ell}{\rho_m} \right)^\gamma$$

yields

$$C_\ell - C_m = \sqrt{\gamma} \left( \frac{P_\ell}{\rho_\ell^\gamma} \right)^{\frac{1}{2\gamma}} \left[ P_\ell^{\frac{\gamma-1}{2\gamma}} - P_m^{\frac{\gamma-1}{2\gamma}} \right]$$

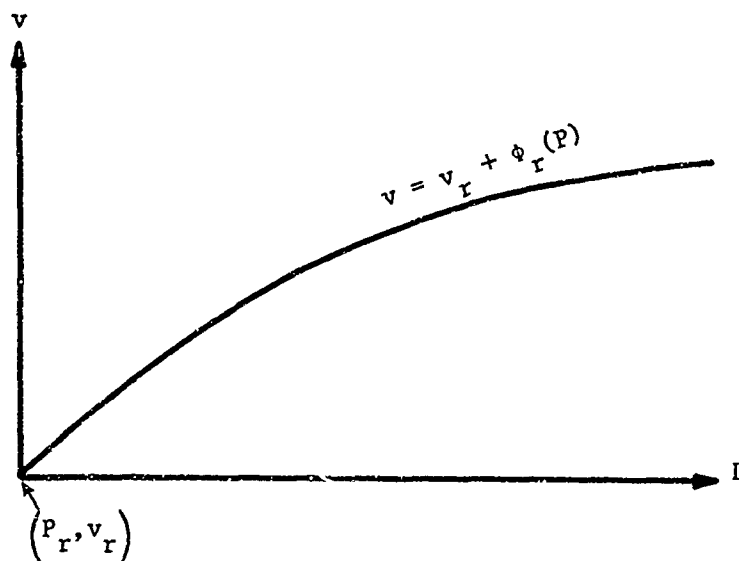


Figure 5g. P, v Plot for Right Facing, Right Specified Shock

So, for a rarefaction wave moving to the left,

$$v_m = v_\ell + \frac{2}{\gamma-1} (c_\ell - c_m)$$

or

$$v_m = v_\ell + \frac{2\sqrt{\gamma}}{\gamma-1} \left( \frac{p_\ell}{\rho_\ell^\gamma} \right)^{\frac{1}{2\gamma}} \left[ p_\ell^{\frac{\gamma-1}{2\gamma}} - p_m^{\frac{\gamma-1}{2\gamma}} \right]$$

If we define  $\psi_\ell(P)$  as

$$\frac{2\sqrt{\gamma}}{\gamma-1} \left( \frac{p_\ell}{\rho_\ell^\gamma} \right)^{\frac{1}{2\gamma}} \left[ p^{\frac{\gamma-1}{2\gamma}} - p_m^{\frac{\gamma-1}{2\gamma}} \right]$$

then

$$v_m = v_\ell - \psi_\ell(p_m)$$

We summarize and review the action: In the shock tube problem, if  $p_\ell > p_r$ , a shock will travel to the right and a rarefaction wave will travel to the left. To the right of the rarefaction and the left of the shock will be a region constant in pressure and velocity but having one discontinuity in density at the point in the fluid of the initial discontinuity. Other than this jump, the density is constant (it takes on only two values) in the middle region. See figures 5d, 5e, and 5f. Proceeding from left to right, the density is  $\rho_\ell$  in the left constant wave; then it drops continuously through the rarefaction wave to  $\rho_{m\ell}$ ; then it jumps up across the initial discontinuity to  $\rho_{mr}$ ; then it jumps down as it crosses the shock to  $\rho_r$ . If the initial discontinuity has the Lagrangian label  $x = 0$ , then the line  $x = 0$  in the Lagrangian wave plot is the path of the initial discontinuity. Therefore, the line  $x = 0$  is the path of the contact or tangential discontinuity. See figure 5c for the Lagrangian wave plot.

Shock relation:

$$v_m = v_r + \phi_r(p_m)$$

Rarefaction relation:

$$v_m = v_\ell - \psi_\ell \left( \frac{P_m}{P_\ell} \right)$$

These two relations determine  $v_m$  and  $P_m$ . The equation for  $P_m$  obtained by equating the two right sides of the above relations is

$$\left( \frac{P_m - P_r}{P_\ell} \right) \sqrt{\frac{2V_r}{(\gamma+1) \frac{P_m}{P_\ell} + (\gamma-1) \frac{P_r}{P_\ell}}} = + \frac{2\sqrt{\gamma}}{\gamma-1} \frac{P_\ell^{\frac{1}{2\gamma}}}{\rho_\ell^{\frac{1}{2}}} \left( P_\ell^{\frac{\gamma-1}{2}} - P_m^{\frac{\gamma-1}{2}} \right)$$

or

$$\left( \frac{\frac{P_m}{P_\ell} - \frac{P_r}{P_\ell}}{\frac{P_m}{P_\ell} + \frac{P_r}{P_\ell}} \right) \sqrt{\frac{2}{(\gamma+1) \frac{P_m}{P_\ell} + (\gamma-1) \frac{P_r}{P_\ell}}} = \frac{2\sqrt{\gamma}}{\gamma-1} \left( \frac{\rho_r}{\rho_\ell} \right)^{\frac{1}{2}} \left( 1 - \left( \frac{P_m}{P_\ell} \right)^{\frac{\gamma-1}{2\gamma}} \right)$$

or for  $\gamma = 1.4$ ,

$$\left( \frac{\frac{P_m}{P_\ell} - \frac{P_r}{P_\ell}}{\frac{P_m}{P_\ell} + \frac{P_r}{P_\ell}} \right) \sqrt{\frac{5}{6 \left( \frac{P_m}{P_\ell} \right) + \frac{P_r}{P_\ell}}} = \sqrt{35} \left( \frac{\rho_r}{\rho_\ell} \right)^{\frac{1}{2}} \left( 1 - \frac{P_m}{P_\ell} \right)^{\frac{1}{7}}$$

$\rho_{m\ell}$  is determined by the isentropy condition

$$\frac{P_\ell}{P_m} = \left( \frac{\rho_\ell}{\rho_{m\ell}} \right)^\gamma$$

$v_{mr} \equiv \rho_{mr}^{-1}$  is determined by (5:RH):

$$0 = e_{mr} - e_r + \frac{P_m + P_r}{2} (v_{mr} - v_r)$$

where

$$e = \frac{PV}{\gamma-1}$$

The shock velocity is determined by the shock speed-pressure relation, (7:SS(P)), derived for SCTP-I:

$$v_s = v_r + \sqrt{v_r \left( \frac{\gamma+1}{2} p_m + \frac{\gamma-1}{2} p_r \right)}$$

The velocity in the rarefaction wave linearly connects  $v_\ell = 0$  to  $v_m$  as was shown in SCTP-II. Then in the rarefaction wave,

$$P = p_\ell \left( 1 - \frac{\gamma-1}{2} \frac{v}{c_\ell} \right)^{\frac{2\gamma}{\gamma-1}}$$

$$\rho = \rho_\ell \left( 1 - \frac{\gamma-1}{2} \frac{v}{c_\ell} \right)^{\frac{2\gamma}{\gamma-1}}$$

as was shown for SCTP-II. The left side of the rarefaction wave is at

$$X_C(t) \equiv X_S(0) - c_\ell t$$

and the right side is at

$$X_R(t) \equiv X_S(0) - \left( c_\ell - \frac{\gamma+1}{2} v_m \right) t$$

as was shown for SCTP-II. The shock wave is at

$$X_S(t) \equiv X_S(0) + v_s t$$

The initial discontinuity point of the fluid is at

$$X_D(t) \equiv X_S(0) + v_m t$$



Solution summary:

Left Region	{	For $X \leq X_C(t)$ , the values are $P_\ell, \rho_\ell, v_\ell$
Rarefaction Region	{	<p>For <math>X_C(t) \leq X \leq X_R(t)</math>, the values are</p> $v(X,t) = \frac{X - X_C(t)}{X_R(t) - X_C(t)} v_m$ $C = C_\ell \left( 1 - \frac{\gamma-1}{2} \frac{v}{C_\ell} \right)$ $P = P_\ell \left( \frac{C}{C_\ell} \right)^{\frac{2\gamma}{\gamma-1}}$ $\rho = \rho_\ell \left( \frac{C}{C_\ell} \right)^{\frac{2}{\gamma-1}}$
Middle Region	{	<p>For <math>X_R \leq X &lt; X_S(t)</math>, the values are <math>P_m, v_m</math></p> <p>For <math>X_R(t) \leq X &lt; X_D(t)</math>, the density is <math>\rho_{m\ell}</math></p> <p>For <math>X_D(t) &lt; X &lt; X_S(t)</math>, the density is <math>\rho_{mr}</math></p>
Right Region	{	For $X > X_S(t)$ , the values are $P_r, \rho_r, v_r$

c. Application as a Test Problem

(1) Eulerian Input

(a) Initial values

For  $X < X_S(0)$ ,

$$P_{\ell} > 0$$

$$\rho_{\ell} > 0$$

$$v_{\ell} = 0$$

For  $X < X_S(0)$ ,

$$P_r > 0$$

$$\rho_r > 0$$

$$v_r = 0$$

$$P_{\ell} > P_r$$

(b) Boundary values

At  $X = 0$ , hold the values at  $P_{\ell}$ ,  $\rho_{\ell}$ , and  $v_{\ell}$

(2) Lagrangian Input

(a) Initial Values

For  $X < X_S(0)$ ,

$$P_{\ell} > 0$$

$$\rho_{\ell} > 0$$

$$v_{\ell} = 0$$

For  $X > X_S(0)$

$$P_r > 0$$

$$\rho_r > 0$$

$$v_r = 0$$

$$P_{\ell} > P_r$$

(b) Boundary values

At  $x = 0$ , hold the values at  $P_l, \rho_l, v_l$

(3) Numerical Values for SCTP-V

(a) SCTP-V-A

$$X_S(0) = 100 \text{ meters}$$

$$\Delta X = 1 \text{ meter}$$

$$P_l = 10^8 \text{ dynes/cm}^2$$

$$\rho_l = 10^{-5} \text{ gm/cm}^3$$

$$v_l = 0$$

$$P_r = 10^4 \text{ dynes/cm}^2$$

$$\rho_r = 10^{-6} \text{ gm/cm}^3$$

$$v_r = 0$$

Right boundary at 250 meters

These imply the following values:

$$P_m \doteq 1.888 \times 10^7 \text{ dynes/cm}^2$$

$$v_m \doteq 3.964 \times 10^6 \text{ cm/sec}$$

$$\rho_{ml} \doteq 3.040 \times 10^{-6} \text{ gm/cm}^3$$

$$\rho_{mr} \doteq 5.982 \times 10^{-6} \text{ gm/cm}^3$$

$$v_S \doteq 4.760 \times 10^6 \text{ cm/sec}$$

The output recipe we used is: print out at time  $1 \times 10^{-4}$  sec,  $1 \times 10^{-3}$  sec, and  $2 \times 10^{-3}$  sec.

(b) SCTP-V-B

Same as A except

$$X_S(0) = 250 \text{ meters}$$

$$\rho_l = 10^{-6} \text{ gm/cm}^3$$

Right boundary at 500 meters

These imply the following values:

$$\begin{aligned}P_m &\doteq 4.610 \times 10^7 \text{ dynes/cm}^2 \\v_m &\doteq 6.196 \times 10^6 \text{ cm/sec} \\\rho_{ml} &\doteq 5.751 \times 10^{-7} \text{ gm/cm}^3 \\\rho_{mr} &\doteq 5.992 \times 10^{-6} \text{ gm/cm}^3 \\v_s &\doteq 7.437 \times 10^6 \text{ cm/sec}\end{aligned}$$

(c) SCTP-V-C

Same as A except

$$X_S(0) = 250 \text{ meters}$$

$$\rho_l = 10^{-6} \text{ gm/cm}^3$$

$$\rho_r = 10^{-5} \text{ gm/cm}^3$$

Right boundary at 500 meters

These imply the following values:

$$\begin{aligned}P_m &\doteq 7.406 \times 10^7 \text{ dynes/cm}^2 \\v_m &\doteq 2.484 \times 10^6 \text{ cm/sec} \\\rho_{ml} &\doteq 8.070 \times 10^{-7} \text{ gm/cm}^3 \\\rho_{mr} &\doteq 5.995 \times 10^{-5} \text{ gm/cm}^3 \\v_s &\doteq 2.981 \times 10^6 \text{ cm/sec}\end{aligned}$$

(4) Comments on the Computer Solution

(a) General

The variations A, B, C were made to explore the three possibilities  $\rho_l > \rho_r$ ,  $\rho_l = \rho_r$ ,  $\rho_l < \rho_r$ . The solution is good until the rarefaction wave reaches the left hand boundary or the right hand boundary. At the last time, we have the active zone situation as presented in table V-A.

(b) PUFF

ACCURACY: On SCTP-V-A, the most noticeable error was a smearing of the density discontinuity at  $X_j$  (see figure 5h). The only other errors were the typical round unders and round overs at corners. (See figure 5h and table V-B. On SCTP-V-B, there was a bit of oscillation in the

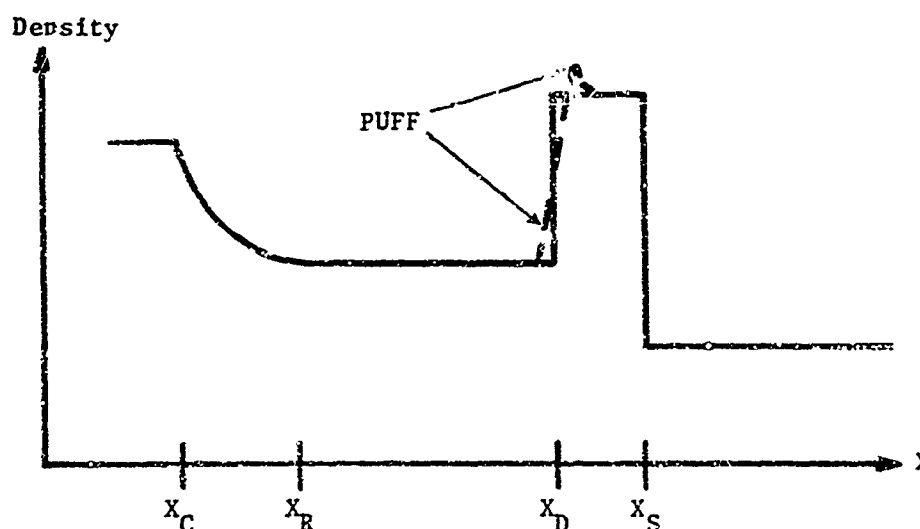


Figure 5h. PUFF Error Graph on SCTP-V-A

density in the compressed region and a little overshoot in velocity and an undershoot in pressure at  $X_R$ . See figure 5i and table V-C. On SCTP-V-C, the dominant error was the overshoot in velocity as shown in figure 5i. The other error was a slight undershoot in the pressure at  $X_R$ . See table V-D.

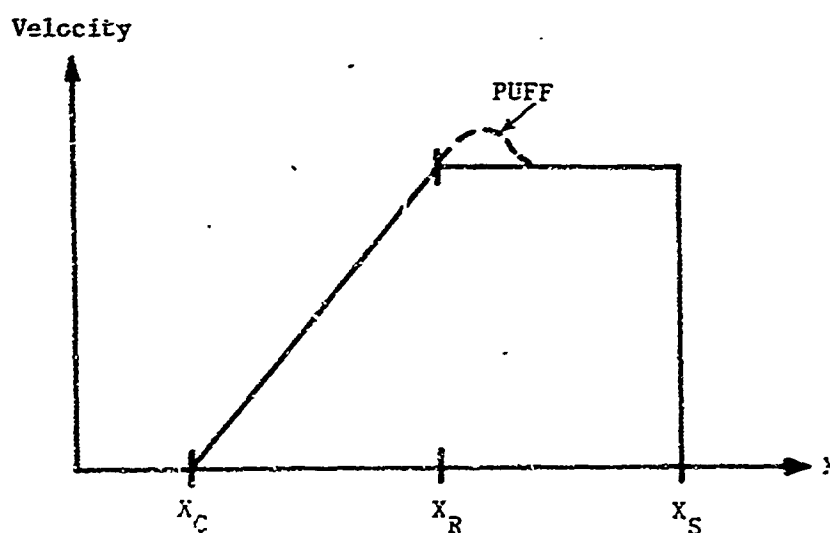


Figure 5i. Error Graph for SCTP-V

AFWL-TR-67-127

TIMING: Sctp-V-A took 976 cycles and 61 seconds CDC 6600  
CP time to run to  $2 \times 10^{-3}$  sec. Sctp-V-B took 1527 cycles and 168 seconds CDC  
6600 CP time to run to  $2 \times 10^{-3}$  sec. Sctp-V-C took 611 cycles and 71 seconds  
CDC 6600 CP time to run to  $2 \times 10^{-3}$  sec.

Table V-A

ACTIVITY TABLE AT TIME  $2 \times 10^{-3}$  SECOND ON SCTP-V

	$X_C$ (meters)	$X_S$ (meters)
SCTP-V-A	25	195
SCTP-V-B	14	400
SCTP-V-C	14	310

Table V-B

PUFF ERROR TABLE FOR SCTP-V-A

Problem time =  $2 \times 10^{-3}$  sec

PUFF cycle = 976

Computer time = 61 sec

Number of active zones = 202

	<u>Sum Sqr. Err.</u>	<u>Max. Err.</u>	<u>Position of Max. Err.</u>
Pressure	0.0061	-0.0545	$X_S$
Velocity	0.0795	+0.875	$X_S$
Density	0.0271	+0.172	$X_S$
	<u>Sum Int. Energy</u>	<u>Sum Kin. Energy</u>	<u>Sum Tot. Energy</u>
EXACT	$2.177 \times 10^{12}$	$3.232 \times 10^{11}$	$2.500 \times 10^{12}$
PUFF	$2.178 \times 10^{12}$	$3.218 \times 10^{11}$	$2.500 \times 10^{12}$

Table V-C

## PUFF ERROR TABLE FOR SCTP-V-B

Problem time =  $2 \times 10^{-3}$  sec

PUFF cycle = 1527

Computer time = 168 sec

Number of active zones = 405

	<u>Sum Sqr. Err.</u>	<u>Max. Err.</u>	<u>Position of Max. Err.</u>
Pressure	0.0137	-0.263	$X_s$
Velocity	0.4447	+0.748	$X_s$
Density	0.0306	-0.415	$X_s$

	<u>Sum Int. Energy</u>	<u>Sum Kin. Energy</u>	<u>Sum Tot. Energy</u>
EXACT	$5.668 \times 10^{12}$	$5.834 \times 10^{11}$	$6.251 \times 10^{12}$
PUFF	$5.669 \times 10^{12}$	$5.814 \times 10^{11}$	$6.250 \times 10^{12}$

Table V-D

## PUFF ERROR TABLE FOR SCTP-V-C

Problem time =  $2 \times 10^{-3}$  sec

PUFF cycle = 611

Computer time = 71 sec

Number of active zones = 316

	<u>Sum Sqr. Err.</u>	<u>Max. Err.</u>	<u>Position of Max. Err.</u>
Pressure	0.0282	-0.478	$X_s$
Velocity	0.0487	+0.701	$X_s$
Density	0.0360	-0.471	$X_s$

	<u>Sum Int. Energy</u>	<u>Sum Kin. Energy</u>	<u>Sum Tot. Energy</u>
EXACT	$6.005 \times 10^{12}$	$2.460 \times 10^{11}$	$6.251 \times 10^{12}$
PUFF	$6.007 \times 10^{12}$	$2.434 \times 10^{11}$	$6.250 \times 10^{12}$



6. HYDROCODE TEST PROBLEM Sctp-VIa. Description of Problem

This problem is the collision of two shock waves. Proceeding from left to right, the values are  $P_\ell, \rho_\ell, v_\ell$  connected by a right facing shock to  $P_o, \rho_o, v_o$  which in turn is connected by a left facing shock to  $P_r, \rho_r, v_r$ . As a convenient convention, always take  $P_\ell \geq P_r$ . Figure 6 gives a graphical description.

b. Derivation of Solution

After collision, the pressure profile looks like figure 6d. Now by the analysis in Sctp-V,  $v_m = v_r + \phi_r(P_m)$  for a shock facing to the right and similarly,  $v_m = v_\ell - \phi_\ell(P_m)$  for a shock facing to the left, where

$$\phi_a(P) \equiv (P - P_a) \frac{2v_a}{(\gamma+1)P + (\gamma-1)P_a}$$

From these two equations,  $P_m$  and  $v_m$  are determined. Then by the Rankine-Hugoniot relation, (5:RH),  $\rho_{m\ell}$  and  $\rho_{mr}$  are determined. Let

$$v_{m\ell} = \rho_{m\ell}^{-1}$$

and

$$v_{mr} = \rho_{mr}^{-1}$$

Then by (5:RH),

$$\frac{1}{\gamma-1} (P_\ell v_\ell - P_m v_{m\ell}) = \frac{P_\ell + P_m}{2} (v_{m\ell} - v_\ell)$$

and

$$\frac{1}{\gamma-1} (P_m v_{mr} - P_r v_r) = \frac{P_m + P_r}{2} (v_r - v_{mr})$$

Let  $t_c$  be the time of collision,  $X_{sl}(t)$  be the position of the left shock prior to collision, i.e.,  $t < t_c$ , then

$P_l, v_l, \rho_l$	$P_o, v_o, \rho_o$	$P_r, v_r, \rho_r$
--------------------	--------------------	--------------------

Figure 6a. Pipe Plot for Sctp-VI Initial Values

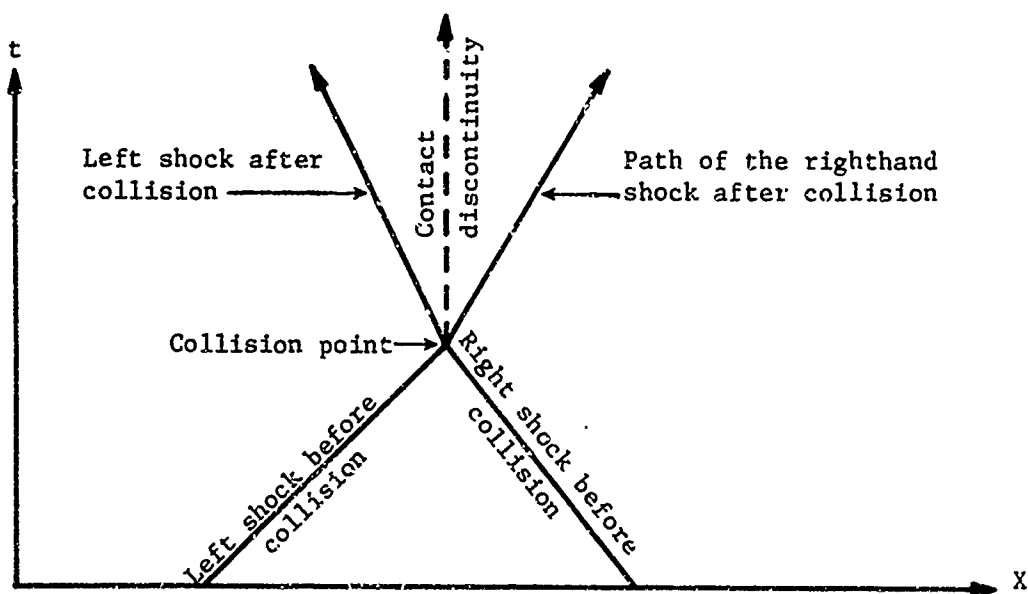


Figure 6b. Lagrangian Wave Plot for Sctp-VI

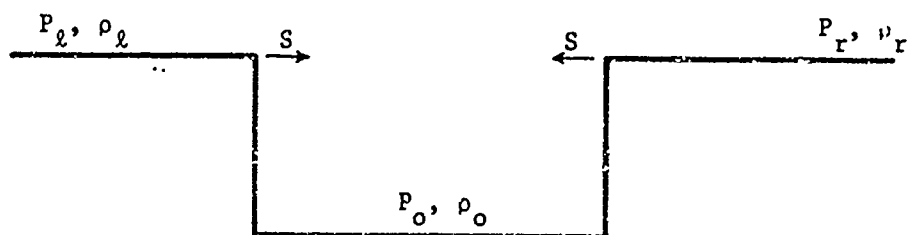


Figure 6c. Pressure-Density Plot Prior to Collision

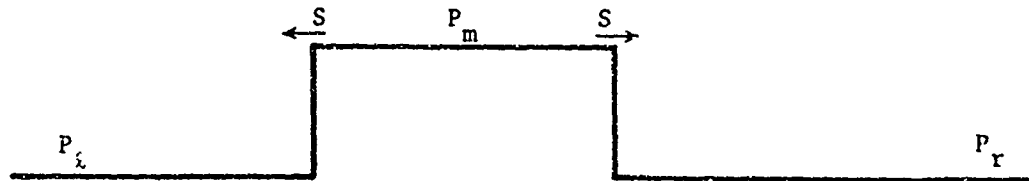


Figure 6d. Pressure Plot after Collision

$$X_{sl}(t) = X_{sl}(0) + V_{sl}t$$

Likewise, let  $X_{sr}(t)$  be the position of the right shock for  $t < t_c$ , then

$$X_{sr}(t) = X_{sr}(0) + V_{sr}t$$

Let  $X_{sl}^*(t)$  be the position of the left hand shock after collision ( $t > t_c$ ), then

$$X_{sl}^*(t) = X_{col} + v_{sl}^*(t-t_c)$$

where  $X_{col}$  is the place the collision occurs. Likewise, let  $X_{sr}^*(t)$  be the position of the right hand shock after collision; then

$$X_{sr}^*(t) = X_{col} + v_{sr}^*(t-t_c)$$

For  $t < t_c$ ,

$X < X_s(t)$  implies the values are  $P_l, \rho_l, v_l$

$X_{sl} < X < X_{sr}(t)$  implies the values are  $P_o, \rho_o, v_o$

$X_{sr}(t) < X$  implies the values are  $P_r, \rho_r, v_r$

For  $t > t_c$ ,

$X < X_{sl}^*(t)$  implies the values are  $P_l, \rho_l, v_l$

$X_{sl}^*(t) < X < X_{col} + v_m(t-t_c)$  implies the values are  $P_m, v_m, \rho_{ml}$

$X_{col} + v_m(t-t_c) < X < X_{sr}^*(t)$  implies the values are  $P_m, v_m, \rho_{mr}$

$X > X_{sr}^*(t)$  implies the values are  $P_r, v_r, \rho_r$

c. Application as a Test Problem

(1) Eulerian Input

(a) Initial values

For  $X < X_{sl}(0)$ , the values are

$$P_l > 0$$

$$\rho_l > 0$$

$$v_l > 0$$

For  $X_{sl}(0) < X < X_{sr}(0)$ , the values are

$$P_o > 0$$

$$\rho_o > 0$$

$$v_o = 0$$

For  $X > X_{sr}(0)$ , the values are

$$P_r > 0$$

$$\rho_r > 0$$

$$v_r = 0$$

where

$$P_l \geq P_r > P_o$$

Give

$$P_o > 0$$

$$\rho_o > 0$$

$$v_o = 0$$

and one of the quantities  $P_l, v_l, \rho_l$ , then all left quantities are determined. Also give one of the quantities  $P_r, \rho_r, v_r$ , and all right quantities are determined. Therefore,

$$\rho_l \geq \rho_r > \rho_o$$

and

$$v_l \geq |v_r| > 0$$

For example, suppose  $P_l$  and  $P_r$  are given by (7:SS(P)):

$$v_{sl} = v_o + v_o \left( \frac{\gamma+1}{2} P_l + \frac{\gamma-1}{2} P_o \right)$$

$$v_{sr} = v_o - v_o \left( \frac{\gamma+1}{2} P_r + \frac{\gamma-1}{2} P_o \right)$$

By (1:CM) and (2:N2L),

$$v_l = \frac{v_o}{v_{sl}} (P_l - P_o)$$

$$v_r = \frac{v_o}{v_{sr}} (P_r - P_o)$$

By (1:CM),

$$\rho_l = \frac{v_{sl}}{v_{sl} - v_l} \rho$$

$$\rho_r = \frac{v_{sr}}{v_{sr} - v_r} \rho_o$$

(b) Boundary values

At  $X = 0$ , hold the values at  $P_l$ ,  $\rho_l$ ,  $v_l$  and at the right hand boundary, hold the values at  $P_r$ ,  $\rho_r$ ,  $v_r$ .

(2) Lagrangian Input

(a) Initial values

Same as Eulerian just given

(b) Boundary values

Same as Eulerian just given

(3) Numerical Values for Sctp-VI

(a) Sctp-VI-A

$$X = 1 \text{ meter}$$

$$X_s(0) = 75 \text{ meters}$$

$$X_{sr}(0) = 125 \text{ meters}$$

and let the right hand boundary be at 200 meters initially

$$P_o = 10^4 \text{ dynes/cm}^2$$

$$\rho_o = 10^{-6} \text{ gm/cm}^3$$

$$v_o = 0$$

$$F_l = 10^8 \text{ dynes/cm}^2$$

$$P_r = 10^7 \text{ dynes/cm}^2$$

These values then determine the remainder of the values to be

$$\rho_l \doteq 5.997 \times 10^{-6} \text{ gm/cm}^3$$

$$\rho_r \doteq 5.97 \times 10^{-6} \text{ gm/cm}^3$$

$$v_l \doteq 9.13 \times 10^6 \text{ cm/sec}$$

$$v_r \doteq -2.88 \times 10^6 \text{ cm/sec}$$

$$v_{sl} \doteq 1.095 \times 10^7 \text{ cm/sec}$$

$$v_{sr} \doteq -3.46 \times 10^6 \text{ cm/sec}$$

$$t_c \doteq 3.468 \times 10^{-4} \text{ sec}$$

$$X_{col} \doteq 1.13 \times 10^4 \text{ cm}$$

$$P_m \doteq 3.66 \times 10^8 \text{ dynes/cm}^2$$

$$\rho_{ml} \doteq 1.43 \times 10^{-5} \text{ gm/cm}^3$$

$$\rho_{mr} \doteq 3.09 \times 10^{-5} \text{ gm/cm}^3$$

$$v_m \doteq 1.96 \times 10^6 \text{ cm/sec}$$

$$v_{sl}^* \doteq 3.75 \times 10^5 \text{ cm/sec}$$

$$v_{sr}^* \doteq 5.72 \times 10^6 \text{ cm/sec}$$

A reasonable output recipe seems to be to print out at  $1 \times 10^{-4} \text{ sec}$ ,  $t_c \doteq 3.468 \times 10^{-4} \text{ sec}$ , and  $7 \times 10^{-4} \text{ sec}$ .

## (b) SCTP-VI-B

Same as A, but  $P_l = P_r = 10^8$  dynes/cm<sup>2</sup>. This yields the following values:

$$\begin{aligned}\rho_l &= \rho_r \doteq 5.997 \times 10^{-6} \text{ gm/cm}^3 \\ v_l &= -v_r \doteq 9.13 \times 10^6 \text{ cm/sec.} \\ v_{sl} &= -v_{sr} \doteq 1.095 \times 10^7 \text{ cm/sec} \\ t_{col} &\doteq 2.282 \times 10^{-4} \text{ sec} \\ X_{col} &= 1.00 \times 10^4 \text{ cm} \\ P_m &\doteq 7.995 \times 10^8 \text{ dynes/cm}^2 \\ v_m &\doteq 9.24 \times 10^6 \text{ cm/sec} \\ \rho_{ml} &= \rho_{mr} \doteq 2.098 \times 10^{-5} \text{ gm/cm}^3 \\ -v_{sl}^* &= v_{sr}^* \doteq 3.65 \times 10^6 \text{ cm/sec}\end{aligned}$$

A reasonable output recipe seems to be to print out at  $1 \times 10^{-4}$  sec,  $t_c \doteq 2.282 \times 10^{-4}$  sec, and  $7 \times 10^{-4}$  sec.

## (4) Comments on the Computer Solution

## (a) General

The solution should be correct until the shocks hit the left or right boundaries of the hydrocode. Note that SCTP-VI-B can be interpreted as the reflection of a shock wave off a wall where the wall is at the collision position. Because of its symmetry, SCTP-VI-B gives a code symmetry test on shocks.

## (b) PUFF

SCTP-VI-A took 1283 cycles and 87 seconds CP time on the CDC 6600 computer. The major errors in evidence were the spikes in the density and internal energy. Hot-thin spikes resulted from the initial discontinuities as we have observed before in SCTP-I-A. A cold-thick spike resulted from the shock collision. See figure 6e.

SCTP-VI-B took 1500 cycles and 113 seconds CDC 6600 CP time. The major errors were again in the density and specific internal energy. The hot-thin and cold-thick spots occurred as in A. No asymmetries were observed.

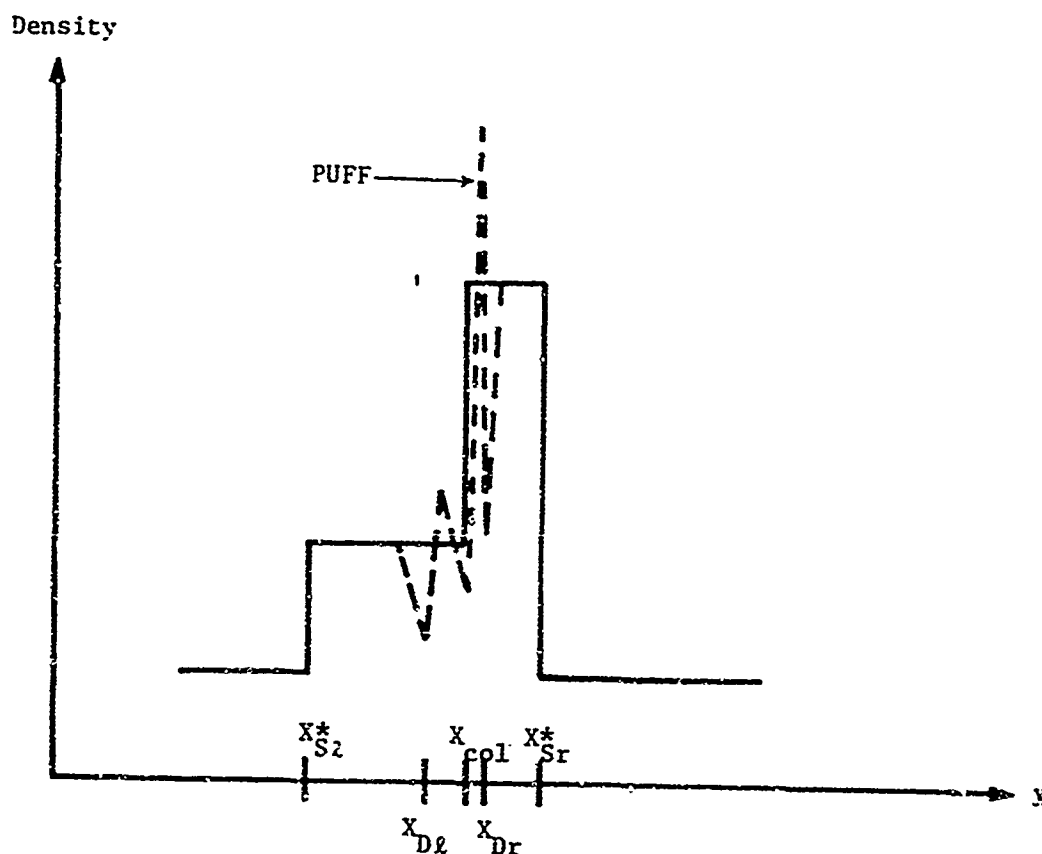


Figure 6e. SCTP-VI-A Error Graph

See table VI for a tabulation of the errors at the final time,  $7 \times 10^{-4}$  sec. See figure 6f. For tables VI-A and VI-B, we define  $X_{Dl}$  and  $X_{Dr}$  to be the position of the fluid particle which was initially at the left and right hand shock positions, respectively.  $X_{Dl}$  and  $X_{Dr}$  will also be used in figures 6e and 6f.



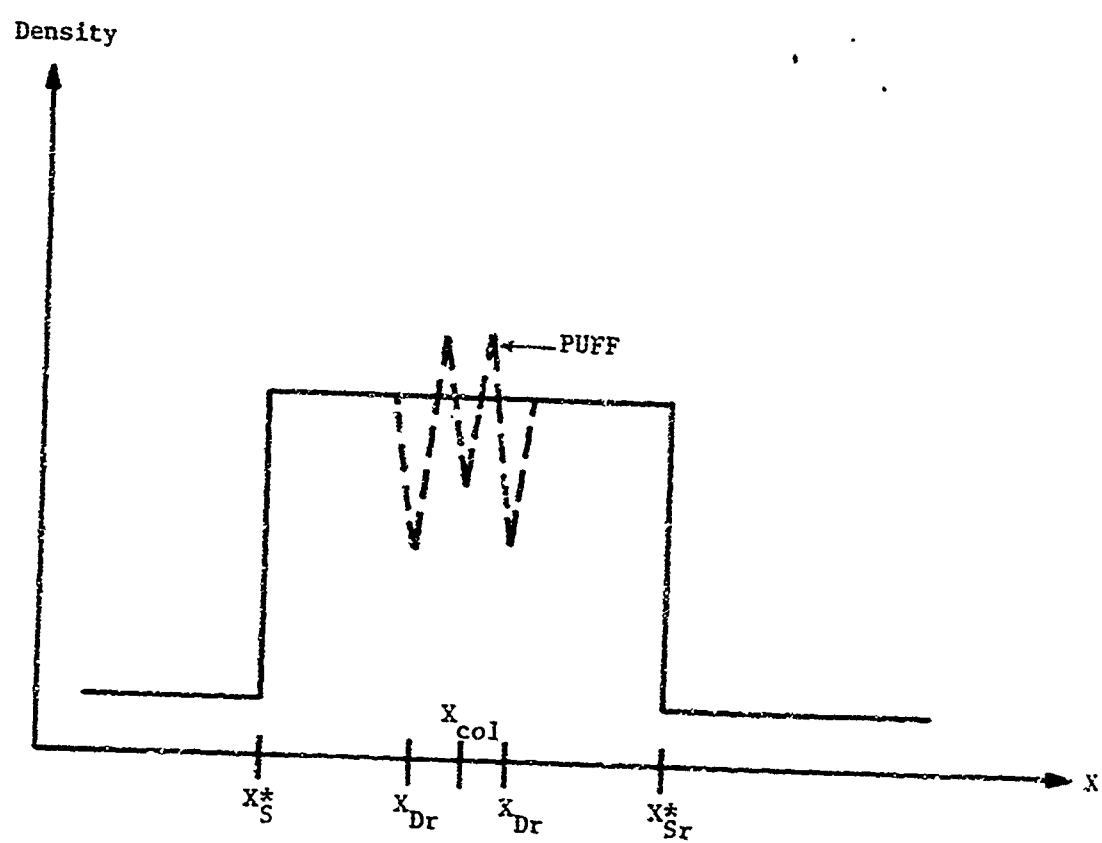


Figure 6f. SCTP-VI-B Error Graph

Table VI-A

## PUFF ERROR TABLE FOR SCTP-VI-A

Problem time =  $7 \times 10^{-4}$  sec

PUFF cycle = 1283

Computer time = 87 sec

Number of active zones = 201

	<u>Sum Sqr. Err.</u>	<u>Max. Err.</u>	<u>Position of Max. Err.</u>
Pressure	0.0392	+0.352	$X_{sr}^*$
Velocity	0.0485	+0.514	$X_{sr}^*$
Density	0.103	+0.640	$X_{col}$
	<u>Sum Int. Energy</u>	<u>Sum Kin. Energy</u>	<u>Sum Tot. Energy</u>
EXACT	$3.104 \times 10^{12}$	$1.375 \times 10^{12}$	$4.480 \times 10^{12}$
PUFF	$3.126 \times 10^{12}$	$1.657 \times 10^{12}$	$4.782 \times 10^{12}$

Table VI-B

## PUFF ERROR TABLE FOR SCTP-VI-B

Problem time =  $7 \times 10^{-4}$ 

PUFF cycle = 1500

Computer time = 113

Number of active zones = 201

	<u>Sum Sqr. Err.</u>	<u>Max. Err.</u>	<u>Position of Max. Err.</u>
Pressure	0.0411	+0.332	$X_{sr}^*$ and $X_{sl}^*$
Velocity	0.0700	+0.602	$X_{sr}^*$ and $X_{sl}^*$
Density	0.0907	-0.516	$X_{Dl}$ and $X_{Dr}$
	<u>Sum Int. Energy</u>	<u>Sum Kin. Energy</u>	<u>Sum Tot. Energy</u>
EXACT	$7.832 \times 10^{12}$	$9.430 \times 10^{11}$	$8.775 \times 10^{12}$
PUFF	$7.882 \times 10^{12}$	$8.940 \times 10^{11}$	$8.776 \times 10^{12}$

## 7. HYDROCODE TEST PROBLEM SCTP-VII

### a. Description of Problem

Two shock waves are traveling in the same direction which is taken to the right. When two shock waves are traveling in the same direction, the one behind will always overtake the one in front.

After overtake time, a rarefaction travels back to the left (for  $\gamma \leq 5/3$ ) and a stronger shock travels on to the right.

Graphical representation is presented in figure 7.

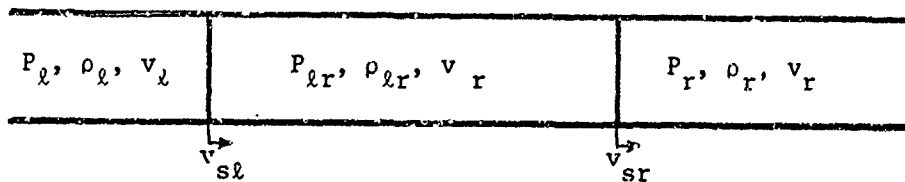


Figure 7a. Pipe Plot for Initial Values in SCTP-VII

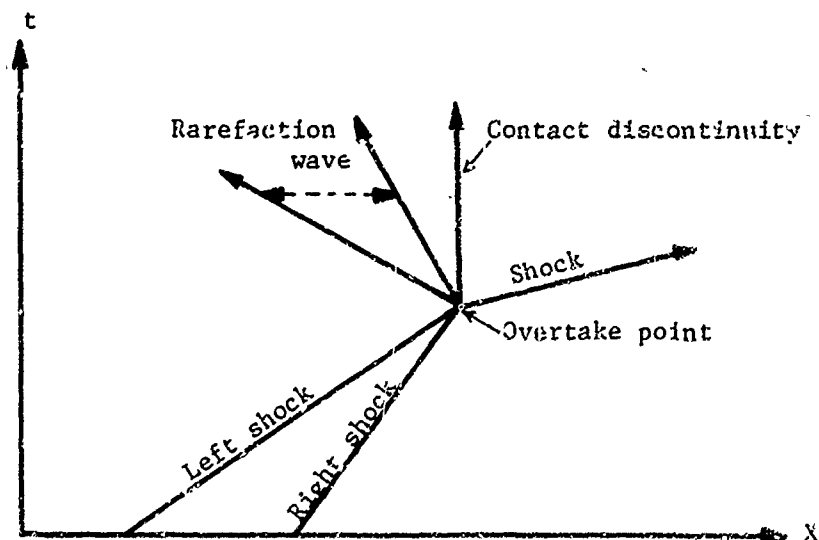


Figure 7b. Lagrangian Wave Plot for SCTP-VII

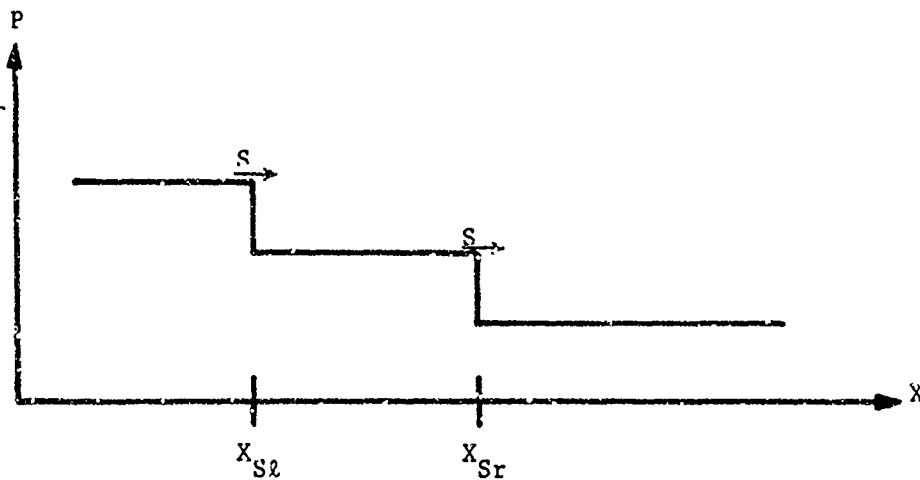


Figure 7c. Initial Pressure Plot for Sctp-VII

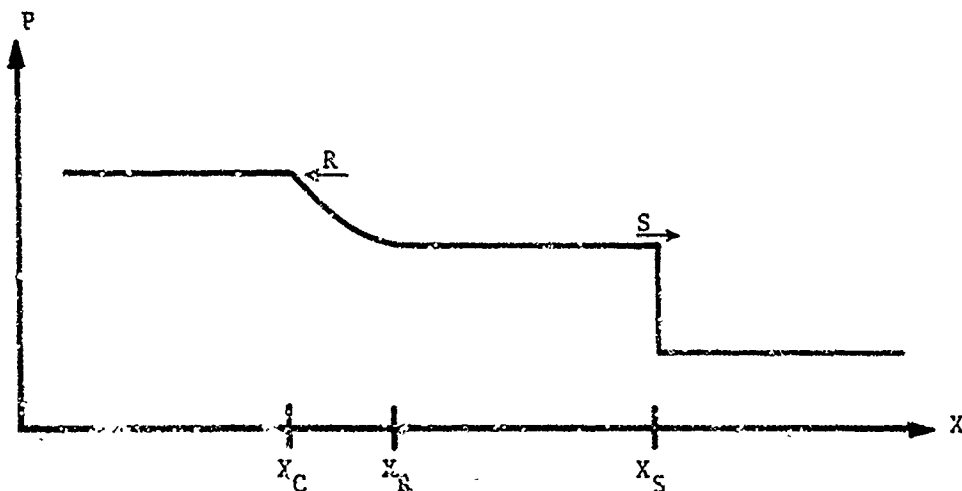


Figure 7d. After Overtake Pressure Plot for Sctp-VII

#### b. Derivation of Solution

After overtake  $v_m = v_r + \phi_r(P_m)$  for the shock traveling to the right and  $v_m = v_l - \psi_l(P_m)$  for the rarefaction traveling to the left. ( $\phi_r(P_m)$  and  $\psi_l(P_m)$  are defined in Sctp-V.) From the above relations,  $v_m$  and  $P_m$  are determined, then  $V_{mr}$  is determined from the Rankine-Hugoniot relation (5:RH)

$$\frac{1}{\gamma-1} (P_{mr} V_{mr} - P_r V_r) = \frac{P_{mr} + P_r}{2} (v_r - v_{mr})$$

$\rho_{lm}$  is determined from the fact that the entropy does not change through a rarefaction; therefore,

$$\frac{P_l}{P_m} = \left( \frac{\rho_l}{\rho_{lm}} \right)^\gamma$$

Let  $v_s, X_s$  be the velocity and position of the shock after overtake. Let  $v_{sl}, X_{sl}$  and  $v_{sr}, X_{sr}$  be the velocities and positions of the left and right shocks (defined only prior to overtake). Let  $(X_o, t_o)$  be the point where overtake occurs.

For  $t \leq t_o$  and  $X < X_{sl}(t)$ , the values are  $P_l, v_l, \rho_l$

For  $t \leq t_o$  and  $X_{sl}(t) < X < X_{sr}(t)$ , the values are  $P_{lr}, v_{lr}, \rho_{lr}$

For  $t \leq t_o$  and  $X > X_{sr}(t)$ , the values are  $P_r, v_r, \rho_r$

On the other hand, for  $t > t_o$ , in the region

$$X < X_o + (v_l - c_l)(t - t_o) \equiv X_c(t)$$

the values are  $P_l, v_l, \rho_l$ . In the region

$$X_x(t) < X < X_o + \left( -c_x + \frac{1+\gamma}{2} v_m + \frac{1+\gamma}{2} v_l \right) (t - t_o) \equiv X_R(t)$$

The velocity  $v$  goes linearly from  $v_l$  on the left up to  $v_m$  on the right and

$$\rho = \rho_l \left( 1 + \frac{\gamma-1}{2} \frac{v_l - v}{c_l} \right)^{\frac{2}{\gamma-1}}$$

$$P = P_l \left( 1 + \frac{\gamma-1}{2} \frac{v_l - v}{c_l} \right)^{\frac{2\gamma}{\gamma-1}}$$

In the region

$$X_R(t) < X < X_o + v_m (t - t_o)$$

the values are  $P_m$ ,  $\rho_{lm}$ , and  $v_m$ . In the region

$$X_o + v_m(t-t_o) < X < X_o + v_s(t-t_o)$$

the values are  $\rho_{mr}$ ,  $P_m$ ,  $v_m$ . In the region

$$X > X_o + v_s(t-t_o)$$

the values are  $P_r$ ,  $\rho_r$ ,  $v_r$ .

c. Application as a Code Test Problem

(1) Eulerian Input

(a) Initial values

For  $X \leq X_{sl}(0)$ , the values are  $P_l$ ,  $v_l$ ,  $\rho_l$

For  $X_{sl}(0) < X \leq X_{sr}(0)$ , the values are  $P_{lr}$ ,  $v_{lr}$ ,  $\rho_{lr}$

For  $X > X_{sr}(0)$ , the values are  $P_r$ ,  $v_r$ ,  $\rho_r$

These values are determined when  $P_r$ ,  $v_r$ ,  $\rho_r$ ,  $P_{lr}$ , and  $P_l$  are given.

(b) Boundary values

At  $X = 0$ , hold the values at  $P_l$ ,  $v_l$ ,  $\rho_l$

(2) Lagrangian Input

(a) Initial values

Same as Eulerian

(b) Boundary values

At  $X(0,t) = v_l t$ , the values should be  $P_l$ ,  $v_l$ ,  $\rho_l$

(3) Numerical values for Sctp-VII

(a) Sctp-VII-A

$$\Delta X = 1 \text{ meter}$$

$$X_{sl}(0) = 75 \text{ meters}$$

$$X_{sr}(0) = 100 \text{ meters}$$

$$P_r = 10^4 \text{ dynes/cm}^2$$

$$\rho_r = 10^{-6} \text{ gm/cm}^2$$

$$v_r = 0$$

$$P_{lr} = 10^6 \text{ dynes/cm}^2$$

$$P_l = 10^{12} \text{ dynes/cm}^2$$

Right boundary at 200 meters

These values yield

$$c_l \doteq 1.97 \times 10^8 \text{ cm/sec}$$

$$v_l \doteq 3.82 \times 10^8 \text{ cm/sec}$$

$$\rho_l \doteq 3.60 \times 10^{-5} \text{ gm/cm}^3$$

$$v_s \doteq 4.56 \times 10^8 \text{ cm/sec}$$

$$v_{sr} \doteq 1.095 \times 10^7 \text{ cm/sec}$$

$$t_o \doteq 1.683 \times 10^{-5} \text{ sec}$$

$$X_o \doteq 1.018 \times 10^4 \text{ cm}$$

$$P_m \doteq 3.32 \times 10^{11} \text{ dynes/cm}^2$$

$$v_{lr} \doteq 9.13 \times 10^6 \text{ cm/sec}$$

$$\rho_{lr} \doteq 5.997 \times 10^{-6} \text{ gm/cm}^3$$

$$v_m \doteq 5.26 \times 10^8 \text{ cm/sec}$$

$$v_s \doteq 6.31 \times 10^8 \text{ cm/sec}$$

$$\rho_{ml} \doteq 1.63 \times 10^{-5} \text{ gm/cm}^3$$

$$\rho_{mr} \doteq 6.000 \times 10^{-6} \text{ gm/cm}^3$$

A reasonable output recipe is print at  $1 \times 10^{-5}$ ,  $1.683 \times 10^{-5}$  (time of overtake), and  $3 \times 10^{-5}$  sec.

(b) SCTP-VII-B

Same as A except

$$\Delta X = 1 \text{ centimeter}$$

$$X_{sl}(0) = 75 \text{ centimeters}$$

$$X_{sr}(0) = 100 \text{ centimeters}$$

Right boundary at 200 centimeters

A reasonable output recipe is print at  $1 \times 10^{-7}$ ,  $1.683 \times 10^{-7}$  (time of overtake), and  $3 \times 10^{-7}$  sec.

(4) Comments on the Computer Solution

(a) General

The computer solution should be in agreement until the rarefaction wave or the shock wave reaches a boundary. The difference between A and B is just the scaling of the space mesh. This variation was introduced to see what, if any, changes in the computer solution that space scaling would introduce. It, of course, should not produce any changes in the computer if the code behaves properly.

(b) PUFF

There was no discernible difference in the PUFF solutions of A and B other than the scale change. They both took 1642 cycles and about 110 seconds CP time to run to  $3 \times 10^{-5}$  sec. Density-specific internal energy spikes are the most noticeable errors. Hot-thin spikes were formed at the initial shock positions and a cold-thick spike was formed at the overtake position. See tables VII-A and VII-B. In the tables,  $X_{Dl}$  stands for the position of the fluid particle that was at the left hand shock front at time zero.



Table VII-A

## PUFF ERROR TABLE FOR SCTP-VII-A

Problem time =  $3 \times 10^{-5}$  sec

PUFF cycle = 1642

Computer time = 108 sec

Number of active zones = 201

	<u>Sum Sqr. Err.</u>	<u>Max. Err.</u>	<u>Position of Max. Err.</u>
Pressure	0.0151	-0.184	$X_s$
Velocity	0.0399	+0.467	$X_s$
Density	0.0301	-0.234	$X_{D\ell}$
	<u>Sum Int. Energy</u>	<u>Sum Kin. Energy</u>	<u>Sum Tot. Energy</u>
EXACT	$9.374 \times 10^{15}$	$1.489 \times 10^{16}$	$2.426 \times 10^{16}$
PUFF	$9.370 \times 10^{15}$	$1.488 \times 10^{16}$	$2.425 \times 10^{16}$

Table VII-B

## PUFF ERROR TABLE FOR SCTP-VII-B

Problem time =  $3 \times 10^{-7}$  sec

PUFF cycle = 1642

Computer time = 109 sec

Number of active zones = 201

	<u>Sum Sqr. Err.</u>	<u>Max. Err.</u>	<u>Position of Max. Err.</u>
Pressure	0.0151	-0.184	$X_s$
Velocity	0.0399	+0.467	$X_s$
Density	0.0301	-0.234	$X_{D\ell}$
	<u>Sum Int. Energy</u>	<u>Sum Kin. Energy</u>	<u>Sum Tot. Energy</u>
EXACT	$9.374 \times 10^{13}$	$1.489 \times 10^{14}$	$2.426 \times 10^{14}$
PUFF	$9.370 \times 10^{13}$	$1.488 \times 10^{14}$	$2.425 \times 10^{14}$

AFWL-TR-67-127

This page intentionally left blank.

## APPENDIX I

## ON THE EQUATIONS MODELING LINEAR FLOW GAS HYDRODYNAMICS

We are going to inspect the typical mathematical model of an air-like gas; that is, a gas which nearly satisfies the following characteristics:

homogeneous

compressible

inviscid (nonviscous, no internal friction)

nonconducting (no heat transfer)

ideal or perfect equation of state  $(PV = RT = (\gamma - 1) e)$

The terms gas and fluid will be used interchangeably in the following.

Consider fluid flowing in a frictionless, insulated pipe. Let us establish some coordinate systems. We will label points in the fluid and call this the Lagrangian coordinate system. We will label points on the pipe and call that the Eulerian coordinate system. Stated another way, the Lagrangian coordinate system is fixed in the fluid and the Eulerian coordinate system is fixed on the pipe. As to notation,  $x$  will be used as a label for the fluid points and  $X$  will be used as a label for the pipe points.

Let  $A$  be the cross-sectional area of the pipe.  $A$  is taken as a constant independent of  $X$  and time. Also, the cross-sectional shape is taken as a constant independent of  $X$  and time. Therefore, the pipe and the fluid may be thought of as one-dimensional continuums, i.e., topologically equivalent to some interval of the real line, e.g., the unit interval from 0 to 1. This is because in any cross section of the fluid perpendicular to the axis of the pipe, all the properties of the fluid are constant, e.g., fluid velocity, density, pressure, etc. The foregoing defines what we mean by linear flow.

Consider the mass  $m$  of fluid between the fluid points labeled  $x - \Delta x$  and  $x + \Delta x$ . This mass is constant because  $x - \Delta x$  and  $x + \Delta x$  are the labels of fixed points in the fluid (not necessarily fixed with respect to the pipe) and we are demanding the conservation of mass. Let  $\chi(x, t)$  denote the Eulerian coordinate at time  $t$  of the fluid point labeled  $x$ . Often  $X(x, 0) = x$  is taken

as a defining relationship between the fluid labels and the pipe labels. We will follow this convention. Likewise,  $\rho(x,t)$  will denote the mass density of the fluid at time  $t$  and at the fluid point labeled  $x$ .

$$\rho(x,t) \geq 0$$

Let

$$\hat{\rho}(X(x,t),t) = \rho(x,t)$$

i.e.,  $\hat{\rho}$  is the density in the Eulerian coordinate system, whereas  $\rho$  is the density in the Lagrangian coordinate system. The mass between the fluid points labeled  $x - \Delta x$  and  $x + \Delta x$  at time  $t$  is defined by

$$m = A \int_{X(x-\Delta x,t)}^{X(x+\Delta x,t)} \hat{\rho}(X,t) dX$$

Now at time  $t = 0$ ,

$$m = A \int_{x-\Delta x}^{x+\Delta x} \rho(x,0) dx$$

Therefore, by conservation of mass,

$$\int_{x-\Delta x}^{x+\Delta x} \rho(x,0) dx = \int_{X(x-\Delta x,t)}^{X(x+\Delta x,t)} \hat{\rho}(X,t) dX$$

Let us make a change of variables; then

$$\int_{X(x-\Delta x,t)}^{X(x+\Delta x,t)} \hat{\rho}(X,t) dX = \int_{x-\Delta x}^{x+\Delta x} \rho(x,t) \frac{\partial X}{\partial x} dx$$

So, we have

$$\int_{x-\Delta x}^{x+\Delta x} \rho(x,0) dx = \int_{x-\Delta x}^{x+\Delta x} \rho(x,t) \frac{\partial X}{\partial x} dx$$

Therefore, under differentiability assumptions, the integral equation can be expressed by the following differential equation:

$$\rho(x,0) = \rho(x,t) \frac{\partial X}{\partial x}(x,t)$$

This is called the conservation of mass equation.

The velocity,  $v(x,t)$ , is defined by

$$v(x,t) = \frac{\partial X}{\partial t}(x,t)$$

Newton's second law says that the sum of the external forces applied to a rigid body is equal to the time rate of change of momentum of the rigid body. Consider the interval of fluid between the fluid points labeled  $x + \Delta x$  and  $x - \Delta x$ . This fluid interval is not a rigid body. However, the law still applies to this body if there are no internal frictional forces in the fluid. In the case of internal frictional forces in the fluid, we must modify Newton's law to say that the external force applied to the fluid interval is equal to the internal frictional forces plus the time rate of change of momentum. We now postulate that our fluid model has no internal frictional forces. Such a fluid is called nonviscous or inviscid. The external force (taken as positive when in the direction of increasing  $x$ ) on the interval at time  $t$  is

$$A(P(x-\Delta x,t) - P(x+\Delta x,t))$$

The momentum of the body at time  $t$  is

$$A \int_{x-\Delta x}^{x+\Delta x} \rho(\zeta,0) v(\zeta,t) d\zeta$$

Thus, Newton's second law yields

$$\int_{x-\Delta x}^{x+\Delta x} \rho(\zeta, 0) (v(\zeta, t+\Delta t) - v(\zeta, t)) d\zeta = \int_t^{t+\Delta t} (P(x-\Delta x, \tau) - P(x+\Delta x, \tau)) d\tau$$

Under differentiability assumptions, this integral equation may be written as the following differential equation:

$$\rho(x, 0) \frac{\partial v}{\partial t}(x, t) = - \frac{\partial P}{\partial x}(x, t)$$

This is called the conservation of momentum equation.

Now we will see what relation the principle of energy conservation will produce. Let  $E(x, t)$  be the specific energy at point  $x$  and time  $t$ , i.e.,  $x - \Delta x$ ,  $x + \Delta x$  at time  $t$  is

$$A \int_{x-\Delta x}^{x+\Delta x} \rho(x, 0) E(x, t) dx$$

The conservation of energy principle states that the increase in the total energy of an interval is equal to the work done on the interval plus any energy in the form of heat which is transferred to the interval. We now postulate that there will be no heat transfer in our fluid model. Therefore, energy conservation in our model is expressed in the following way:

$$\int_{x-\Delta x}^{x+\Delta x} \rho(x, 0) (E(x, t+\Delta t) - E(x, t)) dx = \int_t^{t+\Delta t} P(x-\Delta x, \tau) v(x-\Delta x, \tau) d\tau - \int_t^{t+\Delta t} P(x+\Delta x, \tau) v(x+\Delta x, \tau) d\tau$$

Under differentiability assumptions, this integral equation may be written as the following differential equation:

$$\rho, 0) \frac{\partial E}{\partial t}(x, t) = - \frac{\partial P v}{\partial x}(x, t)$$

This is called the conservation of energy equation. The total energy is composed of the internal energy and the kinetic energy. This is expressed by

$$E(x, t) = e(x, t) + 1/2 v^2(x, t)$$

where  $e(x, t)$  is the specific internal energy. (This could be thought of as the defining equation for  $e$ .) This relation says that the total specific energy is the sum of the specific internal energy and the specific kinetic energy. Using the three foregoing conservation equations, we can derive the following relation:

$$0 = \frac{\partial e}{\partial t} + P \frac{\partial V}{\partial t}$$

The laws of thermodynamics say  $TdS = de + dW$ , and in our fluid model, we postulate that all work is  $PdV$  work (this postulate may be provable from the homogeneous fluid postulate). So the equation

$$0 = \frac{\partial e}{\partial t} + P \frac{\partial V}{\partial t}$$

says that the entropy is constant for each  $x$ . This is called an isentropic process. This process is not necessarily homentropic.\* We postulate the so-called perfect or ideal gas equation of state  $PV = RT = (\gamma-1)e$  where  $R$  and  $\gamma$  are gas constants and  $T$  is the temperature. If we are not undergoing a shock transition or passing through any other discontinuity, then  $PV = (\gamma-1)e$  and  $TdS = de + PdV$  (the first law of hydrodynamics) yield

$$\frac{P}{P_0} = \left( \frac{\rho}{\rho_0} \right)^\gamma e^{\left( \frac{S-S_0}{C_V} \right)}$$

---

\*In general,  $S(x, t)$  is constant in neither  $x$  nor  $t$ . If it is constant in  $t$  but not necessarily in  $x$ , then we say the process is isentropic. If it is constant in both  $t$  and  $x$ , then we say the process is homentropic.

where

$$C_V \equiv \left. \frac{dQ}{dT} \right|_{V \text{ const}}$$

$$C_P \equiv \left. \frac{dQ}{dT} \right|_{P \text{ const}}$$

$$\gamma = \frac{C_P}{C_V}$$

and

$$R = (\gamma - 1)C_V$$

And if  $0 = de + PdV$ , then

$$\frac{P}{P_0} = \left( \frac{\rho}{\rho_0} \right)^\gamma$$

However, for a fluid interval passing in time  $\Delta t$  through a shock traveling to the right where the pressure on the left is  $P_\ell$  and on the right is  $P_r$ , we have

$$\int_t^{t+\Delta t} TdS = e_\ell - e_r + P_\ell v_\ell - P_r v_r$$

as was shown in the shock relations discussion in SCTP-I. Using the shock relations, we can prove that  $e_\ell - e_r + P_\ell v_\ell - P_r v_r > 0$ . Therefore, there is an entropy increase across the shock! But we just "proved" by using the three conservation equations that the process was isentropic! How did this contradiction arise? It arose through the assumption that all quantities were smooth, i.e., that the quantities in the equations

$$\frac{v}{v_0} = \frac{\partial X}{\partial x} \quad (\text{conservation of mass})$$

$$\frac{\partial^2 X}{\partial t^2} = - \frac{1}{\rho_0} \frac{\partial P}{\partial x} \quad (\text{conservation of momentum})$$

$$\frac{\partial E}{\partial t} = - \frac{1}{\rho_0} \frac{\partial Pv}{\partial x} \quad (\text{conservation of energy})$$



were defined. But they are not defined across a shock for there  $E$ ,  $P$ ,  $V$ ,  $v$  are discontinuous by the definition of a shock. (Notice that the derivation did prove, however, that when the flow is smooth, it is isentropic.) Another mistake that is sometimes made is in using the first law of thermodynamics,  $dQ = de + PdV$ , and the statement that the process is adiabatic (no heat transfer) to arrive at the relation  $0 = de + PdV$ . The error in this argument is that  $dQ$  is composed of two parts,  $dQ$  internal +  $dQ$  external. Saying that the process is adiabatic is saying that there is no heat transfer to or from the system, i.e.,  $dQ$  external = 0. But there may also be internal friction in the fluid. If there are internal frictional forces acting, then  $dQ$  internal > 0, so that  $dQ > 0$  when  $dQ$  external = 0. When  $dQ = 0$ , the process is isentropic, for the entropy is defined by  $TdS = dQ$ . But it could happen that the process is adiabatic but not isentropic, i.e.,  $dQ$  external = 0,  $dQ$  internal > 0. And it could happen that the process is isentropic but not adiabatic, i.e.,  $dQ$  internal > 0, but  $dQ$  external < 0 and also  $dQ$  internal +  $dQ$  external = 0. Thus, adiabatic and isentropic are two entirely different processes. Our no-heat-transfer postulate implies that we have an adiabatic process in our model, i.e.,  $dQ$  external = 0. But we have shown that our model is not isentropic when shocks occur. And we have assumed that the fluid was inviscid. The three previous statements are contradictory. Proof: The entropy increases across a shock; therefore,  $dQ > 0$ . The process is adiabatic; therefore,  $dQ$  external = 0. Hence,  $dQ = dQ$  internal > 0 across a shock. Therefore, there are internal frictional forces acting. This is a contradiction since we assumed the fluid to be inviscid! Thus, the postulates assumed for our model are contradictory. Let us review our principles and postulates:

Principle of conservation of mass

Principle of conservation of momentum

Principle of conservation of energy

Principle of monotone increasing entropy

Postulate of homogeneous fluid

Postulate of compressible fluid

Postulate of nonviscous fluid

Postulate of nonconducting fluid

Postulate of ideal equation of state

Postulate of  $dW = PdV$

To produce a self-consistent model, we must throw out or modify some of the postulates. The criteria for this remodeling will come from a closer look at what we are trying to model. So, let us have a closer look at air. The best resolution of the dilemma seems to be to recognize that the fluid we are trying to model has a very small viscosity (it also has a very small heat conductivity but the more satisfactory resolution seems to be in the modification of the inviscid postulate), and that this viscosity is not appreciable except at the places that  $\partial^2 v / \partial X^2$  is large. The inclusion of viscosity prevents the occurrence of shocks. The internal frictional force depends on the product of the viscosity number and  $\partial^2 v / \partial X^2$ . Thus, the entropy increase depends on this product. As the viscosity number goes to zero,  $\partial^2 v / \partial X^2$  can become larger and larger and apparently the limit of the product is finite but not zero. So, we effectively have an "implicit point viscosity." That is, the viscosity effect (entropy increase) is felt only at points where  $\partial^2 v / \partial X^2$  is infinite, i.e., at shocks. The object of the remodeling is, therefore, to define the solution of the limit to be the limit of the solution of the equations including the viscosity as the viscosity goes to zero. So we alter the inviscid postulate to "the fluid is inviscid except at shocks and there the viscosity effects (entropy increase) are those described by the shock relations." Notice that the erroneous derivation of  $0 = de + PdV$  can lead to a success for shocks if it is differenced like the Rankine-Hugoniot relation. That is, the Rankine-Hugoniot relation is

$$0 = e_l - e_r + \frac{P_l + P_r}{2} (v_l - v_r)$$

And if the difference scheme used were

$$0 = e_I^{n+1} - e_I^n + \frac{P_I^{n+1} + P_I^n}{2} (v_I^{n+1} - v_I^n)$$

where  $e_I^n$  is the approximation to  $e(n\Delta t, I\Delta x)$ , then the difference scheme will be correct across shocks. But it does not conserve the entropy in nonshock

regions.\* It also does not explicitly conserve the total energy. Suppose we wish to write the equations in terms of the  $(X,t)$  system instead of the  $(x,t)$  system. That is, suppose the Eulerian formulation is desired instead of the Lagrangian. The transformation from the Eulerian system to the Lagrangian system may be expressed in this manner:

$$\frac{\partial}{\partial t} \text{ in } (x,t) \longleftrightarrow \frac{\partial}{\partial t} + \frac{\partial X}{\partial t} \frac{\partial}{\partial X} \text{ in } (X,t)$$

$$\frac{1}{\rho(x,0)} \frac{\partial}{\partial x} \text{ in } (x,t) \longleftrightarrow \frac{1}{\hat{\rho}(X,t)} \frac{\partial}{\partial X} \text{ in } (X,t)$$

The first relation follows from the chain rule and expresses the so-called convection derivative. The second relation just expresses the conservation of mass

$$\frac{\rho_0}{\rho} = \frac{\partial X}{\partial x}$$

The Lagrangian formulation is

$$\frac{v}{v_0} = \frac{\rho_0}{\rho} = \frac{\partial X}{\partial x} \quad (\text{conservation of mass})$$

$$v = \frac{\partial X}{\partial t} \quad (\text{definition of velocity})$$

$$\frac{\partial v}{\partial t} = - \frac{1}{\rho_0} \frac{\partial P}{\partial x} \quad (\text{momentum conservation})$$

$$\frac{\partial E}{\partial t} = - \frac{1}{\rho_0} \frac{\partial P v}{\partial x} \quad (\text{energy conservation})$$

$$E = e + 1/2 v^2 \quad (\text{definition of internal energy})$$

$$e = \frac{P V}{\gamma - 1} \quad (\text{equation of state})$$

---

\*As a matter of fact, for  $\rho^{n+1}/\rho^n$  near 1, the entropy error is  $\Delta S \sim C_V(\gamma-1/2) (1-\rho^{n+1}/\rho^n)$ . Thus, we have an "entropy increase" if  $\rho^{n+1} < \rho^n$  and an "entropy decrease" if  $\rho^{n+1} > \rho^n$ .

The conservation of mass equation will not transform satisfactorily as it is because  $X$  is to be an independent variable in the Eulerian formulation. So it is expressed in terms of the velocity by taking the time derivative of both sides:

$$\frac{\partial V}{\partial t} = \frac{1}{\rho_0} \frac{\partial v}{\partial x}$$

Notice another differentiability assumption is required here; the transformation yields

$$\frac{\partial V}{\partial t} + \frac{\partial X}{\partial t} \frac{\partial V}{\partial X} = \frac{1}{\rho} \frac{\partial v}{\partial X}$$

$$\frac{\partial v}{\partial t} + \frac{\partial X}{\partial t} \frac{\partial v}{\partial X} = - \frac{1}{\rho} \frac{\partial P}{\partial X}$$

$$\frac{\partial E}{\partial t} + \frac{\partial X}{\partial t} \frac{\partial E}{\partial X} = - \frac{1}{\rho} \frac{\partial P v}{\partial X}$$

And, of course,

$$v = \frac{\partial X}{\partial t}$$

so the Eulerian formulation is

$$\frac{\partial V}{\partial t} + v \frac{\partial V}{\partial X} = \frac{1}{\rho} \frac{\partial v}{\partial X}$$

$$\frac{\partial v}{\partial t} + v \frac{\partial v}{\partial X} = - \frac{1}{\rho} \frac{\partial P}{\partial X}$$

$$\frac{\partial E}{\partial t} + v \frac{\partial E}{\partial X} = - \frac{1}{\rho} \frac{\partial P v}{\partial X}$$

and

$$E = 1/2 v^2 + \frac{Pv}{\gamma-1}$$

APPENDIX II  
SOLUTION METHODS

1. Method of Finite Differences	116
2. Method of Lines	132
3. Method of Characteristics	132
4. Analog Methods	132
5. Hybrid Methods	132

# 1. Method of Finite Differences

For illustrative purposes, we are going to use a linear approximation to the hydrodynamic equations.

The equations describing an isentropic flow may be written (see Appendix I):

$$\frac{\rho_o}{\rho} = \frac{\partial X}{\partial x}$$

$$\frac{\partial^2 X}{\partial t^2} = \frac{1}{\rho_o} \frac{\partial P}{\partial x}$$

$$P = k \rho^\gamma$$

where

$$k \equiv \frac{P_o}{\rho_o^\gamma}$$

and

$$\rho_o \equiv \rho(x, 0)$$

$$P_o \equiv P(x, 0)$$

So,

$$P = P_o \cdot \left( \frac{\partial X}{\partial x} \right)^{-\gamma}$$

and

$$\frac{\partial^2 X}{\partial t^2} = - \frac{1}{\rho_o} \frac{\partial}{\partial x} P_o \left( \frac{\partial X}{\partial x} \right)^{-\gamma} = - \frac{1}{\rho_o} \left( \frac{\partial X}{\partial x} \right)^{-\gamma} \frac{\partial P_o}{\partial x} + \frac{\gamma P_o}{\rho_o} \left( \frac{\partial X}{\partial x} \right)^{-(\gamma+1)} \frac{\partial^2 X}{\partial x^2}$$

Therefore, using

$$\frac{P}{P_o} = \left( \frac{\partial X}{\partial x} \right)^{-\gamma}$$

again, we have

$$\frac{\partial^2 X}{\partial t^2} = - \frac{1}{\rho_o} \frac{P}{P_o} \frac{\partial P_o}{\partial x} + \frac{\gamma P_o}{\rho_o} \left( \frac{P}{P_o} \right)^{\frac{\gamma+1}{\gamma}} \frac{\partial^2 X}{\partial x^2}$$

Under the assumptions that

$$\frac{\partial P}{\partial x} (x, 0)$$

is near zero and  $P/P_0$  is near 1, the above equation is approximated by

$$\frac{\partial^2 X}{\partial t^2} = \frac{\gamma P_0}{\rho_0} \frac{\partial^2 X}{\partial x^2}$$

$$C_0^2 \equiv \frac{\gamma P_0}{\rho_0}$$

$$C_0 > 0$$

$C_0$  is called the ambient isentropic sound speed. Here

$$C_0 = C(x, 0)$$

but we will take it to be a constant for simplicity in the succeeding illustrations. So, our equation for illustrative purposes will be

$$\frac{\partial^2 X}{\partial t^2} = C_0^2 \frac{\partial^2 X}{\partial x^2} \quad (2)$$

This linear second-order hyperbolic partial differential equation is called the wave equation. If central differences are used, the difference equation for the wave equation is

$$\frac{X_I^{n+1} - 2X_I^n + X_I^{n-1}}{\Delta t^2} = C_0^2 \frac{X_{I+1}^n - 2X_I^n + X_{I-1}^n}{\Delta x^2}$$

where  $X_I^n$  is to approximate  $X(I\Delta x, n\Delta t)$ . That is,  $X_I^n$  is the solution to the difference problem at the mesh point  $(n, I)$  which is the point  $(n\Delta t, I\Delta x)$  in the  $tx$  plane and, therefore,  $X_I^n$  is the difference solution which will hopefully approximate  $X(I\Delta x, n\Delta t)$ , the differential solution. At this point, we pose a question known as the Convergence Problem: Will the solutions to the difference

problem,  $x_I^n$ , converge to the solution to the differential problem,  $X(x,t)$ , as  $\Delta x, \Delta t \rightarrow 0$ ? The answer to this problem in the linear case depends upon a number,  $\phi$ , known as the Courant-Friedrichs-Lewy number

$$\phi \equiv \frac{C_o \Delta t}{\Delta x}$$

If  $\phi \leq 1$ , the answer is yes. Sometimes  $\phi$  is referred to as the CFL number. It is called this because the answer to the Convergence Problem in the linear case was established in Courant, Friedrichs, and Lewy's 1928 MATH ANNALEN paper. John von Neumann made a conjecture that generalizes this result to the nonlinear equations. It is essentially that if

$$\frac{C \Delta t}{\Delta x} \leq 1$$

for all  $x$  and  $t$  ( $C = C(x,t)$ ), then convergence would prevail in the nonlinear case also. This conjecture has not been proved. Experience indicates that it is reasonable and this is the condition used in current hydrocodes with only slight modifications. The foregoing difference equation may be arranged in the following form:

$$x_I^{n+1} = 2x_I^n - x_I^{n-1} + \phi^2 (x_{I+1}^n - 2x_I^n + x_{I-1}^n)$$

or

$$x_I^{n+1} = x_I^n (2 - 2\phi^2) - x_I^{n-1} + \phi^2 (x_{I+1}^n + x_{I-1}^n) \quad (3)$$

In this form, the difference equation can be solved in a "time marching" manner. That is, given the values of  $x_I^n, x_I^{n-1}$  for  $L \leq I \leq R$ , we can solve for the values of  $x_I^{n+1}$  for  $L+1 \leq I \leq R-1$ . Suppose we "solved" this difference equation on a machine which introduced round-off errors. That is, if we have a machine that has only a finite number of digits in its numbers, then it will make round-off errors in computing

$$x_I^n (2 - 2\phi^2) - x_I^{n-1} + \phi^2 (x_{I+1}^n + x_{I-1}^n)$$



We denote this round-off error by  $\varepsilon_I^n$ . We denote the machine solution by  $\tilde{X}(n, I)$ . We denote the total deviation of  $X(n, I)$  from  $\tilde{X}_I^n$  by  $\Delta_I^n$ , i.e.,

$$\Delta_I^n = \tilde{X}(n, I) - X_I^n$$

Now we pose a question known as the Stability Problem: Will the round-off errors

$$\varepsilon_I^m, 1 \leq m \leq n$$

introduced in the machine solution cause  $\tilde{X}(n, I)$  to drift so far away from  $X_I^n$  as to be useless as an approximation? As a first attack on the stability problem, we ask: If a single perturbation  $\varepsilon_I^m$  is introduced at the  $m$ th cycle and the resulting solution (with no other errors or perturbations introduced) is

$$X_I^n + \delta_I^n(m)$$

then does  $\delta_I^n(m)$  grow in time (i.e., with increasing  $n$ )? Sometimes the terminology "weak stability," "strong stability" is used in regard to the last two questions. That is, if the answer to the single perturbation question is no, then the difference equation solution is said to be weakly stable. If the answer to the stability problem question is no, then the difference equation solution is said to be strongly stable. Let

$$\Delta_I^n \equiv \tilde{X}(n, I) - X_I^n$$

for  $n = 1, 2, 3, \dots$ . Let  $\delta_I^{n+1}$  be the propagated error due to  $\Delta_I^n$  and  $\Delta_I^{n-1}$ . Then

$$\begin{aligned} X_I^{n+1} + \delta_I^{n+1} &= (X_I^n + \Delta_I^n)(2 - \zeta^2) - (X_I^{n-1} + \Delta_I^{n-1}) \\ &\quad + \zeta^2 (X_{I+1}^n + \Delta_{I+1}^n + X_{I-1}^n + \Delta_{I-1}^n) \end{aligned}$$

Subtracting the unperturbed equation (i.e., equation (3) which was

$$x_I^{n+1} = x_I^n (2 - 2\zeta^2) - x_I^{n-1} + \zeta^2 (x_{I+1}^n + x_{I-1}^n)$$

yields

$$\delta_I^{n+1} = \Delta_I^n (2 - 2\zeta^2) - \delta_I^{n-1} + \zeta^2 (\delta_{I+1}^n + \delta_{I-1}^n)$$

If  $\Delta_I^n, \delta_I^{n-1}$  are just propagated errors themselves, we could write

$$\delta_I^{n+1} = \delta_I^n (2 - 2\zeta^2) - \delta_I^{n-1} + \zeta^2 (\delta_{I+1}^n + \delta_{I-1}^n) \quad (4)$$

This is called the equation of first variation of equation (3). It is the equation for the propagation of perturbations of equation (3). Notice that the equation of first variation of equation (3) is the same equation as equation (3). That is, the equation of first variation of the wave difference equation is again the wave difference equation. This is always true for linear difference equations. Proof: Let

$$L[X+\delta] = L[X] + L[\delta]$$

by linearity. So that

$$L[X+\delta] - L[X] = L[\delta]$$

Therefore, the equation of first variation is

$$L[\delta] = 0$$

Note that in the equation of first variation, the introduction of new round-off errors is not taken into account. Thus, including the total round-off error at the last step,  $\epsilon_I^{n+1}$ , the total error at cycle  $n+1$  is

$$\delta_I^{n+1} + \epsilon_I^{n+1}$$

and this is by definition  $\Delta_I^{n+1}$ ; so

$$\Delta_I^{n+1} = \delta_I^{n+1} + \epsilon_I^{n+1}$$

That is, the machine solution is

$$X(n+1, I) = X_I^{n+1} + \delta_I^{n+1} + \epsilon_I^{n+1} = X_I^{n+1} + \Delta_I^{n+1}$$

Now we ask if there is some restriction on  $\Delta t$  and  $\Delta x$  such that the propagated errors do not grow. The answer to the Stability Problem question turns out to be the same as the Convergence Problem question, i.e.,  $\phi \leq 1$  is the condition on  $\Delta t$  and  $\Delta x$ . That the answers should be the same is plausible from this point of view: The differential and the machine solutions can both be considered as perturbations of the difference solution. Then a necessary condition for both convergence and stability is that perturbations do not grow unboundedly in the difference equation. The condition  $\phi \leq 1$  yields the result that perturbations do not grow.

We will now look at John von Neumann's method of analyzing the perturbation growth or error propagation problem. Consider the propagation equation

$$\delta_I^{n+1} = \delta_I^n (2 - 2\phi^2) - \delta_I^{n-1} + \phi^2 (\delta_{I+1}^n + \delta_{I-1}^n)$$

The solutions to this equation may be written in terms of a Fourier series. A typical term of the series being

$$a_k e^{ikx} e^{\alpha t}$$

where  $k$  is an integer. We plug this term into the above difference equation and solve for  $\alpha$  in terms of  $\phi^2$ .

$$\begin{aligned} a_k e^{ik\Delta x I} e^{\alpha(n+1)\Delta t} &= a_k e^{ik\Delta x I} e^{\alpha n \Delta t} (2 - 2\phi^2) - a_k e^{ik\Delta x I} e^{\alpha(n-1)\Delta t} \\ &+ \phi^2 \left( a_k e^{ik\Delta x (I+1)} e^{\alpha n \Delta t} + a_k e^{ik\Delta x (I-1)} e^{\alpha n \Delta t} \right) \end{aligned}$$

or

$$e^{\alpha \Delta t} = (2 - 2\phi^2) - e^{-\alpha \Delta t} + \phi^2 (e^{i\Delta x k} + e^{-i\Delta x k})$$

So we have  $\alpha$  defined implicitly as a function of  $k$  and  $\phi^2$ . We can prove that if  $\phi^2 \leq 1$ , then the real part of  $\alpha$  is  $\leq 0$ . Therefore, for  $\phi^2 \leq 1$ , the  $k$  frequency component of the solution to the error propagation equation will not

grow in time (because the  $k$  frequency component term is  $a_k e^{ikx} e^{at}$ ). This holds for all  $k$ .

The condition  $\phi^2 \leq 1$  implies  $\phi \leq 1$  which is

$$\frac{C_o \Delta t}{\Delta x} \leq 1$$

This condition is known as the Courant or Courant-Friedrichs-Levy or CFL condition. It is the condition for both convergence and stability of the wave difference equation.

The condition

$$\frac{C_o \Delta t}{\Delta x} \leq 1$$

has a geometric interpretation in terms of the domain of dependence of the solutions to the differential and difference equation. If the initial data are given at time zero as  $X(x,0)$  and

$$\frac{dX}{dt}(x,0)$$

then the solution to the wave differential equation is given by D'Alembert's formula:

$$X(x,t) = 1/2 \left( X(x-C_o t, 0) + X(x+C_o t, 0) + \frac{1}{C_o} \int_{x-C_o t}^{x+C_o t} \frac{dX}{dt}(\xi, 0) d\xi \right)$$

Thus,  $X(x,t)$  depends on the initial data given on the interval

$$[x-C_o t, x+C_o t]$$

We may graphically describe the points that  $X(x,t)$  depends upon in figure A-1.

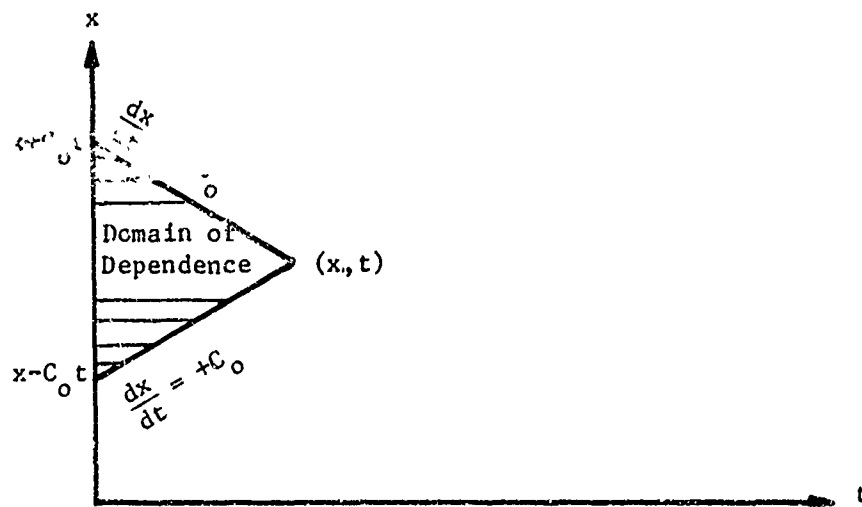


Figure A-1. Domain of Dependence Graph for the Differential Solution

Analogously, the domain of dependence of the difference solution  $x_I^n$  is graphed in figure A-2 and is seen to depend on the values

$$x_{I+1}^0 \text{ for } -n \leq i \leq n$$

and

$$x_{I+1}^1 \text{ for } -n+1 \leq i \leq n-1$$

The CFL condition

$$\frac{C_0 \Delta t}{\Delta x} \leq 1$$

requires that

$$\frac{\Delta x}{\Delta t} \geq C_0$$

This says that the slope of the bottom line should be greater than or equal to  $C_0$  and the slope of the top line should be less than or equal to  $-C_0$ . Superimposing the two graphs in the case  $\Delta x/\Delta t > C_0$  yields figure A-3.

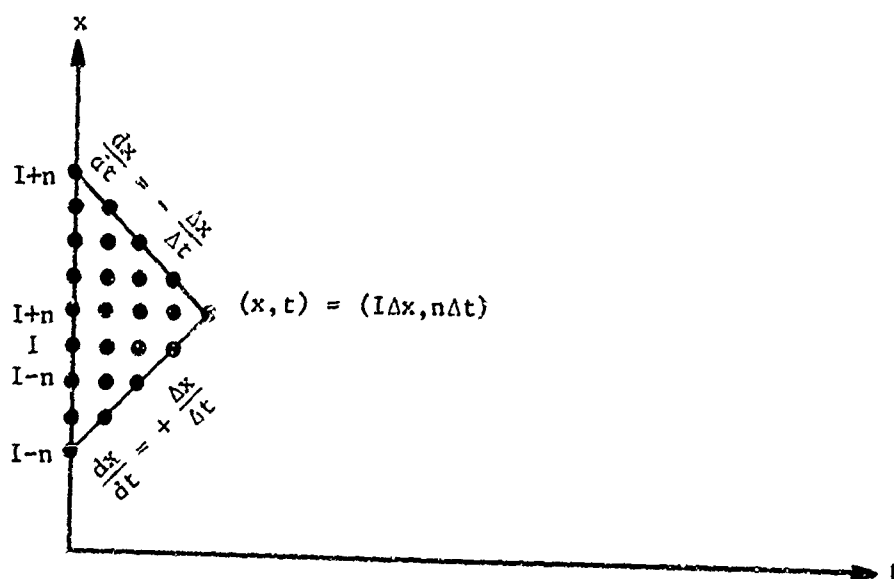


Figure A-2. Domain of Dependence Graph for the Difference Solution

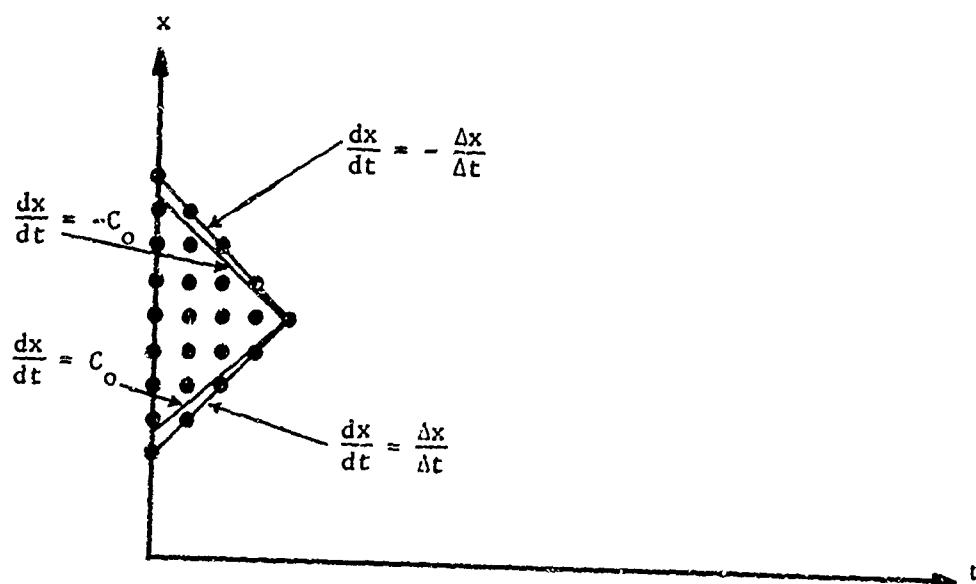


Figure A-3. Relationship of the Domains of Dependence

It is seen that the stability condition requires that the domain of dependence of  $X_I^n$  "overlap" the domain of dependence of  $X(n\Delta t, I\Delta x)$ . In other words,  $X_I^n$  should depend upon at least as much information (in the limit as  $\Delta x, \Delta t \rightarrow 0$ ) as  $X(n\Delta t, I\Delta x)$ .

At this point, we will explore a little farther into the parallel between the convergence problem and the stability problem. To reveal this, let us consider  $X_I^n$  as a perturbed solution of  $X(n\Delta t, I\Delta x)$ . (On the other hand,  $X(n\Delta t, I\Delta x)$  can be thought of as a perturbation of  $X_I^n$ ). That is, in the stability problem, the machine solution is a perturbed solution of the finite difference problem and the perturbations are the machine round-off errors. In the convergence problem, the perturbations are the deviations made in each cycle by using the difference method to advance to the next time level instead of the differential equation. To indicate the parallelism, we will redefine  $\Delta_I^n$ ,  $\epsilon_I^n$ ,  $\delta_I^n(m)$  as follows:

$$\Delta_I^n \equiv X(n\Delta t, I\Delta x) - X_I^n$$

$$\epsilon_I^n \equiv \text{the error introduced in proceeding to time } n\Delta t \text{ from time } (n-1)\Delta t \text{ via the difference equation rather than by the differential equation}$$

$$\delta_I^n(m) \equiv \text{the deviation due to the propagation of } \epsilon_I^m \text{ by the difference equation}$$

To give a precise equation for  $\epsilon_I^n$  and  $\delta_I^n(m)$ , we need to select an interpolation process in space and time to "fill in the gaps" between the  $X_I^n$ . That is, define a function  $X_x^t$  such that  $X_x^t = X_I^m$  (where  $t = m\Delta t$  and  $x = I\Delta x$ ) for  $m \leq n$  and such that

$$\frac{\partial X_x^t}{\partial t}$$

exists and is an approximation to

$$\frac{X_I^n - X_I^{n-1}}{\Delta t}$$

and  $X_x^t$  is defined also at all real  $x$  between the  $I\Delta x$  points.

One of the nicest ways to interpolate in  $x$  is to use the difference equation itself to fill in the gaps. That is, to determine  $X_x^{n\Delta t}$ , set up the original mesh so that for some  $I$ ,  $x = I\Delta x$ , then solve the difference equation for  $X_I^n$ , then set

$$X_x^{n\Delta t} = X_I^n$$

This can be visualized as a translation of the mesh of the difference solution in the space direction. To do something similar in time could be accomplished if we were given a "band of initial data" rather than a line of initial data, that is, initial data from  $t = 0$  to some  $t > 0$ . Then we could do a "time direction translation" of the mesh to determine  $X_{I\Delta x}^t$ . Perhaps a more practical method (because we are not normally given an initial band of data) would be to vary the initial time step in such a way as to produce a time direction translation of the mesh. That is, to define  $X_{I\Delta x}^t$ , let the initial time step be

$$t = \Delta t \cdot GI\left(\frac{t}{\Delta t}\right)$$

(where  $GI$  is the greatest integer function). Then let  $\Delta t$  be the timestep thereafter.

So, assume  $X_x^t$  is defined. Then, using D'Alembert's formula, the advance from  $X^n$  to  $X^{n+1}$  via the differential equation yields

$$X^*(t+\Delta t, x) = \frac{1}{2} \left( X_{x-C_0\Delta t}^t + X_{x+C_0\Delta t}^t + \frac{1}{C_0} \int_{x-C_0\Delta t}^{x+C_0\Delta t} \frac{\partial X_\xi^t}{\partial t} d\xi \right)$$

Then

$$\epsilon_I^{n+1} = X^*(t+\Delta t, x) - X_I^{n+1}$$

(where  $t = n\Delta t$  and  $x = I\Delta x$ ) and then  $\delta_I^{n+1}(m)$  is the propagation of  $\epsilon_I^m$  by equation (4). We know that the condition for the  $\delta_I^n(m)$  not to grow in time is that  $\beta \leq 1$ . So this is a necessary condition for convergence as well as for stability. In view of the geometric interpretation involving the domains of dependence, this is saying that it is necessary that the difference problem take into account at least as much information (initial data domain-wise) as the differential problem if it is to converge to the differential solution.



A physical interpretation of the

$$\frac{C_0 \Delta t}{\Delta x} \leq 1.$$

constraint is to consider the difference equation as a model of the signal propagation process and to interpret the constraint  $C_0 \Delta t \leq \Delta x$  as due to the fact that the difference relation only takes account of the interaction between adjacent zones and so the time step must be restricted so that signals cannot flow from, say, zone I to zone I + 2, but that only the signals from zones I + 1 and I - 1 may reach zone I in one time step.

It turns out that the condition  $\phi \leq 1$  is also sufficient for convergence. For proof, see the CFL paper. For a more general convergence proof for linear problems, see Lax's Equivalence Theorem in Richtmyer's Difference Methods for Initial Value Problems. We will give here the proof for convergence when  $\phi = 1$  because the proof is illuminating. Since

$$x_I^{n+1} = x_{I+1}^n - x_I^{n-1} + x_{I-1}^n + (\phi^2 - 1)(x_{I+1}^n - 2x_I^n + x_{I-1}^n)$$

when  $\phi^2 = 1$ , this becomes

$$x_I^{n+1} = x_{I+1}^n - x_I^{n-1} + x_{I-1}^n$$

One can see that the solution is

$$x_I^n = \sum_{i=0}^{2n} x_{I-n+1}^{\epsilon i} (-1)^i$$

where

$$\epsilon_{\text{even}} = 0$$

$$\epsilon_{\text{odd}} = -1$$

and  $x^0$  and  $x^{-1}$  are the initial conditions. The foregoing equation may be rearranged to

$$X_I^n = \frac{X_{I-n}^0 + X_{I+n}^0}{2} + \sum_{i=0}^{n-1} \frac{X_{I-n+2i+2}^0 + X_{I-n+2i}^0}{2} - X_{I-n+2i+1}^{-1}$$

By D'Alembert's formula

$$X(t, x) = \frac{1}{2} \left( X(0, x - C_0 t) + X(0, x + C_0 t) \right) + \frac{1}{2C_0} \int_{x-C_0 t}^{x+C_0 t} \frac{\partial X}{\partial t}(0, x') dx'$$

This may also be written

$$\begin{aligned} X(n\Delta t, I\Delta x) &= \frac{1}{2} \left( X(0, I\Delta x - nC_0 \Delta t) + X(0, I\Delta x + nC_0 \Delta t) \right) \\ &+ \frac{1}{2C_0} \int_{I\Delta x - nC_0 \Delta t}^{I\Delta x + nC_0 \Delta t} \frac{\partial X}{\partial t}(0, x') dx' \end{aligned}$$

Or using  $C_0 \Delta t$ , it may be written

$$\begin{aligned} X(n\Delta t, I\Delta x) &= \frac{1}{2} \left( X(0, (I-n)\Delta x) + X(0, (I+n)\Delta x) \right) \\ &+ \frac{1}{2C_0} \int_{(I-n)\Delta x}^{(I+n)\Delta x} \frac{\partial X}{\partial t}(0, x') dx' \end{aligned}$$

We also have

$$\frac{1}{2C_0} \int_{(I-n)\Delta x}^{(I+n)\Delta x} \frac{\partial X}{\partial t}(0, x') dx' \sim \sum_{j=0}^{n-1}$$

because the  $\sum$  is a  $\sum \Delta_t X_I$  and if we multiply by

$$\frac{1}{2} \frac{C_o \Delta t}{\Delta x} \left( \frac{2 \Delta x}{C_o \Delta t} \right)$$

we get

$$\frac{C_o \Delta t}{\Delta x} \left( \frac{1}{2 C_o} \sum_{I \text{ odd}} \frac{\Delta_t X_I}{\Delta t} \cdot 2 \Delta x \right)$$

which is

$$\frac{C_o \Delta t}{\Delta x} \frac{1}{2 C_o} \int_{x - \frac{C_o \Delta t}{2}}^{x + \frac{C_o \Delta t}{2}} \frac{\partial X}{\partial t} (0, x') dx'$$

but in this case

$$\phi = \frac{C_o \Delta t}{\Delta x} = 1$$

So, as  $\Delta t, \Delta x \rightarrow 0$  with  $\phi = 1$ , then  $X_I^n \rightarrow X(n \Delta t, I \Delta x)$ .

Moreover, the difference solution will yield the exact solution to the differential problem if  $X_I^{-1}$  is defined properly when  $\phi = 1$ . It is desired that

$$\frac{X_{I+1}^0 + X_{I-1}^0}{2} - X_I^{-1}$$

should approximate

$$\frac{1}{2} C_o \int_{I \Delta x - C_o \Delta t}^{I \Delta x + C_o \Delta t} \frac{\partial X}{\partial t} (0, x') dx'$$

If, after defining  $X_I^0 = X(0, I\Delta x)$ , we define

$$X_I^{-1} = \frac{X_{I+1}^0 + X_{I-1}^0}{2} - \frac{1}{C_0} \int_{I\Delta x - C_0 \Delta t}^{I\Delta x + C_0 \Delta t} \frac{\partial X}{\partial t}(0, x') dx'$$

then

$$\sum_{j=0}^{n-1} \frac{X_{I-n+2j+2}^0 + X_{I-n+2j}^0}{2} - X_{I-n+2j+1}^{-1} = \frac{1}{2C} \int_{I\Delta x - C_0 n \Delta t}^{I\Delta x - n C_0 \Delta t} \frac{\partial X}{\partial t}(0, x') dx'$$

by the additivity of the integral. So the difference solution is exactly the same at all points of the grid. At this point, one can make an interesting observation: By the proofs in the CFL paper, the difference solution converges to the differential solution for  $\mathcal{C} \leq 1$ . But the solution to

$$X_I^{n+1} = X_{I+1}^n - X_I^{n-1} + X_{I-1}^n$$

converges to

$$\frac{1}{2} \left( X\left(0, x - \frac{C_0}{\mathcal{C}} t\right) + X\left(0, x + \frac{C_0}{\mathcal{C}} t\right) \right) + \frac{1}{2C} \int_{x - \frac{C_0}{\mathcal{C}} t}^{x + \frac{C_0}{\mathcal{C}} t} \frac{\partial X}{\partial t}(0, x') dx'$$

For  $\mathcal{C} < 1$ , this amounts to a "smoothing" of the true solution. The actual equation is

$$X_I^{n+1} = X_{I+1}^n - X_I^{n-1} + X_{I-1}^n + (\mathcal{C}^2 - 1) \left( X_{I+1}^n - 2X_I^n + X_{I-1}^n \right)$$

$$\Delta_x^2 X_I^n = X_{I+1}^n - 2X_I^n + X_{I-1}^n$$

AFWL-TR-67-127

Dropping the  $\mathcal{E}^2 - 1 \Delta_x^2 X_I^n$  term when  $\mathcal{E} < 1$  is like adding its negative which we will denote

$$\lambda \Delta_x^2 X_I^n$$

where

$$\lambda \equiv 1 - \mathcal{E}^2 \geq 0$$

If the solution to

$$\begin{aligned} X_I^{n+1} = & X_{I+1}^n - X_I^{n-1} + X_{I-1}^n + (\mathcal{E}^2 - 1) X_{I+1}^n - 2X_I^n + X_{I-1}^n \\ & + \lambda \Delta_x^2 X_I^n \text{ for } 0 \leq \lambda \leq 1 - \mathcal{E}^2 \end{aligned}$$

is a continuous function of  $\lambda$ , then the solution varies from the exact solution at  $\lambda = 0$  to an evidently more and more smoothed solution as  $\lambda$  grows. Thus, the  $\lambda \Delta_x^2 X_I^n$  term seems to have a smoothing effect reminiscent of the viscosity. One might guess that as a function of  $\lambda$  of the solution being converged to would be like

$$\begin{aligned} X(t, x) = & \frac{1}{2} \left( X \left( 0, x - \frac{C_0}{\sqrt{1-\lambda}} t \right) + X \left( 0, x + \frac{C_0}{\sqrt{1-\lambda}} t \right) \right) \\ & + \frac{\sqrt{1-\lambda}}{2C_0} \int_{x - \frac{C_0 t}{\sqrt{1-\lambda}}}^{x + \frac{C_0 t}{\sqrt{1-\lambda}}} \frac{\partial X}{\partial t} (0, x') dx' \end{aligned}$$

since  $\mathcal{E} = \sqrt{1-\lambda}$ .

## 2. Methods of Lines

If, in the differential equation,

$$\frac{\partial^2 X}{\partial t^2} = C_o^2 \frac{\partial^2 X}{\partial x^2}$$

we difference only in space, we would have

$$\frac{\partial^2 X_I(t)}{\partial t^2} = C_o^2 \frac{X_{I+1}(t) - 2X_I(t) + X_{I-1}(t)}{\Delta X^2}$$

Then we have a system of ordinary differential equations. Getting approximate solutions to the partial differential equation by solving this system is called the Method of Lines.

## 3. Method of Characteristics

In Section II in the discussion of SCTP-II, the method of characteristics is discussed. For a discussion of a computer program to solve problems by the method of characteristics, see the report SC 4796(RR), "SWAP--A Computer Program for Shock Wave Analysis." For a discussion of the relative utility of the characteristic method and the fin diff method, see "On the Numerical Solution of the Hydro Equations" by Fyfe, Eng, and Young (Siam Review, Vol 3, No. 4, October 1961), in which the conclusion is: Method of characteristics is good for relatively simple problems. But for problems not so simple, the method of finite differences is to be preferred. Moreover, some problems are too complicated to handle by the Method of Characteristics.

## 4. Analog Methods

An electronic analog computer could be used to electronically solve the system by the method of lines, for example. Other analog techniques might be based upon the analogy between shallow water behavior and gas dynamics behavior. The use of wind tunnels is an Analog Method also.

## 5. Hybrid Computer Methods

A hybrid computer is a combination of analog and digital computers. For a report on this, see AFWL-TR-65-165, "Development of an Automatic Device for Solving Continuum Mechanics Problems."

### APPENDIX III

#### ERROR FORMATS AND ERROR FUNCTIONS

The first thing to be determined when testing a code is at precisely what time and place variables are computed by the code. Example: In PUFF, velocity is computed at the zone boundary, but density, pressure, and internal energy are zone center quantities.

Also, velocity is one half of the time step behind (timewise) the other variables in PUFF. When gradients are steep and fast moving, as in shocks, errors of 5 to 10 percent can easily be made by not plotting the variables at the correct time and place. Example: If one should plot PUFF's zone center quantities at zone boundaries and plot PUFF's velocity as if it were at the same time as the other variables, errors of 5 or 10 percent may be generated.

It is convenient to introduce the term 'primary variable.' By this, we mean a variable that the code actually computes in its cycle advancing routine. Example: In PUFF, the primary variables are X, the zone boundary position; D, the density; S, the stress or pressure; E, the internal energy; V, the velocity. Now, from these we can compute other variables such as momentum, kinetic energy, total energy, etc.

Those nonprimary variables which may be computed from the primary variables will be called secondary variables.

We wish to develop an "error function." This error function is to measure the "distance" between the exact solution and the code's solution. That is, it is to give us a number or numbers indicative of the "closeness" of the code's solution to the exact solution.

This question arises: What should the error function depend on?

In answering this question, the following point should be noted: If we check the error, for example, in momentum in PUFF, we must make an interpolation decision because momentum is the density-velocity product and PUFF computes these primary variables at different places. For this reason, we have answered the error function in this way: The error function should depend only on primary variables at the points in space and time where they

are computed; that is, only at zone boundaries for velocities and only at zone centers for density, internal energy, and pressure; also, only at those times these variables are computed. This eliminates interpolation decisions.

Now actually, PUFF's value at these points is supposed to be the average over the half zone to either side of the point (be it zone boundary or zone center). But the comparisons have all been made with the value of the exact solution at that point. Perhaps it would have been more fair to PUFF to take the exact solution and average it over the region composed of the half zone to the left and the half zone to the right and then compare this average with PUFF. But then the difficulty arises that PUFF may have made an error in its zone boundary positions. So, do we average over the region PUFF is averaging over or over the region the exact solution indicates we should average over?

We have answered the error function question by providing several numbers and graphs. We have provided the maximum error numbers, sum square error numbers, graphs indicating the characteristic and outstanding distortions, etc. We normalized the maximum error number and the sum square error number by dividing by the maximum absolute value of the variable taken on in the exact solution. The "point function" variables in PUFF which we check are the primary variables of PUFF, i.e., D, E, U, S, X. The other variables checked were the "set or interval functions" which were total energy, kinetic energy, and potential energy.

We now give precise definitions of the sum square error numbers and the maximum error numbers. Let  $\tilde{f}_I$  be the value of PUFF or whatever code is being tested. Let  $f_I$  be the exact solutions value at that place. Let N be the number of places or zones which are involved.

$$\text{sum square error} \equiv \sqrt{\frac{\sum_{I=1}^N (\tilde{f}_I - f_I)^2}{N}} \bigg/ \max_{1 \leq I \leq N} |f_I|$$

In PUFF, N is the number of active zones (JSTAR+1 in PUFF).

$$\text{maximum error} \equiv \frac{\max_{1 \leq I \leq N} |\tilde{f}_I - f_I|}{\max_{1 \leq I \leq N} |f_I|} * \text{sgn}(\tilde{f}_{I_{\max}} - f_{I_{\max}})$$



AFWL-TR-67-127

where  $I_{\max}$  is such that

$$|\tilde{f}_{I_{\max}} - f_{I_{\max}}| = \max_{1 \leq I \leq N} |\tilde{f}_I - f_I|$$

(It is possible that there could be more than one  $I_{\max}$ . If so, the program chooses the larger one.)

APPENDIX IV  
SUMMARY OF PUFF TEST RESULTS

PUFF's errors might be categorized into overrounds, underrounds, overshoots, undershoots, hot-thin spikes, and cold-thick spikes. These may be further broken down into compression overrounds, compression underrounds, rarefaction overrounds, and rarefaction underrounds. For graphical description of these distortions, see figure A-r. The hot-thin spikes occur where there are shocks in the initial flow. The cold-thick spikes occur at shock collisions or shock overtakes.

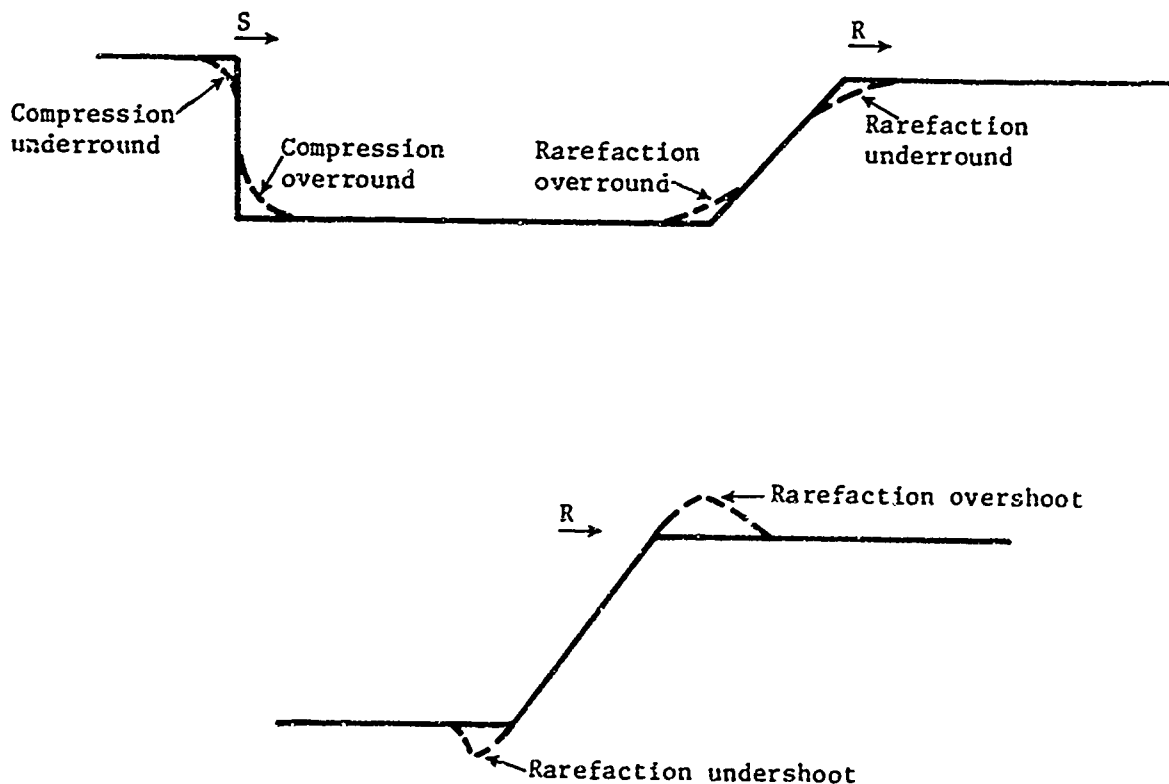


Figure A-4. PUFF Errors

We will now list some examples of these errors.

Compression overround in  $P$ ,  $v$ ,  $\rho$ ,  $e$  in SCTP-I, SCTP-III

Compression underround in  $P$ ,  $v$ ,  $\rho$ ,  $e$  in SCTP-I

Rarefaction overround in the pressure SCTP-V-A

Rarefaction underround in  $P$ ,  $v$ ,  $\rho$ ,  $e$  in SCTP-II

Rarefaction overshoot in the velocity in SCTP-V-C

Rarefaction undershoot in  $P$ ,  $v$ ,  $\rho$ ,  $e$  in SCTP-II-A

Hot-thin spike in SCTP-I, SCTP-VI, SCTP-VII

Cold-thick spike in SCTP-VI, SCTP-VII

The pressure and velocity are the best behaved variables in PUFF while the density and internal energy are the worst behaved.

## INDEX

	<u>Page</u>
A, A-I	105
accelerating piston problems, SCTP-III, SCTP-IV	47
adiabatic, A-I	111
analog methods, A-II	132
artificial viscosity, I	4
C, SCTP-I	11
CE, SCTP-I	14
CFL number, A-II	118
$C_g$ , SCTP-I	11
CM, SCTP-I	12
$C_o$ , A-II	117
$C_r$ , SCTP-I	11
$C_{\pm}$ characteristic, SCTP-II	30
characteristics, SCTP-II	30
characteristics method, A-II	32
code, I	1
compression wave, SCTP-III	47
contact discontinuity, SCTP-V	69
continuity equation, SCTP-I	12
continuous solution, A-I	105
conservation laws, A-I	105
DELTA, see $\Delta X$ , $\Delta t$	---
$\Delta X$ = space mesh increment	---
$\Delta t$ = time mesh increment	---
discrete solution, I	115

## INDEX (cont'd)

	<u>Page</u>
$E$ = specific total energy, A-I	109
$e$ = specific internal energy, SCTP-I	14
effective CFL number, SCTP-I	23
EOS = equation of state relation, SCTP-I	14
energy balance equation, SCTP-I	14
energy partition, SCTP-I	22
equation of continuity, SCTP-I	12
equations of hydrodynamics, A-I	105
equation of motion, SCTP-I	12
equation of state, SCTP-I	14
escape speed, SCTP-II	41
Eulerian formulation, A-I	114
finite difference methods, A-II	115
first law of thermodynamics, A-I	109
gas constant, SCTP-I	14
gamma, see $\gamma$ and $\Gamma$	---
$\gamma$ , SCTP-I	14
$\lambda_{\pm}$ characteristic, SCTP-II	30
isentropic, A-I	109
hybrid methods, A-II	132
hydrocode, I	1
ideal gas, SCTP-I	14
isotropic, A-I	109
Lagrangian equations, A-I	105
Lagrangian formulation, A-I	105
method of characteristics, A-II	137

## INDEX (cont'd)

	<u>Page</u>
Method of lines, A-II	132
Newton's second law, SCTP-I	13
$N2L$ $\equiv$ Newton's second law relation, SCTP-I	13
overround, A-IV	136
overshoot, A-IV	136
$P$ $\equiv$ pressure	---
pipe problem, SCTP-I	10
piston-in-pipe problem, SCTP-I	10
$P_Q$ , SCTP-I	11
$P_T$ , SCTP-I	11
PUFF	3
$Q$ $\equiv$ symbol for artificial viscosity in PUFF	---
$R$ $\equiv$ gas constant, SCTP-I	14
Rankine-Hugoniot relation, SCTP-I	15
rarefaction, SCTP-II, SCTP-IV	27
rarefaction relation, SCTP-V	76
$RH$ $\equiv$ Rankine-Hugoniot relation, SCTP-I	15
$\rho$ , see $\rho$	---
$\rho$ $\equiv$ density	---
$\rho_2$ , SCTP-I	11
$\rho_1$ , SCTP-I	11
Riemann invariant, SCTP-II	29
Riemann problem, SCTP-V	69
$S$ $\equiv$ entropy, A-I	109
SCTP-I	10
SCTP-II	27

## INDEX (cont'd)

	<u>Page</u>
SCTP-III	47
SCTP-IV	62
SCTP-V	69
SCTP-VI	87
SCTP-VII	97
shock, SCTP-I	10
shock relation, SCTP-V	74
shock speed formulas, SCTP-I	16
shock transition region, SCTP-I	22
shock tube problem, SCTP-V	69
shock width, SCTP-I	22
simple wave, SCTP-II	31
simple wave formulas, SCTP-II	54
slab geometry, II	8
steady profile, SCTP-I	10
SS(P) $\equiv$ shock speed as a function of pressure relation, SCTP-I	17
SS(V) $\equiv$ shock speed as a function of specific volume, SCTP-I	17
SS(u) $\equiv$ shock speed as a function of fluid velocity, SCTP-I	16
T $\equiv$ temperature	14
t $\equiv$ time	---
U $\equiv$ symbol for velocity in PUFF	---
underground, A-IV	136
undershoot, A=IV	136
utility, I	1
V $\equiv$ specific volume	11

INDEX (cont'd)	<u>Page</u>
$v \equiv$ velocity	11
vacuum, SCTP-II, SCTP-IV	30
$V$ , SCTP-I	11
$v$ , SCTP-I	11
$v_p$ , SCTP-I	11
$V_r$ , SCTP-I	11
$v_r$ , SCTP-I	12
$v_s$ , SCTP-I	12
$X \equiv$ Eulerian position	105
$x \equiv$ Lagrangian label, A-I	105
ZM $\equiv$ symbol for zone mass in PUFF	---



UNCLASSIFIED  
Security Classification

DOCUMENT CONTROL DATA - R & D		
(Security classification of title, body of abstract and indexing annotation must be entered when the overall report is classified)		
1. ORIGINATING ACTIVITY (Corporate author) Air Force Weapons Laboratory (WLRT) Kirtland Air Force Base, New Mexico 87117		2a. REPORT SECURITY CLASSIFICATION UNCLASSIFIED
		2b. GROUP
3. REPORT TITLE HYDROCODE TEST PROBLEMS		
4. DESCRIPTIVE NOTES (Type of report and inclusive dates) October 1966-October 1967		
5. AUTHOR(S) (First name, middle initial, last name) Darrell Hicks		
6. REPORT DATE	7a. TOTAL NO. OF PAGES 156	7b. NO. OF REFS 2
8a. CONTRACT OR GRANT NO.		9a. ORIGINATOR'S REPORT NUMBER(S) AFWL-TR-67-127
b. PROJECT NO. 5710		
c. Subtask No. 15.018		9b. OTHER REPORT NO(S) (Any other numbers that may be assigned this report)
d.		
10. DISTRIBUTION STATEMENT This document is subject to special export controls and each transmittal to foreign governments or foreign nationals may be made only with prior approval of AFWL (WLRT), Kirtland AFB, NM, 87117. Distribution is limited because of the technology discussed in the report.		
11. SUPPLEMENTARY NOTES		12. SPONSORING MILITARY ACTIVITY AFWL (WLRT) Kirtland AFB, NM 87117
13. ABSTRACT (DISTRIBUTION LIMITATION STATEMENT NO. 2) The utility (accuracy, speed, etc.) of a hydrocode in solving the equations of hydrodynamics may be estimated by applying the hydrocode test problems described in this report. Given the estimations of the utilities of a pair of hydrocodes, we may decide which is the preferred hydrocode to use. The hydrocode test problems described in this report have solutions which are known exactly. Seven hydrocode test problems involving shocks, rarefactions, and interactions are investigated and applied to a typical hydrocode, AFWL's PUFF.		

DD FORM 1 NOV 66 1473

UNCLASSIFIED  
Security Classification

14. KEY WORDS	LINK A		LINK B		LINK C	
	ROLE	WT	ROLE	WT	ROLE	WT
Hydrocodes Hydrocode test problems PUFF hydrocode						